PYRIDINE NUCLEOTIDE TRANSHYDROGENASE

H. W. J. VAN DEN BROEK

PYRIDINE NUCLEOTIDE TRANSHYDROGENASE

Dit proefschrift met stellingen van

HENDRIKUS WILHELMUS JOHANNES
VAN DEN BROEK,

landbouwkundig ingenieur, geboren te Zevenbergen, 30 juni 1940, is goedgekeurd door de promotor, Dr. C. VEEGER, hoogleraar in de Biochemie.

De Rector Magnificus van de Landbouwhogeschool,
J. M. POLAK

Wageningen, 31 maart 1971

PYRIDINE NUCLEOTIDE TRANSHYDROGENASE

(with a summary in Dutch)

PROEFSCHRIFT

TER VERKRIJGING VAN DE GRAAD
VAN DOCTOR IN DE LANDBOUWWETENSCHAPPEN
OP GEZAG VAN DE RECTOR MAGNIFICUS, MR. J. M. POLAK,
HOOGLERAAR IN DE RECHTS- EN STAATSWETENSCHAPPEN
VAN DE WESTERSE GEBIEDEN,
TE VERDEDIGEN TEGEN DE BEDENKINGEN VAN EEN
COMMISSIE UIT DE SENAAT
VAN DE LANDBOUWHOGESCHOOL TE WAGENINGEN
OP WOENSDAG, 26 MEI 1971 TE 16.00 UUR

DOOR

H. W. J. VAN DEN BROEK

H. VEENMAN & ZONEN N.V. - WAGENINGEN 1971

This thesis is also published as Mededelingen Landbouwhogeschool Wageningen 71-8 (1971).
(Communications Agricultural University Wageningen, The Netherlands)

STELLINGEN

I

De gewoonte, om uit niet-lineaire relaties tussen de reactiesnelheid en substraatconcentraties te concluderen, dat men te maken heeft met een regulerend enzym, moet op zijn minst als voorbarig gezien worden

Dit proefschrift

II

Bij het gebruik van regenererende systemen in enzymatische activiteitsbepalingen dient men zich te realiseren dat een foutenbron kan worden geïntroduceerd.

III

De gemiddelde levensduur van de fluorescentie-emissie van gereduceerd nicotine adenine dinucleotide, zoals bepaald door CHEN et al., is onjuist.

R. F. CHEN, G. C. VUREK en N. ALEXANDER, Science, 156 (1967) 949

IV

De suggestie van YOURNO et al., dat genenfusie een aanvaardbare verklaring vormt voor het ontstaan van eiwitcomplexen, is zeer aantrekkelijk; het model, dat deze auteurs voorstellen voor de vorming van het complex histidinol dehydrogenase-aminotransferase in Salmonella typhimurium, wordt echter onvoldoende door hun experimentele gegevens ondersteund.

J. YOURNO, T. KOHNO en J. R. ROTH, Nature, 228 (1970) 820

V

Het ontbreken of aanwezig zijn van iedere intrinsieke infectiositeit van de nucleoproteïne-componenten van meer-componenten virussen is nog onvoldoende bewezen.

A. VAN KAMMEN, Virology, 34(1968)312
A. VAN KAMMEN en L. J. L. D. VAN GRIENSVEN, Virology 41(1970)274
R. W. FULTON, Virology, 41(1970)288

VI

De tegenstrijdigheden, die bestaan tussen de experimentele gegevens en het door Staal en Veeger voorgestelde reactie-mechanisme voor glutathion reductase uit erythrocyten, zijn met behulp van de reactie-parameters te verklaren.

G. E. J. STAAL en C. VEEGER, Biochim. Biophys. Acta 185(1969) 49

VII

De conclusie van FORGET, dat de respiratoire nitraatreductase uit Micrococcus denitrificans een niet-haem-ijzereiwit is, druist in tegen de algemeen verbreide opvatting dat molybdeen betrokken zou zijn bij de dissimilatorische nitraatreductie van bacteriën.

P. FORGET, Eur. J. Biochem., 18(1971)442

VIII

De verklaring die IMAMOTO geeft voor de genetische polariteit van nonsense mutaties in het tryptofaan operon van Escherichia coli (voortijdige beëindiging van transcriptie van dit operon) is gebaseerd op gegevens welke ook gebruikt kunnen worden ter ondersteuning van de opvatting van MORSE en YANOFSKY (afbraak van boodschapper-RNA, distaal ten opzichte van het nonsense codon van het gemuteerde gen).

D. E. MORSE en C. YANOFSKY, Nature, 224(1969)329
F. IMAMOTO, Nature, 228(1970)232

IX

Het gebruik van synthetische chemicaliën, in de vorm van landbouwchemicaliën, bestrijdingsmiddelen, meststoffen, reuk-, kleur- en smaakstoffen in voedingsmiddelen, geneesmiddelen en huishoudchemicaliën, dient door middel van een duidelijk omschreven, internationaal geldende wetgeving geregeld te worden, terwijl de gegevens omtrent deze middelen, inclusief toetsmethodiek en recente toetsresultaten, volledig gepubliceerd dienen te zijn op het moment dat deze stoffen in de handel worden gebracht.

X

De stuurgroep, welke in het MC KINSEY-rapport wordt voorgesteld als dirigerend orgaan van wetenschappelijk onderwijs en onderzoek, dient op democratische wijze te worden samengesteld.

H. W. J. VAN DEN BROEK
Wageningen, 26 mei 1971.

Aan An, Jos en Frank

VOORWOORD

De voltooiing van dit proefschrift stelt mij in de gelegenheid dank te betuigen aan allen, die, op welke manier dan ook, hebben meegewerkt aan het tot stand komen van de bundeling van wetenschappelijke gegevens in deze vorm.

In de eerste plaats dank aan mijn ouders, die mij in de gelegenheid hebben gesteld in Wageningen te gaan studeren.

De hoogleraren, docenten en leden van de wetenschappelijke staf van de Landbouwhogeschool dank ik voor het genoten onderwijs. Met genoegen denk ik terug aan mijn ingenieursstudie, waarin ik op de afdelingen Virologie, Entomologie, Microbiologie en Organische Chemie onderzoek mocht leren bedrijven; de belangstelling voor het wetenschappelijk onderzoek werd door een goed voorbeeld, een ideale begeleiding en een prettige werksfeer in positieve zin beïnvloed en was doorslaggevend bij de bepaling van mijn studiekeuze.

Hooggeleerde Veeger, hooggeachte Promotor, U ben ik zeer veel dank verschuldigd voor de wijze waarop U mij in het onderzoek hebt weten te stimuleren en voor de vrijheid, die U mij hierbij hebt gelaten. Uw ervaring, enthousiasme, interesse en intuïtie vormden een voortdurende stimulans gedurende de gehele periode van dit onderzoek. Ik beschouw het als een voorrecht onder Uw leiding te hebben mogen werken en ik dank U voor alles wat ik van U en op Uw laboratorium heb mogen leren. De steun, die ik van U mocht ontvangen bij het begin van mijn verdere loopbaan, waardeer ik ten zeerste en ik hoop, dat de contacten met U en Uw laboratorium in de toekomst gehandhaafd zullen mogen blijven.

Hooggeleerde van Bruggen, waarde Heer van Breemen, met vreugde denk ik terug aan de periode, dat ik gastvrijheid genoot op het Laboratorium voor Structuurchemie te Groningen. Dank zij een ideale, effectieve vorm van samenwerking kon dit kortstondige verblijf resulteren in het meest spectaculaire hoofdstuk van dit proefschrift. Ik hoop een dergelijke samenwerking in de toekomst, ook met andere laboratoria, nog vaak te mogen meemaken.

Hooggeleerde van der Veen, van de gelegenheid die U mij gaf mijn proefschrift af te ronden, heb ik dankbaar gebruik gemaakt. Uw positieve opstelling ten aanzien van de biochemische aspecten van de genetica vormt een ideaal uitgangspunt voor een verblijf op Uw laboratorium. Voor de moeite die U zich heeft getroost, om een eventuele pioniersperiode voor mij op Uw afdeling tot een minimum te willen bekorten, ben ik U zeer erkentelijk.

Mijn collega's op de afdeling Biochemie wil ik gaarne danken voor de belangstelling, die zij voor mijn werk getoond hebben; hun samenwerking, suggesties en kritische opmerkingen heb ik ten zeerste gewaardeerd. Voor de morele en daadwerkelijke steun welke ik van velen Uwer, in welke vorm dan ook, mocht ontvangen mijn welgemeende dank.

Mijn bijzondere waardering gaat uit naar de Heren Jillert Santema, en Hans Wassink; zonder hun steun zouden een aantal van de in dit proefschrift be-

schreven experimenten nog op uitvoering liggen wachten. In belangrijke mate is dit onderzoek dan ook het hunne geweest en zij verdienen meer dan dank.

De typevaardigheid van Mevrouw Odink-Los en de dames van de typekamer heb ik ten zeerste op prijs gesteld.

Tenslotte wil ik jou, An, danken voor de steun die jij mij gedurende de positieve en negatieve fasen van dit onderzoek voortdurend hebt weten te geven.

CONTENTS

LIST OF ABBREVIATIONS

A	absorbance
ADP	adenosine 5′-diphosphate
2′AMP	adenosine 2′-monophosphate
3′5′AMP	adenosine 3′5′-monophosphate
5′AMP	adenosine 5′-monophosphate
ATCC	american type culture collection
ATP	adenosine 5′-triphosphate
BSA	bovine serum albumin
CD	circular dichroism
$D_{20.w}$	diffusion coefficient in water at 20° at a finite protein concentration
DCIP	2,6-dichlorophenol indophenol
DEAE	diethyl amino ethyl
EDTA	ethylene diaminetetra acetate
EPR	electron spin resonance
FAD	flavin adenine dinucleotide, oxidised form
$FADH_2$	flavin adenine dinucleotide, reduced form
FMN	flavin mononucleotide
GDP	guanosine 5′-diphosphate
GTP	guanosine 5′-triphosphate
K_{ass}	association constant of enzyme-substrate (prosthetic group) complex
K_D	dissociation constant of enzyme-substrate complex
K_i	dissociation constant of enzyme-inhibitor complex
K_m	Michaelis constant
k_{+n}, k_{-n}	reaction constants of step n in a reaction mechanism
L-B plot	Lineweaver-Burk plot
$lipS_2$	lipoic acid, oxidised form
$lip(SH)_2NH_2$	lipoamide, reduced form
M	molecular weight
$NAD(P)^+$	nicotinamide adenine dinucleotide (phosphate), oxidised form
NAD(P)H	nicotinamide adenine dinucleotide (phosphate), reduced form
nm	nanometer
ORD	optical rotatory dispersion
PDC	pyruvate dehydrogenase complex
QAE	quaternary diethyl-(2-hydroxypropyl)-aminoethyl
r.p.m.	revolutions per minute
$s_{20,w}$	sedimentation coefficient in water at 20°
$TNAD(P)^+$	thionicotinamide adenine dinucleotide (phosphate), oxidised form
TNAD(P)H	thionicotinamide adenine dinucleotide (phosphate), reduced form
Tris	Tri (hydroxymethyl) amino methane
v	velocity at a finite substrate concentration
V_{max}	maximum velocity at infinite substrate concentration

LIST OF ENZYMES USED THROUGHOUT THIS THESIS

In this thesis the non-systematic names of the enzymes are used. This list includes the trivial and the systematic names of the enzymes; also is included the enzyme number according to the Report of the Commission for Enzymes of the International Union of Biochemistry.

EC number	Systematic name	Trivial name
1.1.1.1.	Alcohol-NAD^+ oxidoreductase	Alcohol dehydrogenase
1.1.1.49.	D-Glucose-6-phosphate: $NADP^+$ oxidoreductase	Glucose-6-phosphate dehydrogenase
1.6.4.3.	Reduced-NAD^+: lipoamide oxidoreductase	Lipoamide dehydrogenase
1.6.1.1.	Reduced-$NADP^+$: NAD^+ oxidoreductase	$NAD(P)^+$ transhydrogenase
1.11.1.6.	Hydrogen: peroxide oxidoreductase	Catalase
3.2.2.5.	$NAD(P)^+$ glycohydrolase	NADase

1. INTRODUCTION

Pyridine nucleotide transhydrogenases are widespread in nature and have been identified in micro-organisms e.g. *Pseudomonas aeruginosa* (COLOWICK et al., 1952; COHEN, 1967; COHEN and KAPLAN, 1970a), *Azotobacter vinelandii* (KAPLAN et al., 1952; VAN DEN BROEK and VEEGER, 1968, 1970; CHUNG, 1970), *Chromatium* (KEISTER and HEMMES, 1966), *Rhodospirillum* (KEISTER and YIKE, 1966, 1967), *Rhodopseudomonas* (ORLANDO et al., 1966; KEISTER and YIKE, 1967), *Escherichia coli* (MURTHY and BRODY, 1964), *Micrococcus denitrificans* (ASANO et al., 1967) and higher organisms (KAPLAN et al., 1953; DANIELSON and ERNSTER, 1963 a,b). Only a few systems have been extensively investigated. In this introduction our attention will mainly be directed to the studies on the *Pseudomonas* and *Azotobacter* systems and to the energy dependent transhydrogenases in animal tissue mitochondria and the photosynthetic bacteria.

In the course of their investigations on isocitric dehydrogenase in extracts of *Pseudomonas fluorescens*, COLOWICK et al. (1952) were able to demonstrate the presence of an enzyme catalyzing the following reaction

$$NADPH + NAD^+ \rightleftharpoons NADP^+ + NADH \qquad (1)$$

It was supposed that the pyridine nucleotide transhydrogenase could play an important role in regulating the pathway of electron transport. It was even suggested that the transhydrogenase might serve to regulate the conversion of oxidation energy into phosphate-bound energy. Studies with ^{14}C-nicotinamide-labeled NAD^+ (KAPLAN et al., 1953) and NAD^+ analogues (KAPLAN et al., 1952) indicated that the *Pseudomonas* transhydrogenase reaction proceeds without an exchange of the nicotinamide moieties, or a transfer of the monoester phosphate group. SAN PIETRO et al. (1955) showed from studies with deuterium labeled reduced pyridine nucleotides that the catalysed reaction involved transfer of hydrogen rather than a pair of electrons. It was demonstrated that deuterium was transferred from NADPD to form NADD, without exchange of label with the medium. Furthermore this transfer was stereospecific for the B position of NADH; the stereospecificity of transfer with respect to NADPH was not determined. Recent studies regarding the stereospecificity of pyridine nucleotide transhydrogenase from *Pseudomonas aeruginosa* (LOUIE and KAPLAN, 1970 a,b) showed that the enzyme is stereospecific for the 4B hydrogen atom with respect to both NADH and NADPH. From the requirement for the 4B position of both donor and acceptor pyridine nucleotide coenzymes, and the inability to exchange the label with the medium, these authors suggested (1970 a,b) that the enzyme catalyses a reversible direct transfer of hydrogen between the two nucleotides. With partially purified *Azotobacter* transhydrogenase preparations they found (1970a) an incomplete direct transfer, and proposed that the flavin is more exposed in the latter system.

The *Pseudomonas* enzyme is also different from the mammalian mitochondrial transhydrogenases, in that the latter are specific for the 4A position of NADH and the 4B position of NADPH and its analogues (KAWASAKI et al., 1964; LEE et al., 1965; ROBERTON and GRIFFITHS, 1965). There is, however, some similarity with the pyridine nucleotide-dependent flavoenzyme, NADH dehydrogenase, which has also been shown to be specific for the 4B position of NADH as donor and acceptor, but this enzyme exchanges a proton with the medium (LEE et al., 1965).

It was demonstrated (KAPLAN et al., 1953) for the *Pseudomonas* enzyme that reaction (1) was only partially reversible, the reversibility being dependent on the use of low concentrations of $NADP^+$ and phosphate. 2'AMP and compounds containing the ribose 2'-phosphate moiety readily induced a reversal of this reaction and behaved as competitive antagonists of the inhibitory effects of $NADP^+$ and thus as activators of the enzyme. Purification of the *Pseudomonas* enzyme to an apparent homogeneity and crystallisation (COHEN, 1967; COHEN and KAPLAN, 1970a) did not change this phenomenon, although the reverse reaction proceeded directly and the equilibrium constant for the system was as expected near unity. In the reactions in which the reducing substrate did not contain a 2'-phosphate group, 2'AMP was strongly activating; since 2'AMP also showed the ability to disaggregate the enzyme, it was suggested that the disaggregation resulted in an enzyme form which was able to react with NADH. Kinetic studies (COHEN, 1967; COHEN and KAPLAN, 1970b) revealed that in the presence of 2'AMP the NADPH → $TNAD^+$ and the NADH → $TNAD^+$ systems behaved according to a ping-pong bi-bi catalytic mechanism. In the absence of 2'AMP, however, in the NADPH → $TNAD^+$ system, the reaction velocity showed a second order dependence on NADPH, but a first order dependence on $TNAD^+$; the experiments were interpreted in terms of enzyme activation by both NADPH and 2'AMP. The effect of 2'AMP on the NADH → $TNAD^+$ reaction was explained by accepting an increase of the rates of steps in the reaction sequence involving reduction of the enzyme by NADH. The experiments with $NADP^+$ pointed to a failure of $NADP^+$ to activate the enzyme, making NADH a less effective substrate, resulting in a failure of the transhydrogenase to catalyse the reaction between NADH and $NADP^+$. Furthermore the formation of a dead end complex of $NADP^+$ with enzyme was proposed. A ternary complex mechanism, although not favoured, was not excluded. In later studies (LOUIE and KAPLAN, 1970b), however, it was suggested that a modified Theorell-Chance mechanism might give a better explanation, accounting also for the absence of the NADH → NAD^+ exchange reaction.

Spectral experiments suggested that the flavin prosthetic group of the enzyme might participate in the direct transhydrogenation reactions (COHEN, 1967; COHEN and KAPLAN, 1970a; LOUIE and KAPLAN, 1970b). Supporting evidence came from experiments in the presence of 1 M ureum (LOUIE and KAPLAN, 1970b); these experiments also suggested that the flavin might normally be shielded from the aqueous environment.

As already indicated by KAPLAN et al. (1953) the *Azotobacter* transhydrogenase showed many similarities with the *Pseudomonas* enzyme with respect to its behaviour towards 2'AMP and phosphate. The $NADP^+$ inhibition phenomenon, however, was much more pronounced in the case of the *Azotobacter* enzyme. It was suggested this latter effect may be the result of endogeneous $NADP^+$ bound to the enzyme (KAPLAN et al., 1953; LOUIE and KAPLAN, 1970a). Recent studies with the *Azotobacter* enzyme (VAN DEN BROEK and VEEGER, 1968, 1970; CHUNG, 1970) partially confirmed these observations. From kinetic experiments CHUNG suggested that the enzyme might contain a specific '*hydrogen donor*' site for NAD^+ and $TNAD^+$ and a specific '*hydrogen acceptor*' site for NADPH and NADH; upon changing the hydrogen donor subtle differences in the enzyme structure might be brought about. On the basis of the unusual kinetics in the presence of $NADP^+$ the possibility of a third binding site was assumed, having a binding capacity for the inhibitor $NADP^+$ and the activator 2'AMP.

An $NAD(P)^+$ transhydrogenase, also known as TD-transhydrogenase, in animal tissue was found by KAPLAN et al. (1952); the preparations always contained varying amounts of NADH:NAD^+ oxidoreductase (KAPLAN et al., 1952; KAUFMAN and KAPLAN, 1961), known as DD-transhydrogenase. Both activities were not due to one single lipoprotein as proposed by PESCH and PETERSON (1965), but the DD-transhydrogenase was due to lipoamide dehydrogenase (KRAMAR et al., 1968). The basic reaction was catalysed in both directions by the mitochondrial system, with an equilibrium constant near unity, although the reaction in the direction of $NADP^+$ was catalysed more rapidly under the conditions employed. It was assumed that their metabolic function was mainly concerned with the mediation of NADPH to the NADH oxidase system, thereby facilitating the operation of $NADP^+$-dependent dehydrogenases (KAPLAN et al., 1956; NAVAZIO et al., 1958).

The possible existence of reactions in which NADPH could be generated by pathways other than $NADP^+$-linked dehydrogenases was first stressed by KREBS and KORNBERG (1957). They envisaged a mechanism involving an ATP-dependent reduction of $NADP^+$ by a reduced flavoprotein. The findings of KLINGENBERG and SLENCZKA (1959) of a rapid and almost complete reduction of the intramitochondrial $NADP^+$ upon incubation of isolated liver mitochondria with NAD^+-specific substrates or succinate in the absence of phosphate acceptor, led to the postulation of an ATP-controlled transhydrogenase reaction. A similar conclusion was reached by ESTABROOK and NISSLEY (1963). A transhydrogenase which catalyses the transfer of hydrogen atoms from NADH to $NADP^+$ in an energy-dependent reaction was discovered by DANIELSON and ERNSTER (1963) and it was shown that sub-mitochondrial particles catalyse an ATP-dependent reduction of $NADP^+$ by NADH; ATP could be replaced by high-energy intermediates generated during the oxidation of succinate. The requirement for energy in the ATP driven transhydrogenation between NADH and $NADP^+$ was stoichiometric, and its apparent equilibrium constant was of the order of 500 (LEE and ERNSTER, 1964). The sub-mitochondrial

particles also contained the non-energy dependent transhydrogenase. Several indications favoured the view that the two types of reactions involved one common transhydrogenase e.g. both the energy-linked and the non-energy-linked enzyme catalysed a stereospecific transfer between the B-side of NADPH and the A-side of NADH (KAWASAKI et al., 1964; LEE et al., 1965; ROBERTON and GRIFFITHS, 1965). Furthermore antibodies produced for the purified non-energy-linked transhydrogenase suppressed the energy-linked transhydrogenase activity of sub-mitochondrial particles (KAWASAKI et al., 1964). It was suggested that the transhydrogenase may act in a coupled or uncoupled fashion; the coupled reaction will involve an energised form of either NADH or $NADP^+$ as a reactant, thus differing from the non-coupled reaction with respect to reactants and products and to thermodynamic equilibrium.

In recent studies on the mitochondrial transhydrogenase system (RYDSTRÖM et al., 1970), however, an alternative mechanism was proposed, which involved an enzyme-linked alteration of the transhydrogenase molecule itself. The authors proposed the existence of two conformational states of the transhydrogenase, an active and an inactive one. The formation of the active state would be promoted by the presence of NAD^+ and NADPH whereas NADH and $NADP^+$ promoted the formation of the inactive state. It was assumed that in the presence of an energy supply the transhydrogenase reaction involved an energy-linked activation of the enzyme while the overall energy-linked transhydrogenase system operates as a cycling process. The existence of different conformational states of the same enzyme, induced by ATP, was also assumed by SWEETMAN and GRIFFITHS (1970) in their studies on the energy-linked pyridine nucleotide transhydrogenase in *E.coli*. These authors, however, also favoured the hypothesis that more than one hydrogen-transfer enzyme responsible for the formation of NADPH from NADH occurred in *E.coli*. The latter idea was based on the selectivity towards Mg^{2+}, the specificity towards nicotinamide nucleotides and the differences obtained with uncouplers of oxidative phosphorylation.

An energy-dependent reduction of $NADP^+$ by NADH was also observed in the photosynthetic bacteria *Rhodospirillum rubrum* (KEISTER and YIKE, 1966) and *Rhodopseudomonas spheroides* (ORLANDO et al., 1968). Since the reaction appeared to be similar to the ATP-dependent reaction in animal mitochondria (DANIELSON and ERNSTER, 1963) it was concluded that the energy source for the enzyme appeared to be a high-energy intermediate of phosphorylation (KEISTER and YIKE, 1967). An alternative mechanism, involving disulfides and sulfhydryl groups in the transfer reaction was recently proposed by ORLANDO (1970). According to ORLANDO light is required to produce a cyclic electron flow resulting in the partial reduction of chromatophore-bound disulfide groups by thiol derivatives such as reduced thioctic acid or dithiothreitol or a soluble transhydrogenase factor. ATP was proposed to function in a similar way in the presence of the thiol derivatives. The partial reduction of the chromatophores then leads to an unmasking or activation of the transhydrogenase.

Until now no conclusive evidence has been obtained about the function of

pyridine nucleotide transhydrogenase *in vivo*. It was suggested that the transhydrogenase plays an important role in regulating the pathway of electron transport (COLOWICK et al., 1952) or the conversion of oxidation energy into phosphate-bound energy (KAPLAN et al., 1953). The transhydrogenase could also be involved in mediating NADPH to the NADH oxidase system, thus facilitating the operation of $NADP^+$-dependent dehydrogenases (KAPLAN et al., 1956; KEISTER and YIKE, 1967) or in regulating the transfer of reducing equivalents from pyruvate to either N_2 or O_2 (MORTENSON et al., 1963; VAN DEN BROEK and VEEGER, 1968). However, the possibility that the transhydrogenase behaves like a reductase, as shown for several pyridine nucleotide dependent flavoenzymes (WEBER and KAPLAN, 1957; MASSEY, 1963; ZANETTI and FORTI, 1966) and exists in the organism to catalyse reduction or oxidation of a non-pyridine nucleotide substrate by pyridine nucleotides cannot be excluded. The existence of a ternary complex mechanism would support the role of the enzyme as a transhydrogenase *in vivo* (COHEN and KAPLAN, 1970b), but this question has not been answered satisfactorily yet.

In the course of our investigations on succinic dehydrogenase and non-heme iron proteins from *Azotobacter vinelandii* (VAN DEN BROEK and VEEGER, unpublished) a very high level of flavoproteins was found. The detection of an NAD^+-dependent NADPH-lipoate reductase led us to investigate this activity and we were able to separate it in different enzyme fractions, resulting in a method for the purification of the reversible pyridine nucleotide transhydrogenase (CHAPTER 3). Study of the characteristics of the enzyme revealed that we were dealing with a high molecular weight flavoprotein. Its flavin nature led us to investigate the spectral characteristics, with special attention to $NADP^+$ since spectral shifts were obtained upon dialysis of the purified enzyme (CHAPTER 5). The fact that the transhydrogenase had an extremely high molecular weight made it very interesting to study the morphology of the enzyme (CHAPTER 4). At that time LOUIE and KAPLAN (1970a) reported their helical-like structures in *Pseudomonas* transhydrogenase. Kinetic studies were performed (CHAPTER 6) to obtain some information concerning the reaction mechanism and to correlate these results with the spectral studies.

A close interaction was observed between transhydrogenase and lipoamide dehydrogenase activity. Since the latter enzyme could be easily purified from side fractions of the large scale purification procedure developed for the transhydrogenase, some studies were performed with lipoamide dehydrogenase (CHAPTER 7). Most of the latter studies were done by MR. J. SANTEMA.

2. MATERIALS AND METHODS

2.1. MATERIALS

2.1.1. *Enzymes*

The reversible NADH:$NADP^+$ transhydrogenase was purified from cell free extracts of *Azotobacter vinelandii* (ATCC 478) by the method described in CHAPTER 3. Solutions of transhydrogenase in 0.1 M potassium phosphate buffer (pH 7.5), containing 1 mM EDTA were stored at 4° and dialyzed before use for 24 to 48 hours against the same buffer. For the electron microscopic studies the enzyme was dialysed against 0.05 M Tris – HCl (pH 7.5), containing 0.5 mM EDTA and diluted to an appropiate concentration with either the same buffer, 0.1 M ammonium acetate or with bidistilled water. All spectral studies were performed with preparations of a specific activity at 25° as measured under the conditions of the standard assay procedure, of at least 200 units per min per mg of protein (cf. 2.2.2.1).

The apoenzyme of transhydrogenase was prepared by the modified procedure of WARBURG and CHRISTIAN (1938) or by the method of KALSE and VEEGER (1968) (cf. CHAPTER 3). Before spectral measurements were performed, the apoenzyme was dialysed for 4 hours against 0.1 M phosphate buffer (pH 7.5), containing 1 mM EDTA.

Lipoamide dehydrogenase (E.C. 1.6.4.3.) was isolated from *Azotobacter vinelandii* (ATCC 478) and purified from side fractions obtained in the large scale procedure developed for the isolation and purification of the transhydrogenase, according to the method of MASSEY (1960) and MASSEY et al. (1960). All buffers used were potassium phosphate buffers (pH 7.5), containing 0.3–0.5 mM EDTA.

Lipoamide dehydrogenase apoenzyme was prepared by the acid ammonium sulfate method used by STRITTMATTER (1961) for cytochrome b_5 reductase and modified by KALSE and VEEGER (1968) and VISSER (1970) for the pig heart lipoamide dehydrogenase. The precipitated apoenzyme was dissolved in 0.3 M potassium phosphate buffer (pH 7.2), containing 3 mM EDTA at 25° and diluted with cold 0.03 M buffer (pH 7.2) and stored on ice. Also the method of BRADY and BEYCHOK (1968, 1969), i.e. dialysis against 1.5 M guanidine-HCl in 0.03 M phosphate buffer (pH 7.6) in the absence and presence of FMN, was used for the preparation of an apoenzyme of the *Azotobacter* lipoamide dehydrogenase. Dialysis was performed at 4°, spectral measurements at 10°.

Pyruvate dehydrogenase complex was isolated from *Azotobacter vinelandii* cell free extracts according to the method of REED et al. (1969) or from side fractions obtained in the large scale procedure developed for the isolation and purification of the transhydrogenase by calcium phosphate gel, DEAE-cellulose and Sepharose 4B column chromatography.

$NAD(P)^+$ nucleosidase [$NAD(P)^+$ glycohydrolase, E.C.3.2.2.6], purified

from extracts of *Neurospora crassa* according to the method of KAPLAN (1965) was a gift from DR. J. DE VIJLDER, University of Amsterdam.

Yeast alcohol dehydrogenase, catalase and glucose-6-phosphate dehydrogenase were purchased from Boehringer and Soehne.

2.1.2. *Reagents*

NAD^+, NADH, $NADP^+$, NADPH, thio-NAD^+, ATP, 2'AMP, GTP, FAD, FMN, riboflavin, lipoic acid, bovine serum albumin were obtained from Sigma Chemical Co; thio-$NADP^+$ from Schuchardt. Glucose-6-phosphate was purchased from Boehringer and Soehne; QAE-Sephadex, DEAE-Sephadex, CM-Sephadex, Sepharose 2 B or 4 B and blue dextran 2000 from Pharmacia (Uppsala); DEAE-cellulose from Serva. DCIP and $K_3Fe(CN)_6$ were obtained from the British Drug House; ovalbumin and β-mercaptoethanol from Koch-light and sodium dithionite, analytical grade, from Merck.

Reduced lipoamide, synthesised according to the method of REED et al. (1959) was kindly provided by DR. J. KRUL from our laboratory.

All other chemicals used were Reagent Grade and solutions were made up in bidistilled water.

2.2. METHODS

2.2.1. *Preparation of calcium phosphate gel*

The procedure is basically the method used by SWINGLE and TISELIUS (1951). A filtered calcium sucrate solution, prepared from sucrose and calcium oxide, is brought to pH 9.5 at room temperature by slowly adding concentrated phosphoric acid and held at this pH for the next four hours by adding diluted NaOH. The gel is washed with bidistilled water until sucrose free, suspended in bidistilled water at a concentration of 70–80 mg (dry weight) per ml and stored at 4°. The pH of preparation is very critical for the purification of the transhydrogenase. At a pH of preparation > 9.5 the resulting gel has a good adsorbing capacity, however, the transhydrogenase sticks irreversible to the gel; at a pH of preparation below 9.5 the resulting gel has a very poor adsorbing capacity. The most reproducible results are obtained with somewhat aged calcium phosphate gel preparations. The same gel was used for the purification of lipoamide dehydrogenase.

2.2.2. *Determination of activities and concentrations*

The assays were carried out at 25° with a Zeiss spectrophotometer PMQ II in combination with either a Photovolt recorder model 43 or a Honeywell Elektronik 16 high-speed recorder, or with a Cary model 14 recording spectrophotometer in 1 cm cuvettes by following the change in absorbance at the wavelength indicated. The activity was calculated from the initial rate of absorbance change. Maximal absorbance changes at highest substrate concentrations did not exceed 0.1–0.2 per min. On the average tracings were reasonably linear under these conditions for the first half min.

2.2.2.1. The enzymatic assay of *Azotobacter* transhydrogenase, lipoamide dehydrogenase and pyruvate dehydrogenase complex

The standard transhydrogenase assay was performed in 0.05 M Tris-HCl (pH 7.5) in a final volume of 2.5 ml, containing 50 μM $TNAD^+$ and 100 μM NADPH. The assay was initiated by the addition of enzyme, diluted in 0.1 M phosphate buffer (pH 7.5)-1mM EDTA and the absorbance change at 398 nm due to the formation of TNADH was followed. Assuming a molar extinction coefficient of 11,300 M^{-1} cm^{-1} for TNADH at 398 nm (KEISTER and HEMMES, 1966) a unit of activity can be defined as the amount of enzyme required to reduce 1 μmole $TNAD^+$ per min under the conditions mentioned above. The specific activity is defined as units per mg of protein.

The reduction of $TNAD^+$ and $TNADP^+$ by NAD(P)H was determined in an analogues manner at the same concentrations of donor and acceptor, unless otherwise indicated.

The transhydrogenase activities, NADH $\rightarrow$ $NADP^+$ and NADPH $\rightarrow$ NAD^+, were estimated by modifications of previous methods (COLOWICK et al., 1952; KAPLAN et al., 1953). The reduction of NAD^+ by NADPH was carried out in 0.1 M Tris-HCl (pH 8.0), containing 3–6 mM glucose-6-phosphate, excess glucose-6-phosphate dehydrogenase and pyridine nucleotides, as indicated. The reduction of $NADP^+$ by NADH was performed in 0.1 M Tris-HCl buffer (pH 8.0 or pH 7.6), containing 0.04% bovine serum albumin, 0.15 M ethanol, 4 mM semicarbazide, and excess yeast alcohol dehydrogenase; NADH, $NADP^+$ and $MgCl_2$ as indicated. Both reactions were initiated by the addition of the transhydrogenase and the increase in absorbance at 340 nm was measured. An extinction coefficient of 6,220 M^{-1} cm^{-1} for NADH and NADPH was assumed.

Calculation of catalytic centre activity is based on a minimum molecular weight of 60,000 daltons per mole of enzyme flavin (cf. CHAPTER 3).

The diaphorase activities of the transhydrogenase were assayed in 0.05 M phosphate buffer (pH 7.2) at donor concentrations of 100 μM in a final volume of 2.5 ml. The concentration of $K_3Fe(CN)_6$ was 0.8 mM and that of DCIP 0.04 mM; the molar extinction coefficients assumed were $\varepsilon_{420\ nm}$ = 1,030 $M^{-1}cm^{-1}$ and $\varepsilon_{600\ nm}$ = 20,000 $M^{-1}cm^{-1}$, respectively.

The standard lipoamide dehydrogenase assay was performed in 0.8 M tri-sodium citrate-H_3PO_4 buffer (pH 6.5), in a final volume of 2.5 ml, containing 0.1% bovine serum albumin, 1 mM EDTA, 0.8 mM lipoic acid, 100 μM NAD^+ and 100 μM NADH. The activity with reduced lipoamide was determined in 0.05 M potassium phosphate buffer (pH 7.6), containing 1 mM EDTA, 0.1 % BSA; concentrations of $lip(SH)_2NH_2$ and NAD^+ as indicated. DCIP activity was determined in 0.06 M potassium phosphate buffer (pH 7.2), 0.1% BSA, 1 mM EDTA, 40 μM DCIP and 100 μM NADH. In all cases the reaction was initiated by the addition of enzyme and activities corrected for the non-enzymic reaction. Activities are expressed as μmoles NADH oxidized or NAD^+ reduced per mg per min or in % of the original activity. Calculation of catalytic centre activity is based upon a flavin content of 1 mole FAD per 50,000 g of protein.

Pyruvate dehydrogenase complex activity was determined by the dismutation assay (REED and WILLMS, 1966).

Alcohol dehydrogenase and catalase activities were assayed as described by EISENKRAFT (1969).

2.2.2.2. Determination of concentrations

Protein concentration was determined by the biuret method of GORNALL et al. (1949) or by the micro-biuret method of ITZHAKI and GILL (1964).

The absorbance at 340 nm was a measure for the concentration of the freshly prepared NADH and NADPH (extinction coefficient of 6,220 $M^{-1}cm^{-1}$). The concentrations of NAD^+, $TNAD^+$, $NADP^+$ and $TNADP^+$ were either enzymatically determined with ethanol and alcohol dehydrogenase (NAD^+ and $TNAD^+$) or with glucose-6-phosphate and glucose-6-phosphate dehydrogenase ($NADP^+$ and $TNADP^+$) or were assayed as the pyridine nucleotide cyanide complexes assuming extinction coefficients for NAD^+ at 327 nm of 6,000 $M^{-1}cm^{-1}$, for $NADP^+$ at 327 nm of 5,900 $M^{-1}cm^{-1}$, for $TNAD^+$ at 355 nm of 10,000 $M^{-1}cm^{-1}$ and for $TNADP^+$ at 355 nm of 9,000 $M^{-1}cm^{-1}$ (Biochemica Catalogue, Boehringer, Mannheim).

Solutions of dithionite, used in the anaerobic titration experiments, were standardised by titration with lumiflavin assuming a molar extinction coefficient of 10,800 $M^{-1}cm^{-1}$ (FOUST et al., 1969b) for oxidized minus reduced flavin at 445 nm. Lumiflavin was titrated with dithionite, which was made up in anaerobic buffer, and the concentration of the dithionite solution was calculated from the slope of the plot relating the absorbance change at 445 nm with the amount of dithionite added. The oxygen contamination in the titration system was determined from the lag at the beginning of the titrations where no changes in absorbance at 445 nm occurred and the calculations were corrected for the observed contamination.

2.2.3. *Thin layer chromatography of flavins*

Thin layer chromatography was performed with *n*-butyl alcohol-acetic acid-water (4:3:3), 5% Na_2HPO_4 in water and *tert.* butyl alcohol-water (6:4) as developing solvents (KILGOUR et al., 1957), using silica gel powder plates (Baker-flex, Silica Gel 1 B, Baker Chemical Co., Phillipsbury, New Yersey). Flavins were detected by their fluorescence.

2.2.4. *Absorption spectrophotometry*

Absorption spectra were recorded on a Cary model 14, recording spectrophotometer, thermostated at 25° in cells with a 1 cm light path and corrected for the absorbance of the additions. The difference spectra were recorded with the 0–0.1 absorbance indicating slidewire; measurements were performed in tandem cells to correct for absorbance of the added substances.

Anaerobic titrations were performed under a nitrogen atmosphere in an anaerobic titration assembly as described by FOUST et al., (1969b). The apparatus consisted of three parts: a somewhat modified quartz Thunberg cuvette

with one side arm, a burette and a reservoir for titrant. Each part could be independently made anaerobic, thus permitting several titrations with the same titrant solution. Anaerobic conditions were obtained by evacuation and refilling of the cuvettes with oxygen free nitrogen. The latter was obtained by passing the nitrogen through alkaline pyrogallol or alkaline sodium hydrosulfite solution to which sodium-β-anthraquinone sulfonate was added as catalyst (FIESER, 1924). This procedure was repeated at least five times. De-gassing of the contents of the cuvette was assisted by shaking and stirring whilst under vacuum, keeping the solution cold by immersion in ice water to minimise evaporation and foaming. Volume losses due to evaporation were taken into account.

2.2.5. *Fluorescence*

Fluorescence emission spectra were recorded on a Hitachi Perkin-Elmer MPF-2A spectrofluorimeter, equipped with a thermostated cuvette holder. The emission spectra are corrected for scatter of the solvent.

2.2.6. *Ultracentrifugation*

Sedimentation and diffusion patterns were obtained using an MSE analytical ultracentrifuge. Sedimentation velocity runs were performed in 20 mm double sector cells at temperatures from 16–20°, and at rotor speeds between 26,000 and 33,000 r.p.m. for transhydrogenase and 50,000 r.p.m. for lipoamide dehydrogenase. Sedimentation coefficients were calculated according to the relation of SVEDBERG and PEDERSON (1940) and corrected to the standard conditions of a water solvent at 20°. Sedimentation equilibrium experiments with the *Azotobacter* lipoamide dehydrogenase apoenzyme were carried out at a rotor speed of 6,000 r.p.m. in the double sector synthetic boundary cell. The diffusion coefficient was calculated from the equation

$$D = (A/H)^2/4\,\pi\,t$$

where A is the area under the Schlieren peak and H is the maximum ordinate of the peak at time t. Values of $(A/H)^2$ are plotted with respect to t and the diffusion coefficient is evaluated; corrections were performed to the standard conditions. A value of the molecular weight of the lipoamide dehydrogenase apoenzyme was calculated from the SVEDBERG equation (1940)

$$M = RTs/D(1 - \bar{V}\rho)$$

where R is gas constant, T is temperature (°K), $\bar{V}$ is partial specific volume (for which a value of 0.73 was assumed), ρ is the density of the solvent, s is sedimentation coefficient and D is diffusion constant, by using the determined values of $s_{20,w}$ and $D_{20,w}$.

Sucrose density gradient centrifugation of the *Azotobacter* lipoamide dehydrogenase holo- and apoenzyme was performed with an MSE 50 superspeed

centrifuge at 3–4° in a 3 × 3 ml swing-out bucket rotor at 37,000 r.p.m. for 17 hours. Linear gradients from 9–25% sucrose in 0.1 M phosphate buffer (pH 8.0), containing 0.3 mM EDTA were used. Fractions for activity measurements were collected by punching a hole in the bottom of the tubes by means of the MSE fractionator. By application of the approximation of MARTIN and AMES (1961) molecular weights can be calculated using markers of known molecular weights (cf. CHAPTER 7).

Sedimentation and diffusion measurements were kindly performed by DR. J. VISSER.

2.2.7. *Gelfiltration*

Gelfiltration of lipoamide dehydrogenase on Sephadex G-200 columns was performed at about 8° according to the method described by VISSER and VEEGER (1968). The calculation of the Stokes radius permits the determination of the diffusion constant, according to the relation (SIEGEL and MONTY, 1966)

$$D_{20,w} = kT/6\,\pi\,\eta\,a$$

where a is Stokes radius (cm), k is the Boltzmann constant, T is temperature (°K), and η is viscosity of water at 20°.

Combination of the Stokes radius and sedimentation coefficient allows the calculation of the molecular weight according to the relation of SIEGEL and MONTY (1965, 1966)

$$M = 6\pi\eta Nas/(1 - \bar{V}\rho)$$

where η is the viscosity of the solvent, N is Avogadros number, a is Stokes radius (cm), s is sedimentation coefficient, $\bar{V}$ is the partial specific volume, ρ is the density of the solvent.

From the Stokes radius a frictional ratio, f/f_o, may also be obtained, using the equation of SIEGEL and MONTY (1965)

$$f/f_o = a/\left(\frac{3\,V\,M}{4\,\pi\,N}\right)^{1/3}$$

2.2.8. *Light-scattering*

Light-scattering data for transhydrogenase were obtained with a Cenco-TNO apparatus at room temperature (22° ± 1). Measurements were kindly performed by MR. VAN MARKWIJK (N.I.Z.O., Ede, The Netherlands).

The relation Kc/R_θ, derived from the Rayleigh ratio

$$R_\theta = i_\theta r^2/I_o = Kc/(1/M + 2Bc + 3Cc^2 + \ldots)\ \mathrm{cm}^{-1}$$

(STACEY, 1956) was calculated and plotted as a function of $(sin^2\,\theta/2) + c$. The optical constant K is defined as

$$K = 2\pi^2\eta_o^2(dn/dc)^2/N\lambda^4 \text{ cm}^2\text{g}^{-2}$$

where η_o is refraction index of the solvent; dn/dc is the refractive increment (accepted value 0.176 cm^3 g^{-1} for *Azotobacter* transhydrogenase); λ is wavelength of the light used (5460 Å) and i_θ/I_o is the ratio of the light scattered under the angle θ and of the incident beam. Benzene was used as a standard. For the optical constant a value of $K = 2.67 \times 10^{-7}$ cm^{2}g^{-2} was calculated. Buffer solutions were filtered before use with a 100 mμ filter and enzyme solutions centrifuged before dilution. Protein concentrations were determined by weight. Values obtained were corrected for contributions of the solvent.

2.2.9. *Electron Microscopy*

Negative staining of the preparations for electron microscopy was performed at room temperature (22° ± 1) using the droplet method, with 0.5% uranyl acetate (pH 4.2) or 0.5% uranyl oxalate (pH 6.4–6.7) as contrast medium according to MELLEMA et al. (1967). The droplet of the cold enzyme solution was left on a carbon coated grid for 30 sec – 1 min and non-adsorbed molecules were removed by blotting and washing with buffer or directly with several drops of the contrast medium; after about 1 min excess medium was carefully removed with filter paper and the stained protein film was dried in air.

Electron micrographs were taken at a magnification of 17,500 to 70,000 on 35 mm film with a Philips EM 300 or EM 200 electron microscope operating at 80 KV. The instrument was provided with an anti-contamination device cooled by liquid nitrogen. The double condensor lens system was used with apertures of 300 and 200 μ. The objective aperture was 50 or 40 μ.

Kodak fine grain positive release (F.R.P. 426) film was used and development was performed at 20° in Kodak HRP for 3–4 min.

Magnification calibration was performed with the aid of a grating replica having 21,600 lines/cm.

Molecular weights are calculated according to the following definitions (STACEY, 1956),

$$\text{number average mol.wt. } (M_n) = \Sigma m_i M_i/\Sigma m_i = \Sigma c_i/\Sigma(c_i/M_i)$$

$$\text{weight average mol.wt. } (M_w) = \Sigma m_i M_i^2/\Sigma m_i M_i = \Sigma c_i M_i/\Sigma c_i$$

$$\text{Z-average mol.wt. } (M_z) = \Sigma m_i M_i^3/\Sigma m_i M_i^2 = \Sigma c_i M_i^2/\Sigma c_i M_i$$

derived for a system of i components of weight concentration c_i(g/ml), of molar concentration m_i, and molecular weight M_i.

2.2.10. *Optical Rotatory Dispersion and Circular Dichroism*

Optical rotatory dispersion measurements were carried out with a Jasco automatic recording spectropolarimeter, Model ORD/UV-5, over the range

200–600 nm at a temperature of 25°, unless otherwise indicated. A path length of 1.0–10 mm was used and the enzyme concentrations were 0.03–2.5 mg/ml for the transhydrogenase and 0.5–2.0 mg/ml for lipoamide dehydrogenase. The mean residue rotation was calculated from the observed rotation, according to the relation:

$$[M']_\lambda = MRW \times \alpha_{obs}/cl$$

where $[M']_\lambda$ is mean residue rotation in degrees $cm^2 dmoles^{-1}$, α_{obs} is observed rotation of sample minus observed rotation of blank, l is pathlength of cell in decimeters, c is concentration of protein in grams per 100 ml, and MRW is mean residue molecular weight, which was assumed to be 115 (FASMAN, 1963).

Circular dichroic absorption curves were recorded on a Jouan Dichrograph II at 25° or 10°. The dichroic absorbance differences for left and right circularly polarized light of the samples are corrected for the dichroism of buffer and free coenzymes and are recalculated as mean residue ellipticities according to the relation:

$$[\theta]_\lambda = \Delta\varepsilon \times MRW \times 3300$$

where $\Delta\varepsilon$ is the dichroic absorbance difference, MRW is mean residue weight and $[\theta]_\lambda$ is mean residue molar ellipticity. The ellipticities are thus expressed in degrees cm^2 $dmoles^{-1}$.

2.2.11. *Photoreduction*

The photoreduction experiments in the presence of EDTA (25 mM) as electron donor were performed with Thunberg cuvettes or with the anaerobic titration assembly and the deoxygenation was accomplished as described under *Absorption spectrophotometry*. The illumination was performed with light from a stabilized 500 W Xenon lamp in a Zeiss spectrofluorimeter (Zeiss LX 501). A solution of $CuSO_4$ (40 g/l), $(NH_4)_2$ SO_4. $Fe_2(SO_4)_3$(2g/l) and concentrated H_2SO_4(1 ml/l) was used as a filter to exclude light below 390 nm. The cuvette was placed in a thermostated holder equipped with a magnetic stirrer to obtain homogeneous photoreduction. The rate of photoreduction was followed by recording the spectra at different times. The temperature was generally maintained between 12 and 16°.

2.2.12. *Recombination*

Recombination of transhydrogenase apoenzyme with FAD was performed in 0.1 M phosphate buffer (pH 7.5), containing 1 mM EDTA; that of lipoamide dehydrogenase in 0.03 M buffer (pH 7.4), containing 0.3 mM EDTA. Samples were withdrawn at the times and temperatures indicated. When the guanidine-HCl apoenzymes of lipoamide dehydrogenase were recombined with FAD, the incubation mixture also contained 0.1 M β-mercaptoethanol or dithiothreitol. Other experimental conditions are described in the text.

3. ISOLATION, PURIFICATION AND CHARACTERIZATION OF *AZOTOBACTER* TRANSHYDROGENASE

3.1. INTRODUCTION

In cell free extracts of *Azotobacter vinelandii* the presence of a reversible NAD^+-dependent NADPH-lipoate reductase was demonstrated (VAN DEN BROEK and VEEGER, 1968). This unusual, interesting activity could be separated in fractions with a coenzyme A-dependent pyruvate lipoate reductase, a reversible NAD^+-dependent NADH-lipoate reductase, a reversible NADH-$NADP^+$ transhydrogenase and a NADPH-$Fe(CN)_6^{3-}$-diaphorase activity.
The possibility that the transhydrogenase in combination with the pyruvate dehydrogenase complex, could be directly involved in the regulation of transfer of reducing equivalents from pyruvate to either N_2 or O_2 (MORTENSON et al., 1963) led us to investigate the pyridine nucleotide transhydrogenase, the pyruvate dehydrogenase complex and the lipoamide dehydrogenase. These studies will mainly deal with the transhydrogenase.

Pyridine nucleotide transhydrogenases are widespread in nature and have been identified and partially purified from several different organisms, e.g. *Pseudomonas fluorescens* (COLOWICK et al., 1952; COHEN, 1967; COHEN and KAPLAN, 1970), animal tissue mitochondria (KAPLAN et al., 1953), *Azotobacter vinelandii* (VAN DEN BROEK and VEEGER, 1968, 1970; LOUIE and KAPLAN, 1970a; CHUNG, 1970), *Chromatium* (KEISTER and HEMMES, 1966) and *Spinacea oleracea* (KEISTER et al., 1960, 1962). The spinach transhydrogenase was identical with the spinach NADPH-diaphorase, ferredoxin-$NADP^+$ reductase and NADPH cytochrome *f* reductase as shown by ZANETTI and FORTI (1966) and SHIN et al., (1963). DANIELSON and ERNSTER (1963) reported about another type of transhydrogenase from submitochondrial particles, which catalyzed the reduction of $NADP^+$ by NADH only in the presence of a high energy intermediate of oxidative phosphorylation or in the presence of ATP. In recent studies it was suggested (RYDSTRÖM et al., 1970) that the energy-linked transhydrogenase reaction does not involve energized forms of nicotinamide nucleotides, but that an energy-linked alteration of the transhydrogenase molecule itself is involved. The occurrence of similar enzymes in the chromatophores of *Rhodospirillum rubrum* (KEISTER and YIKE, 1966; KEISTER, 1966) and in *Rhodopseudomonas spheroides* (ORLANDO et al., 1966) was demonstrated.

Recently (ORLANDO, 1970) the involvement of disulfides, like thiols and reduced thiotic acid, in the energy-linked photoreduction was explained in terms of an unmasking or activation of membrane-bound transhydrogenase.

The similarity of the *Pseudomonas* transhydrogenase to the *Azotobacter* enzyme was already indicated by KAPLAN et al. (1953) and later by other studies confirmed (VAN DEN BROEK and VEEGER, 1970; LOUIE and KAPLAN, 1970a). The differences were thought to be centered around the effects of 2'

AMP, NAD(P)H and $NADP^+$. COHEN (COHEN, 1967; COHEN and KAPLAN, 1970) investigated thoroughly the *Pseudomonas* enzyme and the effect of 2' AMP on the rate of the reaction in which NADH was involved. Recently, whilst this study was in progress, CHUNG (1970) reported about the effects of 2'AMP with the *Azotobacter* transhydrogenase.

In this paper a method is described for obtaining a highly purified enzyme from *Azotobacter vinelandii* and some of the properties are given. Preliminary data of this study have been published (VAN DEN BROEK and VEEGER, 1968, 1970).

3.2. RESULTS

3.2.1. *Distribution of the Azotobacter transhydrogenase*

The results of TABLE 3.1 show how the transhydrogenase activity, the overall pyruvate dehydrogenase activity, the lipoamide dehydrogenase activity and the NADPH-$Fe(CN)_6^{3-}$-diaphorase activities are distributed between the various cell fractions.

The fractions were separated by differential centrifugation at low and high speed (TISSIÈRES et al., 1957; JONES and REDFEARN, 1966)

1. crude extract after ultrasonic disintegration and 10 min 15,000 × *g*,
2. large particles, 30 min 35,000 × *g*,
3. supernatant, 2/3 of the toplayer after centrifugation for 90 min at 150,000 × *g*,
4. fluffy layer, rest of liquid from tube after high speed centrifugation,
5. small particles, homogenized sediment after 90 min 150,000 × *g*.

The fluffy layer and the small particles have both the highest specific activity, whereas in the larger particles there is none. The activities are probably either associated with the small and very small particles, or are coupled to proteins of high molecular weight. Upon performing the first purification steps on the fluffy layer and the small particles the same specific activities with respect to transhydrogenase, pyruvate dehydrogenase complex and NADPH-$Fe(CN)_6^{3-}$ diaphorase were obtained. Because of the fact hardly any purification in terms of specific activity of the transhydrogenase was obtained from this procedure, the crude extract without most of the large particles was used as the source of enzyme upon isolation and purification of the transhydrogenase.

3.2.2. *Growth of Azotobacter vinelandii*

Large scale production of *Azotobacter vinelandii* (ATCC 478) was kindly performed by Royal Yeast and Fermentation Industries, Delft, The Netherlands.

A. vinelandii cells were grown aerobically at 30° on a nitrogen free medium according to PANDIT-HOVENKAMP (1966). 2400 litres of growth medium were inoculated with a 2.5% inoculum and cells were grown for 22 hours under mixing (240 rpm) and aerating (0.2 m^3 air/m^2). Because of foam formation the oxygen pressure had to be decreased occasionally. After 22 hours the cell

TABLE 3.1. Distribution of transhydrogenase, pyruvate dehydrogenase complex, lipoamide dehydrogenase and NADPH-$Fe(CN)_6^{3-}$ diaphorase between cell fractions of *Azotobacter vinelandii*. Fractions obtained as described in the text. Activities measured as described in CHAPTER 2 and expressed as relative activities.

Fraction	Protein Total (%)	Transhydrogenase		Pyr. dehydr. complex		Lipoamide dehydr.		NADPH-$Fe(CN)_6^{3-}$ diaphorase	
		Specific activity	Total activity (%)	Specific activity	Total activity (%)	Specific activity	Total activity (%)	Specific activity	Total activity (%)
Crude extract	100	1	100	1	100	1	100	1	100
Large particles	15	0.2	4	0.6	15	0.4	8	0.1	2
Supernatant	14	0.6	10	0.6	14	0.5	5	1.0	18
Fluffy layer	51	1.8	73	1.5	50	1.6	60	1.4	62
Small particles	20	1.2	17	1.2	20	1.9	30	1.4	20

suspension was cooled to 14° and the cells were harvested in a Westfalia centrifuge at a speed of 300 l per hour. The harvested cells, 7.1 g wet weight per litre of growth medium, were washed in 0.05 M potassium phosphate buffer (pH 7.5) containing 0.5 mM EDTA and stored until used at −20° as a cell paste.

3.2.3. *Isolation and purification of Azotobacter transhydrogenase*

Step 1: Preparation of cell free extracts.

Batches of 500 g (wet weight) frozen cell paste were thawed, washed several times in buffer and in portions of 10 ml per 2 g cells sonically treated for 3 periods of 2 minutes with a 100 Watt Ultrasonic Disintegrator, MSE, London, at 0–4°. The sonically treated cell suspension was centrifuged at 35,000 × *g* in a MSE 18 rotor for 10 min. The resulting supernatant, defined as cell free extract, was used as the source of enzyme. All further steps were performed at 4°, unless otherwise stated.

Step 2: Heat treatment.

The cell free extract was stirred for 24–36 hours with 2% *(w/v)* ammonium sulfate. 5 vol% of 96% ethanol were slowly added to the suspension and stirring was continued for another 30 min. The suspension was then heated to 42° in a waterbath and held at that temperature for 15 min with gentle agitation. The heated solution was rapidly cooled in an ice bath to about 10° and the denaturated protein was removed by centrifugation at 20,000 × *g* for 30 min.

Step 3: First ammonium sulfate fractionation.

To the supernatant obtained in the previous step was added 1/15 volume of di-potassium hydrogen-ortho-phosphate, 0.3 M, for buffering purposes. Solid ammonium sulfate was added to given 30% of saturation. The preparation was allowed to stand for one hour and centrifuged at 20,000 × *g* for 20 min. The precipitate was discarded and the supernatant was brought to 50% of saturation by the slow addition of solid ammonium sulfate. After standing for one hour the suspension was centrifuged again at 20,000 × *g* for 20 min. The supernatant was saved for the isolation of lipoamide dehydrogenase. The whitish precipitate was suspended in 0.05 M phosphate buffer (pH 7.5) containing 0.5 mM EDTA and dialyzed overnight against two times of 3 l of the same buffer. At this stage the preparations could be stored at −20° without any loss of activity.

Step 4: Calcium phosphate gel fractionation.

The dialyzed enzyme fraction obtained in the previous step was diluted with 0.05 M phosphate buffer (pH 7.5), containing 0.5 mM EDTA to a protein concentration of about 10 mg/ml. Calcium phosphate gel in bidistilled water was added to this protein solution at a gel-to-protein-ratio of 0.5–1. After an equilibration period of 10 min the gel was collected by centrifugation at 2,500 × *g* for 10 min and a second batch of calcium phosphate gel was added to the protein solution. This procedure was repeated untill all transhydrogenase activity had disappeared from the supernatant. On the average 8–10 additions of calcium phosphate gel were necessary to adsorb all enzyme activity, most of

the transhydrogenase activity was adsorbed by the last 3 or 4 gel additions. Most of the pyruvate dehydrogenase activity was adsorbed by the preceding gels. The gels which had adsorbed most of the transhydrogenase activity were washed several times with 0.03 M potassium phosphate buffer (pH 7.5) containing 0.5 mM EDTA. The transhydrogenase activity was eluted from the gel with 0.1 M potassium phosphate buffer (pH 7.5), containing EDTA. The elution was repeated three or four times. The eluates with a specific activity of 25 and higher were pooled.

Step 5: Second ammonium sulfate fractionation.

The combined 0.1 M phosphate buffer eluates from the previous step were brought to 25% of saturation by adding solid ammonium sulfate. After standing for an hour the suspension was centrifuged at 20,000 × *g* for 20 min. Sometimes a greenish precipitate was formed, which could only be solubilized in 0.1 M potassium phosphate buffer (pH 7.5), containing 1 mM EDTA and 1 mM $NADP^+$ and in the case of reasonable activity purified separately. This fraction was dialyzed against 0.1 M phosphate buffer (pH 7.5) containing 1 mM EDTA. Solid ammonium sulfate was added to the supernatant to give 50% of saturation. After standing for one hour the suspension was centrifuged and the precipitate redissolved in 0.1 M phosphate buffer (pH 7.5), containing 1 mM EDTA.

Step 6: First differential centrifugation.

The enzyme fraction obtained in the previous step was dialyzed for 24–48 hours against the same buffer and any insoluble material was removed by centrifugation. The protein solution was centrifuged in the MSE preparative ultracentrifuge No. 50, with an angle rotor, at 200,000 × *g* for 45 min. The supernatant, with only about 10–15% of the activity, was decanted and the yellow-green sediment was homogenized in a POTTER-ELVEHJEM in a small volume of 0.1 M phosphate buffer (pH 7.5) containing 1 mM EDTA and 1 mM $NADP^+$. The dissolved material was centrifuged at 10,000 × *g* for 5–10 min to remove insoluble material. This insoluble material had to be homogenized a second time in the same buffer, containing EDTA and $NADP^+$.

Step 7: Second differential centrifugation.

The soluble enzyme fractions obtained in the previous step were centrifuged again at 200,000 × *g*. The brownish-green sediment obtained after centrifugation for 10 min was dissolved in 0.1 M phosphate buffer (pH 7.5), containing 1 mM EDTA and saved for experiments not requiring pure enzyme. The second yellow-green sediment obtained after centrifugation for 45 min at 200,000 × *g* could be easily solubilized in phosphate buffer without addition of $NADP^+$. The solubilized enzyme fraction was dialyzed for 36–48 hours against the same buffer and stored at 4°.

The whole purification procedure is summarized in TABLE 3.2.

In the earlier stages of this study (VAN DEN BROEK and VEEGER, 1968, 1970) a DEAE-cellulose chromatography step preceeded the differential centrifugation at 200,000 × *g*. For several reasons this step was omitted at later stages.

TABLE 3.2. Summary of purification of *Azotobacter* transhydrogenase

Steps of purification	Total volume (ml)	Total Protein (mg)	Total activity (units)	Specific activity (units/mg protein)	Yield (%)	Accumulative purification (-fold)
1	8000	265,000	87,000	0.3	100	1
2	6500	72,000	94,000	1.3	108	4
3	500	27,000	83,000	3.1	95	9
4	1500	1,500	43,000	29	49	88
5	45	880	26,600	30	30	92
6	30	150	16,600	111	19	340
7	20	60	13,300	220–260	15	650–800

The calcium phosphate gel eluates, characterised by the presence of a reversible NAD$^+$-dependent NADPH-lipoate reductase could be separated in several enzyme fractions upon chromatography on DEAE-cellulose. As shown in FIG. 3.1, A the NADPH lipoate reductase can be separated into a NAD$^+$-dependent lipoamide dehydrogenase, a CoA-dependent pyruvate lipoate reductase, a NADPH-ferricyanide reductase and a reversible NADH-NADP$^+$

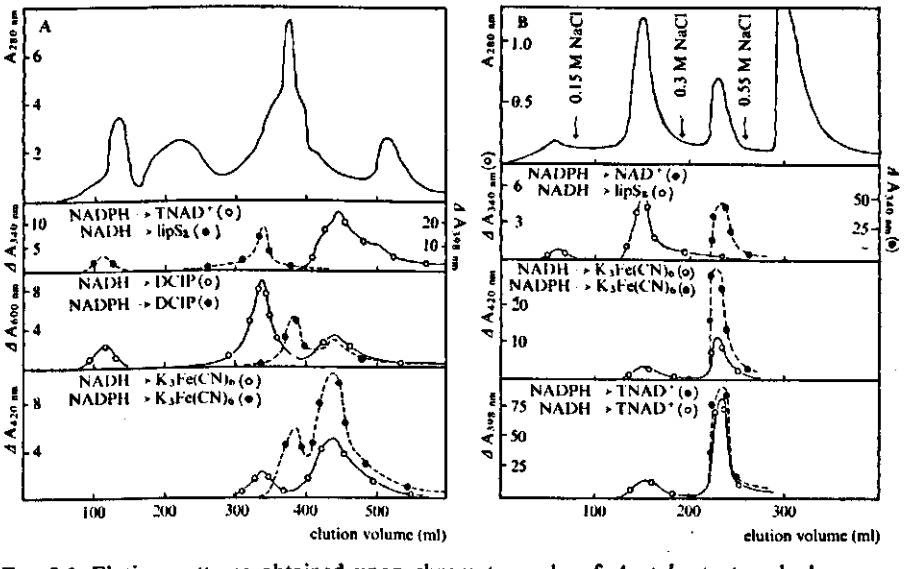

FIG. 3.1. Elution patterns obtained upon chromatography of *Azotobacter* transhydrogenase on DEAE-cellulose. Impure enzyme fractions were applied to a 2 × 40 cm DEAE-cellulose column. A. Continuous elution with a NaCl-gradient from 0–0.75 M NaCl in 0.03 M potassium phosphate buffer (pH 7.5), containing 0.5 mM EDTA. B. Discontinuous elution with NaCl in phosphate buffer; concentrations as indicated. Fractions were collected and monitored for absorbancy at 280 nm and the transhydrogenase (NADPH → NAD$^+$, NADPH → TNAD$^+$, NADH → TNAD$^+$), lipoate reductase (NADH → lip S_2) and diaphorase (NAD(P)H → $K_3Fe(CN)_6$, NAD(P)H → DCIP) activities were measured. Activities are expressed as absorbance change/min/ml column eluate.

transhydrogenase upon continuous elution of the DEAE-cellulose column with a sodium chloride gradient in 0.03 M potassium phosphate buffer (pH 7.5). This procedure, however, always resulted in low recoveries of transhydrogenase in terms of total units and small purification in terms of specific activity. 0.1 M β-mercaptoethanol did not markedly stabilize the transhydrogenase as was observed for the *Pseudomonas* enzyme (COHEN, 1967; COHEN and KAPLAN, 1970).

Better results were obtained upon discontinuous elution of the DEAE-cellulose columns with sodium chloride in 0.05 M phosphate buffer (pH 7.5). FIG. 3.1, B shows a typical elution pattern and the distribution of the activities upon chromatography of a calcium phosphate gel eluate on DEAE-cellulose. However upon removing the different activities the transhydrogenase tends to aggregate. Especially in the case when preparations with a relative high specific transhydrogenase activity (> 25 units/mg protein) and a low pyruvate dehydrogenase content were subjected to DEAE-cellulose chromatography a large loss of enzyme activity, up to 70–80%, occurred. Losses of transhydrogenase activity were even higher if elution with NaCl concentrations between 0.15 and 0.3 M preceeded that with 0.3 M NaCl. Upon raising the NaCl-concentration and the pH only a small fraction of the activity could be eluted, the rest stuck irreversibly to the top of the column. The activity which came off the column could be easily purified by differential centrifugation; the total recovery, however, was in the order of 5%.

The DEAE-cellulose chromatography step could not be replaced by column chromatography on QAE-Sephadex, hydroxyl apatite, carboxymethylcellulose, carboxymethyl-Sephadex, DEAE-Sephadex, Sephadex G-200, Sepharose 2 B, or Sepharose 4 B.

If the calcium phosphate gel eluates, after ammonium sulfate fractionation and dialysis, were directly subjected to differential centrifugation the purification was sometimes complicated by the contaminating pyruvate dehydrogenase overall activity. Because of its high molecular weight (WILLMS et al., 1967) the pyruvate dehydrogenase complex also sediments slowly at these g values. The latter solubilised sediments showed upon standing at 4° a typical association behaviour, which will be dealt with in the electron microscopic studies (CHAPTER 4).

3.2.4. *Reactions catalyzed*

The purified transhydrogenase catalyzes the transfer of hydrogen from NADPH to NAD^+, thio-NAD^+ and thio-$NADP^+$ and from NADH to $NADP^+$, thio-NAD^+ and thio-$NADP^+$; 3-Acetylpyridine-NAD^+ and pyridine-NAD^+ are not reduced. The transhydrogenase is also able to reduce 2,6-dichlorophenol indophenol and potassiumferricyanide with both NADH and NADPH. As measured under identical conditions the activities with NADPH are higher than with NADH. TABLE 3.3 summarizes the different activities for a highly purified transhydrogenase preparation; the velocities given are not the maximum velocities. As will be shown in our kinetic studies, (CHAPTER 6), the maximum

TABLE 3.3. Comparison of the reactions catalyzed by the purified *Azotobacter* transhydrogenase. The transhydrogenase activities were assayed at 25° in 0.05 M Tris-HCl buffer (pH 7.5), the diaphorase activities in 0.05 M potassium phosphate buffer (pH 7.2) at the concentrations of donor and acceptor as indicated in the TABLE. Activities expressed as μmoles NAD(P)H oxidized per min per mg protein, assuming molar extinction coefficients for TNAD(P)H, NAD(P)H, $K_3Fe(CN)_6$ and DCIP of $\varepsilon_{398} = 11{,}300\ M^{-1}cm^{-1}$, $\varepsilon_{340} = 6{,}220\ M^{-1}cm^{-1}$, $\varepsilon_{420} = 1{,}030\ M^{-1}cm^{-1}$, $\varepsilon_{600} = 20{,}000\ M^{-1}cm^{-1}$, respectively.

Reaction catalyzed	Concentration of donor (μM)	Concentration of acceptor (μM)	Activity (μmoles/min/mg protein)
Transhydrogenase reactions			
NADPH → $TNAD^+$	100	50	240
NADPH → $TNADP^+$	100	50	150
NADPH → NAD^+	100	400	300
NADH → $TNAD^+$	100	50	190
NADH → $TNADP^+$	100	50	140
NADH → $NADP^+$	100	50	60
Diaphorase activities			
NADPH → $K_3Fe(CN)_6$	100	800	580
NADPH → DCIP	100	40	30
NADH → $K_3Fe(CN)_6$	100	800	300
NADH → DCIP	100	40	32

velocities are strongly dependent on both substrate concentrations.

The reduction of all mentioned nucleotides, except $NADP^+$, proceeds very quickly. The reduction of $NADP^+$ by NADH is rather slow with respect to the reverse reaction. About five to ten times more enzyme is needed to obtain the same rate of conversion. The activity curves observed for the $NADP^+$ re-

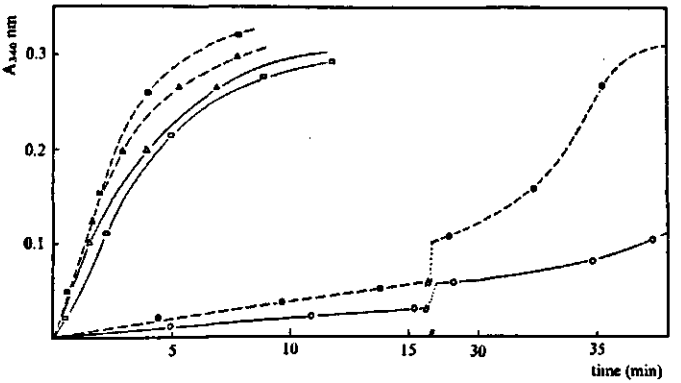

FIG. 3.2. Effect of NADPH and $MgCl_2$ on the reduction of $NADP^+$ by NADH, as catalyzed by an impure enzyme preparation. Time course of the change in absorbance at 340 nm. Reaction mixture as described in CHAPTER 2. [$NADP^+$], 50 μM; [NADH], 50 μM.
Full and dotted lines are without and with $MgCl_2$ (2 mM), respectively. (○, ●), no NADPH; (□, ■), 30 μM NADPH; (△, ▲), 60 μM NADPH.

duction strongly depend on the purity of the enzyme in contrast to the curves obtained for the other reactions. In the cell free extract and in the heat extract the $NADP^+$-reduction is not detectable, besides, upon addition of these extracts to purer preparations the $NADP^+$-reduction is totally inhibited. This is not due to an NADPH oxidase in these fractions. With partly purified preparations the $NADP^+$-reduction is very sluggish in the absence of $MgCl_2$ and NADPH. As shown in FIG. 3.2 a lag period in the activity curve is observed. Upon the addition of the product, NADPH, the lag period shortens and finally disappears; the length of the lag period depends on the ratio $NADPH/NADP^+$. In the presence of 2–4 mM $MgCl_2$ the lag period is much shorter, the rate of the reaction is higher and smaller amounts of NADPH are needed to overcome the lag period. The length of the lag period in both cases also depends on the concentration of NADH, the higher the NADH concentration the higher that of NADPH needed. $MgCl_2$ has no stimulating effect on the other reactions catalyzed.

With highly purified transhydrogenase preparations the lag period in the activity curve is less pronounced and depends on the enzyme concentration. NADPH has only a clear activating effect at higher $NADP^+$ concentrations, but as soon as the ratio $NADPH/NADP^+ \geqslant 0.5$–1.0, inhibition is observed. In the presence of 2–4 mM $MgCl_2$ the rate of the $NADP^+$ reduction is higher than in its absence but the degree of activation depends both on the concentration of $NADP^+$ and NADPH.

In contrast to the observations for the *Pseudomonas* (COHEN, 1967; COHEN and KAPLAN, 1970) and *Azotobacter* (LOUIE and KAPLAN, 1970a; CHUNG, 1970) transhydrogenases we find that the reactions with NADH as hydrogen donor

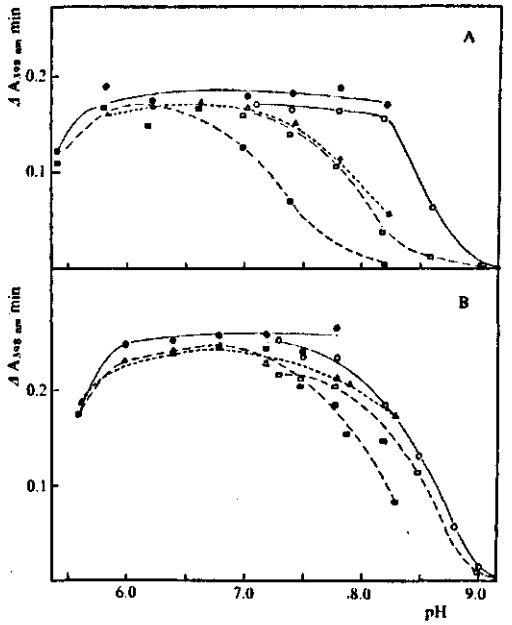

FIG. 3.3. Effect of pH, buffer and 2'AMP on the reduction of $TNAD^+$ and $TNADP^+$ by NADH and NADPH. Conditions as described in CHAPTER 2; [buffer], 0.05 M; [2'AMP], 0.4 mM. Velocity expressed as initial absorbance change at 398 nm per min. A. $TNAD^+$ reduction; B. $TNADP^+$ reduction. Donor NADPH: o —— o, Tris-HCl buffer with and without 2'AMP; • —— •, potassium phosphate buffer, with and without 2'AMP. Donor NADH: □ — — □, Tris-HCl buffer with and without 2'AMP; ■ — — ■, phosphate buffer without 2'AMP; △ ---- △, phosphate buffer with 2'AMP.

are, as measured under our standard conditions, hardly influenced by 2'AMP. By changing the pH and the buffer, however, a clear effect can be observed. FIG. 3.3 shows the effects of buffer, pH and 2'AMP on the reduction of thio-NAD^+ and thio-$NADP^+$ by NADPH and NADH. As can be seen the effect of 2'AMP on the reactions with NADPH is negligible both in Tris-HCl buffer and in phosphate buffer at all pH values. The reduction of thio-NAD^+ by NADH, however, is strongly buffer and pH dependent. In Tris-HCl buffer 2'AMP has no effect, but in potassium phosphate buffer 2'AMP shifts the pH-curve to that obtained for Tris-HCl. Similar effects are observed for the NAD(P)H $\rightarrow$ TNADP$^+$ reactions; the effects, however, are much less pronounced.

All reactions are also influenced by the concentrations of the buffer used. In Tris-HCl, potassium phosphate and pyrophosphate buffer the reaction rates decrease when the buffer concentration exceeds 0.05 M; EDTA, at a concentration of 1 mM, has a slight activating effect at very low buffer concentrations.

3.2.5. *Stability of the enzyme*

The isolated transhydrogenase is stable at 4° in 0.1 M potassium phosphate buffer (pH 7.5) containing 1 mM EDTA; stored under these conditons at protein concentrations of 0.5 mg/ml or higher, practically no loss of activity is observed for several months. Storage at −20° leads to a partly insoluble enzyme due to aggregation of the enzyme at high protein concentration. Such an effect does not occur with less pure preparations.

Dilution of the enzyme to protein concentrations $\leqslant$ 0.01 mg/ml does not lead to significant inactivation of the transhydrogenase in a period of 12 hours. The diluted protein solution is stabilized by 0.2% bovine serum albumin and 1 mM EDTA over a longer period of time; this stabilization effect is more pronounced in 0.1 M potassium phosphate buffer (pH 7.5) than in 0.1 M Tris-HCl (pH 7.5). In contrast to the *Pseudomonas* transhydrogenase (COHEN, 1967; COHEN and KAPLAN, 1970) neither β-mercaptoethanol nor dithiothreitol is needed for stabilization.

The *Azotobacter* transhydrogenase is more heat stable than the *Pseudomonas* transhydrogenase. Heating for one hour at 50° in 0.1 M phosphate buffer (pH 7.5), containing 1 mM EDTA at a protein concentration of either 1.5 mg/ml or 0.015 mg/ml does not lead to a significant loss of activity. However, temperatures higher than 65° lead to denaturation of the protein and result in a complete loss of activity within 15 minutes. Addition of FAD largely protects the enzyme against inactivation under these conditions. FIG. 3.4 shows the effect of NADH and NADPH on the activity upon incubating the enzyme at 50° and the effect of FAD, FMN and $NADP^+$ on the inactivation. As can be seen from the figure in the presence of one or both reducing substrates the inactivation at 50° is dramatically accelerated, the activity declines very quickly to a lower level and remains more or less constant. The rate of inactivation and the final level obtained depends on the concentration of reducing substrate

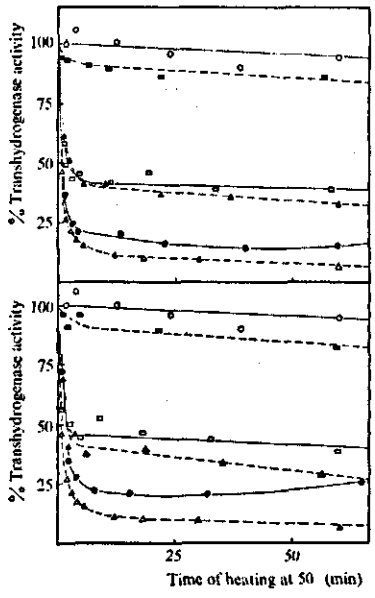

FIG. 3.4. Effect of heating at 50° on *Azotobacter* transhydrogenase. Transhydrogenase (0.02–0.1 mg) in a volume of 2 ml 0.1 M phosphate buffer (pH 7.5), containing 1 mM EDTA incubated at 50° in the presence or absence of different nucleotides. At the times indicated aliquots were removed and assayed in the NADPH → TNAD⁺ standard assay system at 25°. A. Effect of NADH: ○ —— ○, no additions; ● —— ●, 100 μM NADH; □ —— □, 100 μM NADH + 100 μM FMN; ■ —— ■, 100 μM NADH + 100 μM FAD; △ —— △, 100 μM NADH + 100 μM NADPH; ▲ —— ▲, 100 μM NADH + 100 μM NADP⁺. B. Effect of NADPH. The same as under A, but NADH to be replaced by NADPH.

used. At lower temperatures (35–40°) after an initial inactivation some reactivation occurs upon prolonged storage at these temperatures. $NADP^+$ and FMN give partial protection against heating at 50°. FAD, however, provides almost full protection. After inactivation by heat treatment in the presence of reducing substrate the original activity cannot be restored by the addition of FAD as was observed with the *Pseudomonas* enzyme; neither do FMN + FAD nor riboflavin. In the presence of β-mercaptoethanol the activity can partly be restored (TABLE 3.5). Addition of reducing substrates at 0° has no effect on the activity.

Incubation of the enzyme at 25° with deoxycholate at concentrations higher than 0.1% results in a rapid loss of activity; the enzyme is, however, resistent to 1% digitonin.

In the presence of low concentrations of ureum the activity drops very slowly, both at 0° and 25°. In 4 M ureum a 50% decline in activity is observed after about 5–6 hours. In 8 M ureum, however, 50% of the activity is irreversible lost within 5 minutes.

3.2.6. *Spectral characteristics*

FIG. 3.5 presents the absorption spectra of the transhydrogenase before and after dialysis. As isolated by solubilization of the high speed sediment in the presence of $NADP^+$ the transhydrogenase has maxima in its spectrum at 267 nm, 355–370 nm and 438 nm, minima at 320 nm and 398 nm, while shoulders are present at 420 nm and 464 nm. Especially the shoulder at 464 nm is a pronounced one. The absorbance ratios for the different maxima are A_{280}/

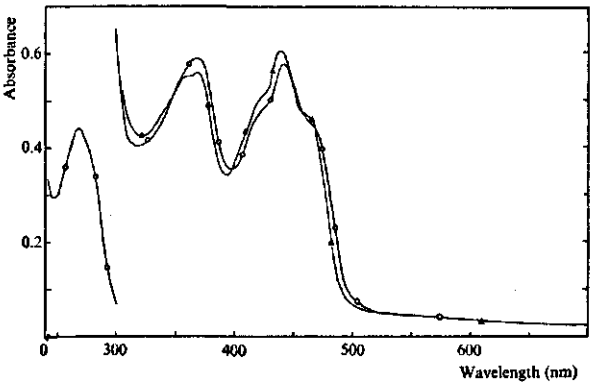

FIG. 3.5. Absorption spectra of *Azotobacter* transhydrogenase before and after dialysis. 2.6 mg of protein per ml in 0.1 M potassium phosphate buffer (pH 7.5), containing 1 mM EDTA. Enzyme spectra recorded versus buffer. ▲ —— ▲, transhydrogenase after solubilisation in the presence of $NADP^+$; o —— o, after dialysis for 48 hours. The U.V. spectrum of the dialyzed preparation was recorded in a tenfold diluted protein solution.

$A_{438} = 8.67$ and $A_{370}/A_{438} = 0.93$. Upon dialysis the spectrum shifts to the red. The shoulder at 464 nm is much less pronounced and maxima are present at 269 nm, 368 nm and 442 nm, minima at 316 nm and 397 nm. The absorbance ratios for the different maxima are $A_{280}/A_{442} = 6.51$, $A_{368}/A_{442} = 1.05$. As will be shown (CHAPTER 5) a spectral shift to the blue can be induced by the addition of $NADP^+$ to the $NADP^+$ free enzyme. Sometimes dialysis only was not sufficient to remove bound $NADP^+$ as concluded from the shift in the spectrum; anaerobic dialysis in the presence of glucose-6-phosphate and traces of glucose-6-phosphate dehydrogenase in the dialysis bag resulted in complete removal of all $NADP^+$ bound to the enzyme.

Extinction coefficients for the oxidized, dialyzed enzyme were calculated according to the method described by MAYHEW et al. (1969) for flavodoxin. The flavin was released from the protein by heating samples in sealed vials protected from light in a boiling waterbath. After removing the precipitate by centrifugation the changes in absorbance at 450 nm and 457 nm are measured. As FIG. 3.6 shows the flavin is already completely released from the transhydrogenase during 15 min of heat; decreases in absorbance at prolonged heating indicate some destruction of the flavin under these conditions. From extrapolation of the data to zero time an extinction coefficient of 11,900 $M^{-1}cm^{-1}$ at 450 nm and of 10,900 $M^{-1}cm^{-1}$ at 457 nm can be calculated for the protein bound flavin. These values have been used for the calculation of the extinction coefficients at other wavelengths. The extinction coefficients for the oxidized enzyme preparation are $\varepsilon_{270} = 104{,}000\ M^{-1}cm^{-1}$, $\varepsilon_{370} = 13{,}000\ M^{-1}cm^{-1}$, $\varepsilon_{440} = 12{,}900\ M^{-1}cm^{-1}$ and $\varepsilon_{450} = 11{,}900\ M^{-1}cm^{-1}$. In the presence of $NADP^+$ the following values were obtained, $\varepsilon_{270} = 128{,}000\ M^{-1}cm^{-1}$, $\varepsilon_{370} = 12{,}100\ M^{-1}cm^{-1}$, $\varepsilon_{440} = 13{,}300\ M^{-1}cm^{-1}$ and $\varepsilon_{450} = 11{,}000\ M^{-1}cm^{-1}$.

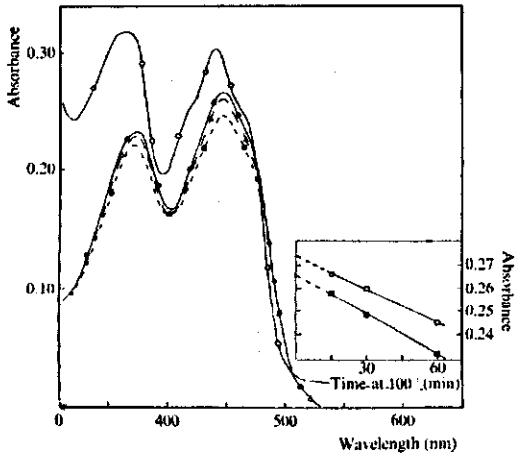

FIG. 3.6. Spectrum of oxidized transhydrogenase (1.5 mg protein/ml) and the released protein-bound flavin upon heating at 100°. Samples in 0.1 M potassium phosphate buffer (pH 7.5), containing 1 mM EDTA. The precipitates were removed by centrigugation. o —— o, untreated transhydrogenase; • —— •, released flavin after 15 min heating; △ —— △, released flavin after 30 min heating; ■ —— ■, released flavin after 60 min heating. Insert: plot for determination of extinction coefficient of protein-bound flavin at 450 nm (□ —— □) and 457 nm (■ —— ■).

As will be shown later (CHAPTER 5) the transhydrogenase can be chemically reduced by either NADH, NADPH or dithionite and photochemically by illumination in the presence of EDTA; $NADP^+$ has a marked influence on both types of reductions.

3.2.7. *Flavin content and minimum molecular weight*

The flavin prosthetic group of *Azotobacter* transhydrogenase dissociates from the apoprotein by heat treatment at 100° or by treatment with 5% trichloracetic acid at 0°. As FIG. 3.6 shows the dissociated flavin is characterized by absorption maxima at 260 nm, 375 nm and 448 nm and minima at 310 nm and 403 nm, with an absorbance ratio of $A_{450}/A_{375} = 1.10$ (cf. FAD released from *Azotobacter* lipoamide dehydrogenase, $A_{450}/A_{375} = 1.13$ and pure FAD, $A_{450}/A_{375} = 1.23$). The flavin was identified by thin layer chromatography in three solvent systems according to KILGOUR et al. (1957). In 5% di-sodium phosphate and *tert.* butylalcohol-water the transhydrogenase flavin behaved identical with authentic FAD and with the dissociated flavin from *Azotobacter* lipoamide dehydrogenase. When butanol-acetic acid - water (4:3:3) was used as solvent system the results did not provide conclusive evidence. The R_f-value of the main component was always between those for FAD and FMN in contrast to the dissociated flavin from lipoamide dehydrogenase; furthermore always more FMN seemed to be present in the extracts from the transhydrogenase than in extracts from free FAD or *Azotobacter* lipoamide dehydrogenase treated in a similar way.

Upon incubation of the dissociated flavin from the transhydrogenase with apoenzyme of lipoamide dehydrogenase from *Azotobacter*, prepared according to KALSE and VEEGER (1968), partial restoration of the lipoate activity was

TABLE 3.4. Extent of restoration of lipoamide dehydrogenase activity upon incubation of *Azotobacter* lipoamide dehydrogenase apoprotein with the dissociated flavins from *Azotobacter* transhydrogenase and lipoamide dehydrogenase. Controls were FAD treated at 100° for the same time and excess FAD (2×10^{-4} M). Solution contained 0.075 M potassium phosphate buffer (pH 7.5), 0.3 mM EDTA, 16 μM flavin in the case of the heated samples and apoprotein (4.3 μM in exp. I and 3.2 μM in exp. II). Mixtures were incubated at 25° for 60 min and lipoate activities measured as described in CHAPTER 2. Activities are expressed as % of the original lipoate activity.

Exp.	Flavin	% lipoate activity
I	30 min heat extract transhydrogenase	56
	30 min heat extract lipoamide dehydrogenase	83
	30 min heat extract FAD	51
	2×10^{-4} M FAD	44
II	15 min heat extract transhydrogenase	48
	15 min heat extract lipoamide dehydrogenase	65
	15 min heat extract FAD	38
	2×10^{-4} M FAD	33

obtained. TABLE 3.4 summarizes the results of incubation of the heated extracts with apoenzyme of lipoamide dehydrogenase. As can be seen, the extent of restoration of the lipoamide dehydrogenase activity with the dissociated flavin from transhydrogenase is in the same order of magnitude as for the heated FAD. It is therefore surprising that the dissociated flavin from lipoamide dehydrogenase shows a higher ability to recombine with the apoenzyme.

The FAD-like character of the flavin from transhydrogenase is underlined, as will be shown later, by the ability of FAD to recombine with the apoenzyme of transhydrogenase while FMN and riboflavin cannot restore the enzymatic activity. In addition only FAD, and not FMN or riboflavin, can fully protect the transhydrogenase from inactivation at higher temperatures (FIG. 3.4); FMN only protects slightly, while riboflavin does not protect at all.

On the basis of a molar extinction coefficient of 10,900 $M^{-1}cm^{-1}$ at 457 nm for the enzyme-bound flavin a flavin content of 1.15–1.35% for five purified enzyme preparations could be calculated, equivalent to a minimum molecular weight of 58,000–68,000 daltons. This value is in good agreement with those obtained for several other flavoproteins.

3.2.8. *Preparation of the apoenzyme and recombination with FAD*

The preparation of the apoenzyme of the *Azotobacter* transhydrogenase has been performed according to the different methods normally used in flavoprotein chemistry. Depending on the method used the remaining activity, the percentage of denaturation and the ability to recombine with FAD may vary enormously. TABLE 3.5 summarizes the results obtained upon recombining the apoenzyme, prepared according to the different methods, with FAD.

TABLE 3.5. Preparation of the *Azotobacter* apoenzyme according to different methods and recombination with FAD. Enzyme (0.1 mg) in 0.1 M potassium phosphate buffer (pH 7.5), containing 1 mM EDTA were treated as indicated. The acid ammonium sulfate precipitates were dissolved in 0.3 M phosphate buffer (pH 7.5) and diluted with 0.03 M buffer to the original volume. The apoenzyme was incubated at 25° for 60–120 min in 0.1 M phosphate buffer (pH 7.5), containing 1 mM EDTA, 2 mM FAD and 0.1 M β-mercaptoethanol where indicated and transhydrogenase activities were measured. Activities are expressed as % of the original activity in the standard assay system.

Treatment	Exp. No.	Remaining activity after treatment (%)	Maximal restored activity upon recombination with FAD	
			+β-mercapto-ethanol	−β-mercapto-ethanol
Acid ammonium sulfate according to KALSE and VEEGER (1968)	I	3	10	7
	II	6	34	22
	III	14	29	22
	IV	30	60	46
Acid ammonium sulfate according to WARBURG (1938)	I	34	60	47
at pH 3.3	II	8	41	24
at pH 3.0	III	14	50	28
	IV	13	47	28
Dialysis against 60% ammonium sulfate at pH 2.5 for 5 hours followed by dialysis against 0.1 M phosphate buffer pH 7.5		36	65	not tested
Ditto, in the presence of 2 mM NADPH under anaerobic conditions		23	45	not tested
Dialysis against 1.5 M Guanidine-HCl at pH 7.5 for 12 hours acc. to BRADY and BEYCHOK (1969)		0	0	0
Heating at 50° for 6–90 min in the presence of 200 μM NADPH		23	38	21
Heating at 50° for 6–90 min in the presence of 200 μM NADH		13	24	15

The best (but still poor) results were obtained when the apoenzyme was prepared according to the method of WARBURG and CHRISTIAN (1938). The enzyme solution in 0.1 M potassium phosphate buffer (pH 7.5), containing 1 mM EDTA was 55% saturated with $(NH_4)_2SO_4$ and brought to pH 3.0 with 1 N HCl. After standing 10 min in an ice bath the apoenzyme was collected by centrifugation, dissolved in 0.3 M phosphate buffer (pH 7.5), containing EDTA and diluted with 0.03 M buffer to a concentration of 0.1 M. Replacing the phosphate buffer by Tris-HCl buffer (pH 7.5) results in complete denaturation of the apoenzyme.

FMN and riboflavin cannot restore the enzymatic activity, only FAD is

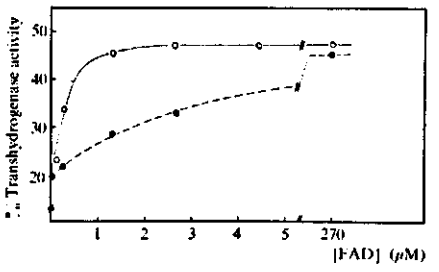

FIG. 3.7. Effect of FAD concentration and temperature on the reactivation of the *Azotobacter* transhydrogenase. Apoprotein prepared according to WARBURG and CHRISTIAN (1938) as described in the text and incubated at 0° (● —— ●) or at 25° (o —— o) at the FAD concentrations indicated. After 30 min incubation samples were withdrawn and activities measured in the NADPH → TNAD⁺ standard assay system. Activities expressed as % of the original activity of the holoenzyme.

active. FAD, however, never gave complete restoration of activity. Recombination is favoured by the presence of 0.1 M β-mercaptoethanol, and to a less extent by 0.1 M dithiothreitol. Addition of bovine serum albumin to the incubation mixture has no influence on the return of transhydrogenase activity.

FIG. 3.7 shows the effect of the FAD concentration and temperature on the partial reactivation of the apoenzyme. The plot clearly indicates that the restoration of activity is temperature dependent. From these data an apparent K_m for FAD of about 0.3 μM and 2.5 μM at 25° and 0°, respectively could be calculated. Corresponding values for K_{ass} are respectively about 3.3×10^6 M^{-1} and 4×10^5 M^{-1}, assuming K_m is identical with the dissociation constant. Preincubation of the apoenzyme with high concentrations of FMN does not retard the restoration by FAD, as was observed for glutathione reductase (STAAL et al., 1969) and lipoamide dehydrogenase (VISSER, 1970; VISSER and VEEGER, 1970). Similarly no decline in activity is observed upon the addition of FMN after maximal restoration of activity with FAD is obtained. Storage of the apoenzyme at −20° or at 0° for 20 hours both resulted in a decline of the remaining transhydrogenase activity and of the ability to recombine with FAD; maximum recombination declined from 46 to 32%.

3.2.9. *Sedimentation velocity and molecular weight*

Sedimentation studies in 0.1 M potassium phosphate buffer (pH 7.5), containing 1 mM EDTA at protein concentrations of 1 to 4 mg/ml revealed sedimentation coefficients ($s_{20,w}$) of about 48 S for a component present in all studied transhydrogenase preparations. A typical sedimentation velocity experiment with one of the purest transhydrogenase preparations purified according to the procedure given in this paper is shown in FIG. 3.8. The gradient curve observed is typical for a polydisperse solution. Furthermore a second component with a much higher sedimentation constant, $s_{20,w} \sim 88$ S, is observable in the first pictures in small amounts. Many preparations purified according to a procedure, which included a DEAE-cellulose chromatography step, however, did not show the presence of the component with the higher S value, but were characterized by the presence of a component with a much lower sedimentation coefficient ($s_{20,w} \sim 24$ S).

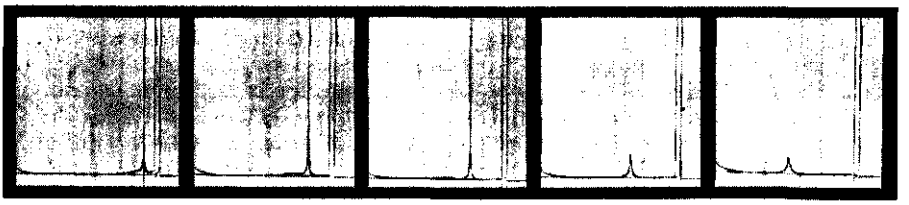

FIG. 3.8. Ultracentrifugal sedimentation patterns obtained with *Azotobacter* transhydrogenase. Enzyme (2.6 mg/ml) in 0.1 M phosphate buffer (pH 7.5) containing 1 mM EDTA. Rotor speed 26,900 r.p.m., temperature 17.3° (±0.1). Photographs taken at 270, 630, 990, 1410 and 2010 seconds after reaching rotor speed. Phase angle for the first three pictures 15°, for the latter 20°. Sedimentation from right to left.

Addition of $NADP^+$ only results in the disappearance of the component with the highest sedimentation coefficient but does not change the sedimentation behaviour of the other components; besides, the gradient curves remained typical for a polydisperse solution. From the solubilizing effect of $NADP^+$ and from the electron microscopic investigations (cf. CHAPTER 4) a much more pronounced dissociating effect of $NADP^+$ was expected.

Sedimentation of the enzyme in the presence of large excess of NADPH which kept the enzyme in its reduced state during the sedimentation run as could be concluded from its colorless state, results in a somewhat different sedimentation pattern with respect to the control. In the presence of NADPH the concentration of the heaviest component is higher then in its absence. Moreover the sedimentation coefficient of the main component is slightly raised to a value of about 55–60 S. After resolubilization of the sediment and re-oxidation of the enzyme, the heaviest component totally disappears and only one component with a sedimentation coefficient ($s_{20,w}$) equal to that obtained for the main component in the control, 48 S, is observed. Representative sedimentation patterns of the transhydrogenase upon sedimentation in the absence and presence of NADPH and $NADP^+$ are shown in FIG. 3.9. Both effects indicate

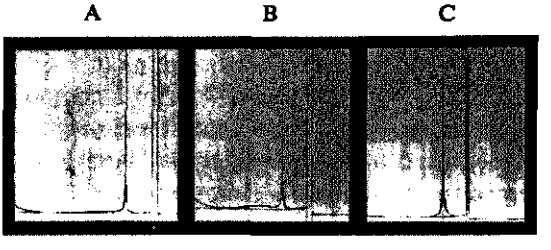

FIG. 3.9. Sedimentation velocity patterns obtained with *Azotobacter* transhydrogenase in the absence and presence of NADPH and $NADP^+$ at 26,900 r.p.m. and 17.3° (±0.1). Enzyme (2.6 mg/ml) in 0.1 M potassium phosphate buffer (pH 7.5) containing 1 mM EDTA. Sedimentation proceeds from right to left. A. No additions; B. in the presence of NADPH (1 mg/0.8 ml enzyme solution); C. in the presence of $NADP^+$ (1 mg/0.8 ml enzyme solution). Time after reaching rotor speed 810, 800, 800 seconds, respectively. Phase angles 15° for A and 20° for B and C.

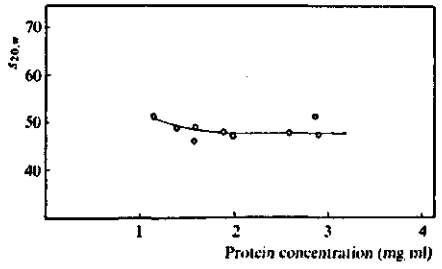

FIG. 3.10. Dependence of sedimentation coefficient of *Azotobacter* transhydrogenase main component on protein concentration. Experimental points calculated from sedimentation velocity studies of several transhydrogenase preparations. Transhydrogenase in 0.1 M phosphate buffer (pH 7.5), containing 1 mM EDTA. Rotor speed 26,000–31,000 r.p.m., temperature 16–20°.

that under these conditons only incomplete dissociation and association is possible. The results obtained here are in good agreement with the electron microscopic investigations where the elongating, associational effect of NADPH and the dissociational effect of $NADP^+$ are observed (cf. CHAPTER 4). In the presence of NADH and NAD^+ none of these typical effects are observable.

Because of the inhomogeneity of the transhydrogenase preparations, as indicated by the broadening of the boundary and confirmed by the electron microscopic investigations, it is rather tentative to determine the sedimentation coefficient as a function of protein concentration. FIG. 3.10 shows the possible relationship between the protein concentrations in the region 1–3 mg/ml and the sedimentation coefficient of the main component. The somewhat scattered experimental points were calculated from sedimentation velocity experiments of several transhydrogenase preparations; protein concentrations for the main component were calculated from the proportional areas under the gradient curves. In the region 1.5–3 mg/ml the $s_{20,w}$ is almost independent of the protein concentration; at lower protein concentrations, however, the tendency for an upward curvature is clearly visible. Such an effect can be expected for elongated macromolecules like DNA and for preparations of very different molecular weight components at very high dilution (SCHACHMAN, 1959).

In order to get a more reliable information about size, shape and molecular weight of the transhydrogenase, light-scattering studies were performed. The preparations studied were characterized by the presence of both the 48 S and 88 S components as could be concluded from sedimentation velocity experiments. Under the electron microscope, at low protein concentrations, structures in the order of 120–150 Å to 15,000 Å were observable in these preparations. Statistical analysis revealed that two components with chain lengths in the order of 400–1000 Å and of a few thousand Å are the most dominant species present.

Light-scattering studies were performed in 0.1 M and 1 mM potassium phosphate buffer (pH 7.5), containing 1 mM EDTA at protein concentrations from 1–18 μg/ml (estimated by the weight difference procedure). The data obtained from measurements of the distribution of light-scattering at different angles were plotted according to the method of ZIMM (1948) and extrapolation along lines of constant angle to zero concentration and along lines of constant concentration to zero angle were performed. A grid-like graph is produced and

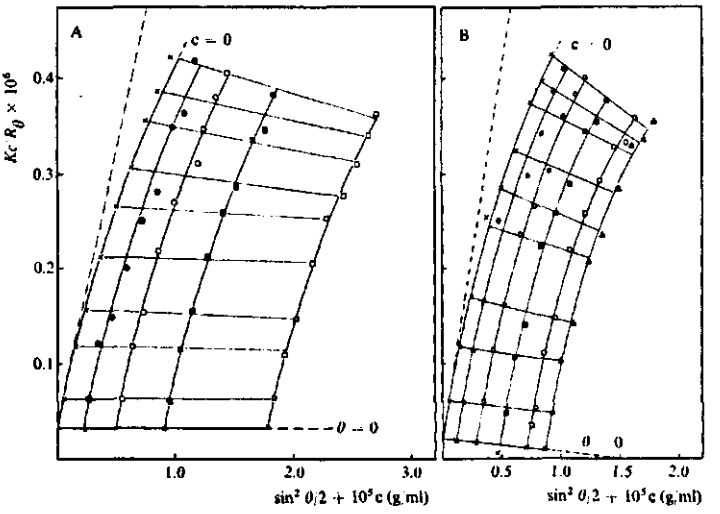

FIG. 3.11. ZIMM plots of angular light-scattering data obtained from *Azotobacter* transhydrogenase in 0.1 M (A) and 1 mM (B) phosphate buffer (pH 7.5), containing 1 mM EDTA at room temperature (22° ± 1). Experimental points (▲, □, ■, ○, ●) obtained at different scattering angles ranging from 30 to 150° and different protein concentrations (1–18 μg/ml) are plotted and extrapolated to $c \rightarrow 0$ and $\theta \rightarrow 0$. The intercept of the extrapolated limiting lines (×—×) in the Y-axis is equal to the reciprocal of the *Z*-average molecular weight. The initial slope of the zero concentration line at the intercept (dotted line) determines the radius of gyration.

the two limiting lines meet at the same intercept. This value $(Kc/R_\theta)_{c\rightarrow 0,\ \theta\rightarrow 0}$ is equal to the reciprocal of the *Z*-average molecular weight (M_z). The slope of the line of zero angle gives the value of *B*, the second virial coefficient.

In 0.1 M phosphate buffer (FIG. 3.11, A) the intercepts of the extrapolated lines on the ordinate are equivalent to a molecular weight af about 30×10^6 daltons, while the slope of the line of $\theta \rightarrow 0$ is equal to zero. In 1 mM buffer (FIG. 3.11, B) however, the intercept is equivalent to a value of about 50×10^6 daltons while an interaction coefficient or 2nd virial coefficient of 1.6×10^{-3} ml g^{-2} can be calculated from the slope of the zero angle line, indicating a greater interaction between the different molecules. The experimental points are also much more scattered in the latter case.

The radius of gyration ρ_z can be related to the dimensions of the model studied. In our case, for a rod-like structure, $\rho_z^2 = L^2/12$ (STACEY, 1956) can be calculated from the ratio of the initial slope of the zero concentration line to its intercept on the Y-axis, according to the equation $\rho_z^2 = \dfrac{\text{initial slope}}{\text{intercept}} \times \dfrac{3\lambda^2}{16\pi^2}$ in which λ is the wavelength used in Å. The radii of gyration calculated in 0.10 M and 1 mM buffer are respectively about 3,000 and 4,500 Å, the corresponding values for the length of the thread-like structures 10,000 and 15,000 Å. On the

basis of the dissymmetry, defined by the angular distribution of light-scattering at two angles chosen to be symmetrical about 90°, $R_{45}/R_{135} = Z$, it could already be predicted that the characteristic dimension should exceed the wavelength (DOTY and STEINER, 1950), since extrapolation to $c \rightarrow 0$ revealed dissymmetry values in 0.1 M and 1 mM buffer of about 3.4.

3.3. DISCUSSION

The *Azotobacter* transhydrogenase as purified by this procedure has a specific activity of 220–260 μmoles NADPH oxidized per min per mg as measured under standard conditions, corresponding to a 700–800 fold purification with respect to the original cell free extract. These data are very similar with those reported by COHEN for the *Pseudomonas* enzyme (COHEN, 1967; COHEN and KAPLAN, 1970) and CHUNG (1970) for the *Azotobacter* enzyme.

The purification behaviour is not hampered by inactivation in the absence of 0.1 M β-mercaptoethanol as observed for the *Pseudomonas* enzyme, but by several 'association-dissociation' phenomena, which may result in a considerable loss of transhydrogenase activity. From the experimental data it was clear that removal of the pyruvate dehydrogenase complex (PDC) activity and the NADPH-ferricyanide activity supported the observed losses in transhydrogenase activity upon DEAE-cellulose chromatography. The idea of a multi-enzyme complex was adopted, but until now no direct evidence for the existence of such a multi-enzyme complex could be obtained by re-association of the different components e.g. transhydrogenase, PDC and NADPH-diaphorase to a large unit (J. KRUL, unpublished). It is known, however, from the work with the bacterial and mammalian PDC (KOIKE and REED, 1961) and 2-oxoglutarate dehydrogenase complexes (HAYAKAWA et al., 1966) that such a re-assembly is difficult to achieve.

On the basis of the long thread-like structures found in the purified transhydrogenase preparation it is not surprising that large losses occur upon column chromatography on DEAE-cellulose, but the question arises what kind of forces induce the formation of these structures at this purification stage? It is of course possible that the transhydrogenase molecules are able to associate as soon as the enzyme concentration reaches a certain level, followed by irreversible aggregation at higher concentrations identical to the aggregation observed upon freezing a pure enzyme solution. The dissociation must be rather irreversible since in highly diluted preparations these polymers can be observed. It is however also possible that the dissociation of a multi-enzyme complex, consisting of PDC, transhydrogenase and perhaps the ferricyanide diaphorase, should preceed the association of the transhydrogenase molecules and that the association is the result of the preceeding dissociation and the removal of the contaminating components. Some experimental evidence for this hypothesis was obtained from the electron microscopic studies (cf. CHAPTER 4). In these studies a relationship was found between the presence of PDC structures (and

activity) and the length of the transhydrogenase molecules; the smaller the amount of PDC structures the longer the transhydrogenase structures. The possibility of a close interaction between the transhydrogenase and the PDC structures was best underlined by the fact that some partial purified preparations showed structures which appeared to consist of transhydrogenase and PDC elements. On the other hand, since also a close relationship was found between the length of the transhydrogenase structures and the specific transhydrogenase activity the first possibility cannot be ruled out.

Another explanation may be found in the idea that *in vivo* the enzyme contains bound $NADP^+$, as proposed by KAPLAN (KAPLAN et al., 1952, LOUIE and KAPLAN, 1970a). Upon purification the protein-bound $NADP^+$ is removed, which results in a more ideal structure for self-association of the transhydrogenase molecules. This idea is supported by the dissociating effects of $NADP^+$ on the thread-like transhydrogenase structures. $NADP^+$ is probably most extensively removed by the calcium phosphate gel treatment, because at this stage the appearance of the thread-like transhydrogenase structures is observed by the electron microscope.

The isolated transhydrogenase is a flavoprotein, characterized by an absorption maximum at 442 nm, with a relative high extinction coefficient $\varepsilon_{440} = 12{,}900\ M^{-1}cm^{-1}$, and some absorbance above 500 nm. This latter absorbance may either be due to an impurity or to scattering phenomena. Several observations indicate that FAD is the prosthetic group. A minimum molecular weight of 58,000–68,000 daltons per mole of FAD can be calculated from the flavin content and turnover numbers in the order of 50,000–60,000 moles per min per mole of enzyme flavin are obtained in the NADPH-$TNAD^+$ assay (cf. CHAPTER 6). The enzyme is rather stable, even at high dilution and elevated temperatures. The reduced enzyme, however, is rather heat-sensitive; protection can be achieved by FAD and to a less extent by $NADP^+$ and FMN, indicating that the oxidized flavin is more firmly bound to the protein than the reduced flavin. The observation that no reactivation is obtained upon treatment with FAD of a heat-inactivated NAD(P)H-reduced enzyme indicates that the apoenzyme is more heat-sensitive than the holoenzyme. This latter observation does not exclude the possibility that also conformational changes are involved, since under reducing conditions $NADP^+$ is also more easily removed.

Though the flavin can be easily removed by different treatments the ability to recombine with FAD is very poor; recombination is favoured by the presence of β-mercaptoethanol, indicating that sulfhydryl or disulfide groups may be involved in the regeneration of activity (BRADY and BEYCHOK, 1969) as observed with guanidine-HCl treated pig heart lipoate reductase. In all cases it was observed that when the residual activity was very low, due to a second or a more intensive treatment, the recombination was much less effective or did not occur. This is in accordance with the findings of KALSE and VEEGER (1968) and KOIKE et al. (1962) for heart and bacterial lipoamide dehydrogenase. Because of the complicated structure of the transhydrogenase it is possible and perhaps very likely that the apoenzyme is partially damaged and that upon recombination

only a partial active FAD-apoenzyme complex can be formed. The formation of this partially active complex is temperature dependent and is hardly influenced by preincubation with FMN; the latter finding is in contrast to the results obtained for lipoamide dehydrogenase (VISSER, 1970; VISSER and VEEGER, 1970) and glutathione reductase (STAAL et al., 1969). Preliminary results indicate that the level of recombination increases with higher protein concentration.

As indicated by the sedimentation velocity studies and confirmed by the light-scattering experiments the transhydrogenase preparations are inhomogeneous and consist of rather large to very large structures. Additional evidence for the large size of the molecules was obtained by electron microscopy (cf. CHAPTER 4). The results indicate that in the two types of transhydrogenase preparations three average forms of the transhydrogenase molecule are present. The differences in the $s_{20,w}$ values observed may be due to the different purification procedures followed, e.g. with or without a DEAE-cellulose chromatography purification step. It may be visualized that the smaller units are predominantly eluted from DEAE-cellulose and that especially in these cases incomplete removal of $NADP^+$ may be responsible for the presence of substantial amounts of smaller enzyme units with respect to the very large molecules. It is, however, striking that addition of $NADP^+$ to the enzyme solutions did not result in the appearance of the slower sedimenting component. When preparations, mainly characterized by the 48 S and 88 S components were treated no shift in the distribution of the components was observed and similarly in the case of preparations characterized by the 48 S and 24 S components, while in the electron microscopic studies a rather pronounced effect of $NADP^+$ was obtained. It must be remembered, however, that in the ultracentrifuge experiments the protein concentration is much higher than in the electron microscopic studies. Furthermore, the possibility that we are dealing with an all-or-none effect of $NADP^+$ cannot be excluded; a similar effect with 2'AMP was observed for the transition of *Pseudomonas* transhydrogenase structures to substructures by LOUIE and KAPLAN (1970). In this respect the buffer used may be of great importance; it has to be pointed out that the sedimentation velocity studies and the light-scattering experiments were performed in phosphate buffer (pH 7.5), while the electron microscopic studies were carried out in Tris-HCl buffer (pH 7.5).

It is of course also possible that some high molecular weight contamination is responsible for the lowest sedimentation value. In this respect pyruvate dehydrogenase complex and transacetylase are on the basis of their sedimentation coefficients as obtained for *E. coli*, open to suspicion (WILLMS et al., 1967). The preparations studied in the analytical ultracentrifuge, however, showed practically no PDC activity or none at all; the transacetylase activity was not checked. The presence of these activities is also unlikely, because on DEAE-cellulose nearly all pyruvate dehydrogenase overall activity is eluted with 0.15 M NaCl. Furthermore, both types of preparations, although varying somewhat in specific activity, did not show gross differences in kinetic and spectral properties.

Although the results do not permit a definite statement, one is inclined to attribute the different S values to the smallest enzyme units, the medium sized thread-like structures and the elongated thread-like structures, respectively. These elongated structures would then have been the determining species in the light-scattering studies. The values of the length of the structure *(L)* calculated from the light-scattering data are in rather good agreement with the electron microscopic investigations (cf. CHAPTER 4). The molecular weight is rather high, but assuming a molecular weight of 1 million daltons for the smallest enzyme unit, preliminary statistical analysis of the electron micrographs revealed a *Z*-average molecular weight which was in the same order.

It is clear that the enzyme from *A. vinelandii* has many characteristics in common with the *Pseudomonas* transhydrogenase; the differences are mainly centered around the effects of $NADP^+$, NADPH and 2'AMP.

4. ELECTRON MICROSCOPIC STUDIES ON *AZOTOBACTER* TRANSHYDROGENASE

4.1. INTRODUCTION

The isolation and purification of the reversible pyridine nucleotide transhydrogenase from *Azotobacter vinelandii* (ATCC 478) is reported. It was shown to be a high molecular weight protein by its sedimentation coefficients and characteristics derived from the light-scattering data (CHAPTER 3).

Although several differences have been found, the enzyme has many properties in common with the transhydrogenase from *Pseudomonas* (cf. VAN DEN BROEK and VEEGER, 1970; COHEN, 1967; COHEN and KAPLAN, 1970a, 1970b). Ouchterlony immunodiffusion and micro-complement fixation analysis showed that both the *Pseudomonas* and the *Azotobacter* transhydrogenase cross-react with the anti-*Pseudomonasserum* (LOUIE and KAPLAN, 1970), suggesting that the two enzymes have somewhat related structures.

The same authors (1969, 1970) reported that the native *Pseudomonas* enzyme appeared to have a long helical-like structure, several thousands *Å* long with a diameter of 100–120 *Å*. Upon treatment with 2'AMP, the activator of the $NADP^+$ reduction, a total population of small circular segments with a diameter of 130–150 *Å* was found and the substructures were characterized by an octahedral leaflet arrangement. The transition of the *Pseudomonas* enzyme structure into subunits was not induced by the normal substrates $NADP^+$ and NADPH, while furthermore the transition process upon treatment with 2'AMP appeared to be an all or none effect.

The effects of 2'AMP and $NADP^+$ on the properties of *Azotobacter* transhydrogenase were different from those of *Pseudomonas* transhydrogenase. Therefore it was of interest to investigate the morphology of native *Azotobacter* transhydrogenase and to compare the results with those of the *Pseudomonas* enzyme. Moreover we have attempted to investigate by electron microscopy the effects of the different substrates and inhibitors on the structure of the native enzyme and to correlate these with the kinetic and chemical effects.

These studies have been performed in collaboration with PROF. DR. E. F. J. VAN BRUGGEN and MR. J. F. L. VAN BREEMEN, Laboratorium voor Structuurchemie, The University, Groningen, The Netherlands.

4.2. RESULTS AND DISCUSSION

The electron micrographs reproduced in FIG. 4.1 were obtained upon examination of negatively stained, highly purified *Azotobacter* transhydrogenase preparations (specific activity 270 units per mg protein). The micrographs clearly demonstrate that we are dealing with very inhomogeneous protein

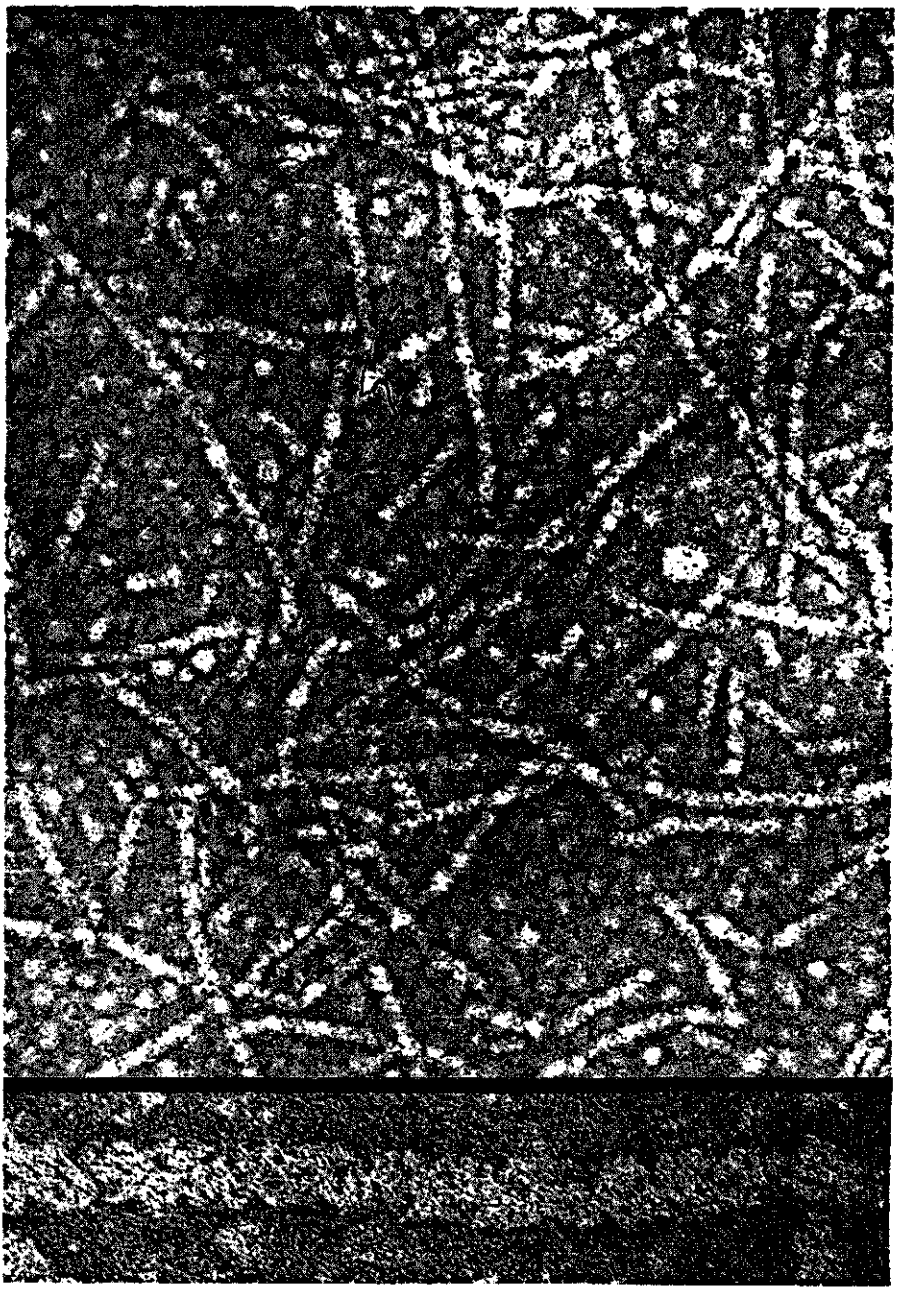

FIG. 4.1. Electron micrograph of *Azotobacter* transhydrogenase. Enzyme, as isolated, extensively dialysed against 0.05 M Tris-HCl buffer (pH 7.5) containing 0.5 mM EDTA, diluted in the same buffer to a protein concentration of 0.1–0.2 mg per ml and stained with 0.5% uranyl oxalate (pH 6.4). Top, × 130,000; bottom, × 560,000.

preparations, as already concluded from sedimentation analysis and light-scattering experiments, performed with the same enzyme preparation (cf. CHAPTER 3, FIGS. 3.8, 3.9 and 3.11). Very long helical-like structures, rod-like structures and separate large units are observable. The threads and rods have a diameter of about 116–120 Å; their lengths vary from a few hundred Å to several thousands Å. Maximal length measured was about 8,000–18,000 Å. Sometimes it is clearly visible that these very long structures are constructed of separate units, because an oblique or perpendicular striping on the structure is sometimes observable; moreover clean-cut constrictions are often present. These pictures may also be due to a flattened spiral structure. The smaller units do not show any specific or characteristic structure and might represent projections of spherical particles, with a diameter of about 120 Å. Sometimes, however, small rosettes and striped rectangles are present in the highly purified preparations with a diameter of about 130 Å, resembling structures found in RNA-polymerase preparations (LUBIN, 1969). If they represent spherical particles of 120–130 Å diameter, the calculated volume per particle is 0.90 to 1.15 $\times 10^{-18}$ g (assuming a protein partial specific volume, $\bar{V}$, of 0.74 cc per g) and a molecular weight of 0.75 to 0.94 $\times 10^6$ daltons. Accepting a minimum molecular weight of 60,000 daltons the 120–130 Å body should be made up of 12–16 subunits if 1 mole FAD per subunit were present or 6–8 subunits if the smallest subunits contained 2 moles FAD. With respect to the *Pseudomonas* enzyme (LOUIE and KAPLAN, 1969, 1970) an octahedral leaflet arrangement may be very likely. Because the true border of the particles is probably poorly defined by the negative stain, the figures given may be under-estimates and the calculations of molecular weight are crude at best.

FIG. 4.2 shows the distribution of the structures found in five different micrographs from the preparation shown in FIG. 4.1. If a molecular weight of 1 million daltons for the 120 Å enzyme units is assumed, from these measurements a Z-average molecular weight or 27 $\times 10^6$ daltons can be calculated; a value which agrees very well with that obtained from the light-scattering experiments in 0.1 M phosphate buffer (cf. CHAPTER 3). The weight average (M_w) and number average (M_n) molecular weights calculated are about 19 $\times 10^6$ and 11 $\times 10^6$ daltons, respectively. For definitions of the different

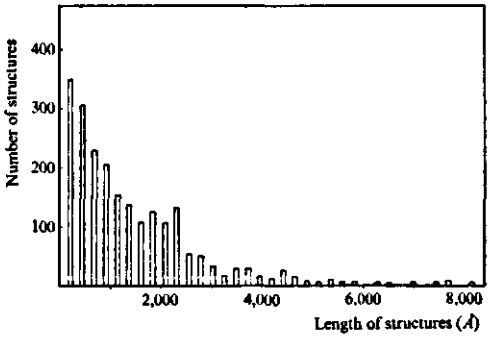

FIG. 4.2. Frequency distribution of measured molecular length. From an *Azotobacter* transhydrogenase preparation (specific activity 270 units per mg) in 0.05 M Tris-HCl buffer (pH 7.5), 0.5 mM EDTA, species for electron microscopy were prepared and stained with uranyl oxalate (pH 6.4). On different electron micrographs about 1060 structures were measured and these numbers were used for the distribution curve.

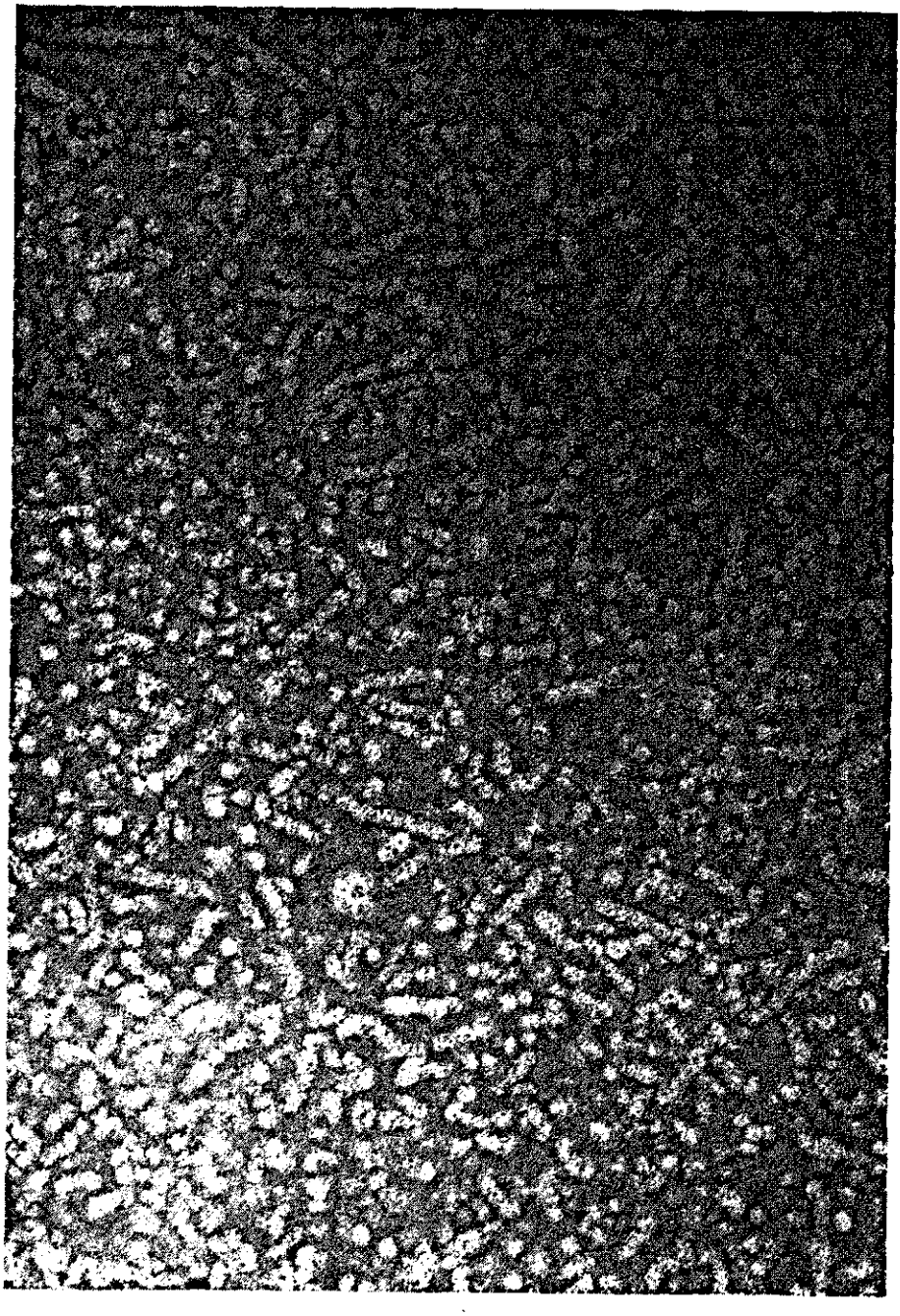

FIG. 4.3. Electron micrograph of *Azotobacter* transhydrogenase. Enzyme (1.3 mg per ml) treated with 2 mM $NADP^+$ and diluted in Tris buffer (pH 7.5), 1 mM EDTA; negatively stained with 0.5% uranyl oxalate (pH 6.4). × 130,000.

molecar weights, see CHAPTER 2. From the weight distribution curve it could be concluded that the two peaks are responsible for the observed sedimentation coefficients.

In the presence of $NADP^+$ a much larger amount of the smallest enzyme units and the small rod-like structures are visible on the electron micrographs than in its absence, indicating $NADP^+$ is able to dissociate the long helical structures. FIG. 4.3 demonstrates the effect of $NADP^+$. The transition of the enzyme into smaller units is never an all or none process, since a complete dissociation never was obtained. The dissociation seems to be dependent on the concentration of $NADP^+$. At low $NADP^+$ concentrations, equimolar amounts with respect to flavin, the helical structures are on the average somewhat shorter in length, but no large amounts of small units are observable. At higher $NADP^+$ concentrations the dissociation is much more pronounced, although still elongated structures can be observed. The dissociation by $NADP^+$ can be prevented by adding NADPH. The pictures even suggested that addition of high concentrations of NADPH to a partly dissociated enzyme preparation results in a partial restoration of the original elongated structures. This behaviour indicates that the length of the protein structure is determined by the ratio NADPH-$NADP^+$ and that in the presence of NADPH the effect of $NADP^+$ is counteracted due to replacement of the enzyme-bound $NADP^+$.

Support for this hypothesis comes from the observation that preparations which were dialyzed anaerobically in the presence of glucose-6-phosphate and traces of glucose-6-phosphate dehydrogenase tended to be more homogeneous in composition and contained more very long structures than preparations which were extensively dialyzed aerobically (FIG. 4.4). Moreover in preparations which were solubilized in the absence of $NADP^+$, very long structures ($> 15{,}000$ Å) next to bundles of the helical structures were observed and nearly no small units were present. Further indications were obtained from experiments in which NADPH was added to a transhydrogenase preparation and the NADPH oxidized by bubbling oxygen through the solution; in these cases typical intermediate stages could be observed (FIG. 4.5). The observed effect of NADPH on the enzyme structure is in good agreement with the effect of NADPH on the sedimentation patterns (cf. CHAPTER 3, FIG. 3.9). Thio-$NADP^+$ is also able to give partial dissociation but its effect is not very pronounced; in the presence of 2'AMP only a tendency towards dissociation is observable. NAD^+, NADH, thio-NAD^+ and ATP, which is a potent inhibitor of the $NADP^+$ reduction (cf. CHAPTER 6), have no effect at all.

These results are contrary to those of the *Pseudomonas* enzyme (LOUIE and KAPLAN, 1969, 1970); in the *Pseudomonas* preparation only the activator, 2'AMP, and not the substrates, $NADP^+$ and NADPH, can give structural changes.

Fragmentation of the long structures was observed in highly diluted enzyme preparations (protein concentration less than 0.02 mg per ml), but the very long structures are still present. This supports the idea that association may be a concentration dependent process; a similar picture was observed in preparations

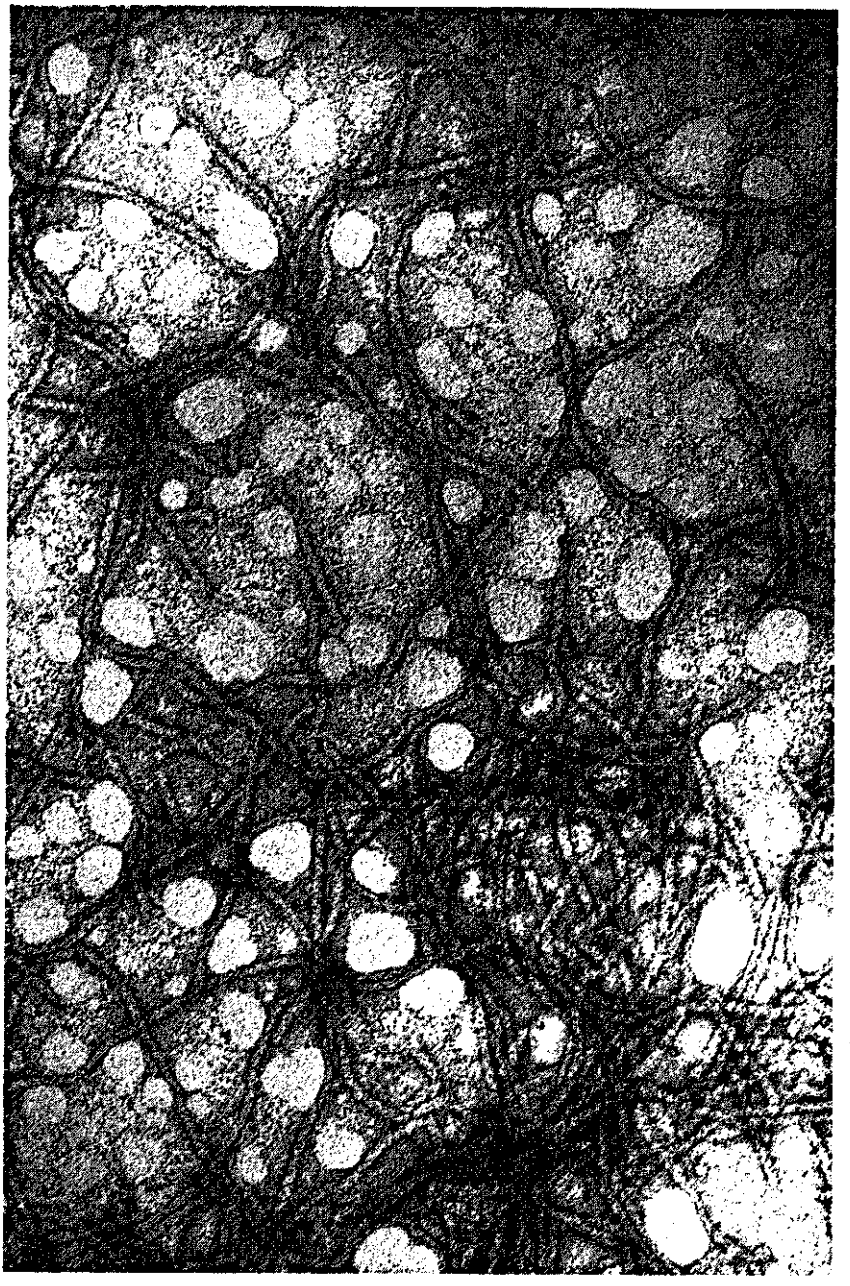

FIG. 4.4. Electron micrograph of *Azotobacter* transhydrogenase. Isolated enzyme dialyzed anaerobically in the presence of glucose-6-phosphate and a trace of glucose-6-phosphate dehydrogenase. Diluted preparations negatively stained with uranyl acetate. × 130,000.

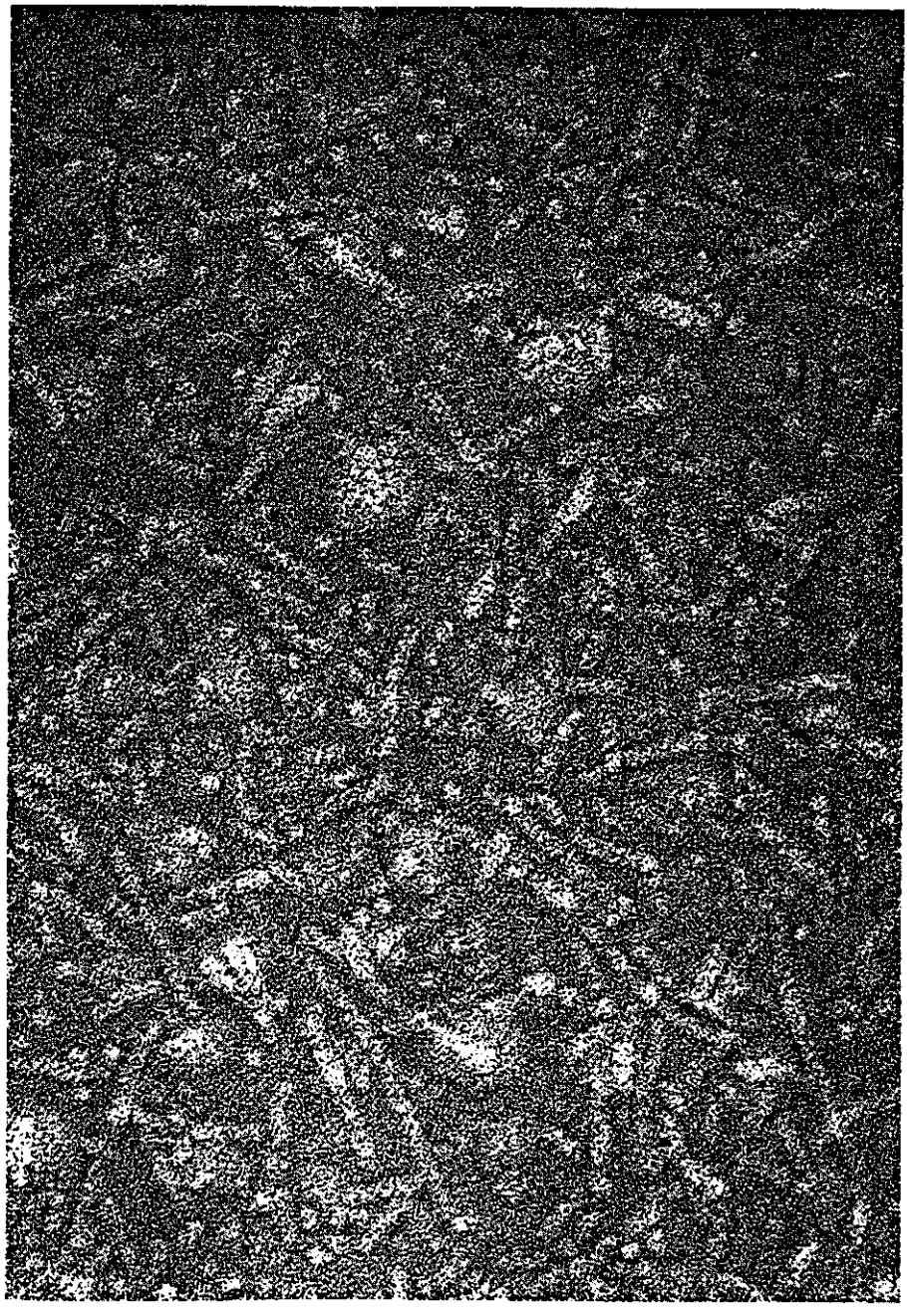

FIG. 4.5. Electron micrograph of *Azotobacter* transhydrogenase. Enzyme reduced with NADPH and slowly re-oxidized by bubbling air through the solution. Before re-oxidation was completed this sample was withdrawn and examined. Protein negatively stained with uranyl oxalate (pH 6.4). × 180,000.

which were stored in diluted states (protein concentration ~ 0.07 mg/ml) at 4° for a period of 6 days.

A very typical, totally unknown structure was found in preparations obtained after sedimentation of eluates from calcium phosphate gel, especially batches which initially had adsorbed both the transhydrogenase and the pyruvate dehydrogenase complex (PDC). The sediments solubilized in the presence of $NADP^+$ and dialyzed against buffer, were stored at 4° for a period of several days to several weeks. These preparations are characterized by a high absorbance in the 300–400 nm region and by an increase in absorbance over the whole wavelength region due to light-scattering; addition of $NADP^+$ only results in a very slight disappearance of the scattering, indicating that large structures are still present. The presence of very large molecules is also indicated by settling down of the solubilized material after standing for some time at 4°; the settled material sediments very easily through a dense sucrose solution. It is characterized by its transhydrogenase activity (150–180 units per mg) and transacetylase activity; no PDC activity could be detected in these heavy structures. Examination of this preparation with the electron microscope revealed the presence of ladder-like structures, consisting of pairs of the typical long helical-like structures with the dimensions of the native transhydrogenase molecules, connected in a regular manner by sets of two rungs. The sets of 2 rungs occur at regular intervals. FIG. 4.6 shows the typical structures next to several other structures. The following mean dimensions were measured: distance between the two elongated structures ~ 120 Å; center to center distance between 2 rungs of one pair ~ 87 Å; external cross-section for a pair ~ 145 Å; center to center distance between two neighbouring pairs of rungs ~ 320 Å.

The structures in between the long helical transhydrogenase structures are, with respect to their appearance and dimensions, almost identical to tetrad-like structures, observed in purified PDC preparations and in preparations which were characterized by both transhydrogenase and PDC activity. A typical picture is shown in FIG. 4.7. The tetrads are completely similar to the transacetylase structures of the PDC complex of *E. coli* (cf. REED and coworkers, 1966). Since in the ladder-like structures only a transacetylase activity and no PDC activity was detectable, the idea of a complex between transhydrogenase and the transacetylase is very likely. The ladder-like structures are able to resist the dissociating effect of $NADP^+$, in contrast to the separate helical structures present. It is striking, however, that only the transacetylase structures could be detected in the different preparations and not the complete PDC structures; according to KOIKE (personal communication) this may be due to the method of negative staining with uranyl acetate or uranyl oxalate and to the lability of the PDC structure itself. As can be seen in FIG. 4.6 the preparations contain apart from the ladder-like structures also several large and small rosettes with diameters of about 170–200 Å and 130–140 Å, respectively; occasionally striped rectangles (175 × 145 Å) are also observable. Because of the lower specific transhydrogenase activity of these preparations some (or all) of these structures may be ascribed to contaminants.

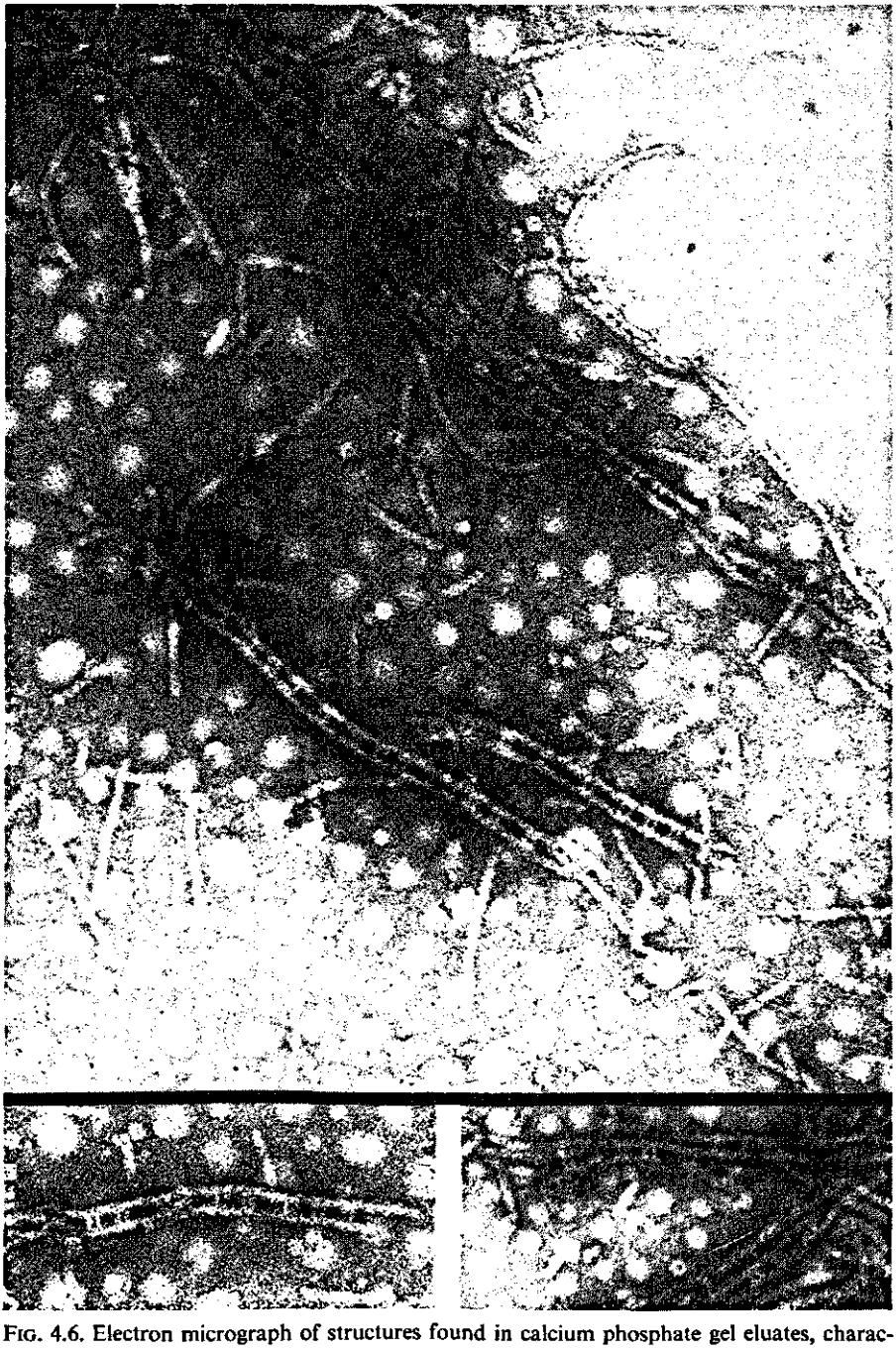

FIG. 4.6. Electron micrograph of structures found in calcium phosphate gel eluates, characterized by transhydrogenase and overall pyruvate dehydrogenase activity, which were sedimented at 200,000 × g, solubilized in the presence of $NADP^+$, dialyzed and stored at 4 °C. Negatively stained with uranyl acetate. × 130,000.

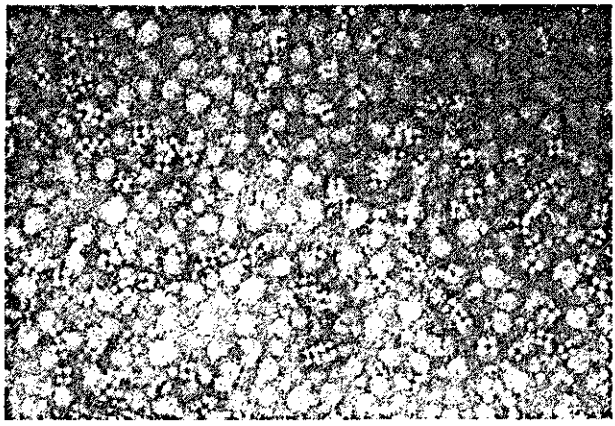

FIG. 4.7. Electron micrograph of structures found in *Azotobacter* preparations, characterized by overall pyruvate dehydrogenase activity. Negatively stained with 0.5% uranyl oxalate. × 130,000.

FIG. 4.8 shows the structures observed in a crystalline transhydrogenase preparation (specific activity before crystallization ~ 180–200 units per mg protein). Apart from transhydrogenase structures – long threads and fragments – bundles of threads and large aggregates with some kind of 'stacked disc' structures were observable. The diameter of the stacked discs cannot be measured. Different types of rosettes can also be observed. Solutions of the crystals in Tris buffer (pH 7.5) only show long helical-like structures and fragments of it, and different types of rosettes are found (FIG. 4.9). Since in solution the number of rosettes seems to be larger, it is possible that the stacked discs are due to the rosettes. The direct connection between the threads, rosettes, and stacked discs, however, still remains uncertain. If the rosettes of about 130–140 Å are really the smaller units of the transhydrogenase molecule then we have a magnificant example of a conformational transition.

Since a large number of structures in the sedimented enzyme preparations could be observed, it was of great interest to investigate whether we were dealing with real native enzyme molecules or with some type of purification artefact. For this reason all purification stages from cell free extract to pure enzyme solution, including the fractions obtained upon differential centrifugation (cf. CHAPTER 3), were examined with the electron microscope; all preparations were stored, diluted and stained according to the same procedure for comparative purposes. In the cell free extract, the heat extract, the 25–50% ammonium sulfate fraction and the different cell fractions a multitude of structures was present (different types of rosettes, rings, tetrads, rectangles, filamentary structures, membrane fragments, and bundles of thick threads). Thread-like structures with identical dimensions as measured for the helical-like transhydrogenase structures were also present, but it appeared very difficult,

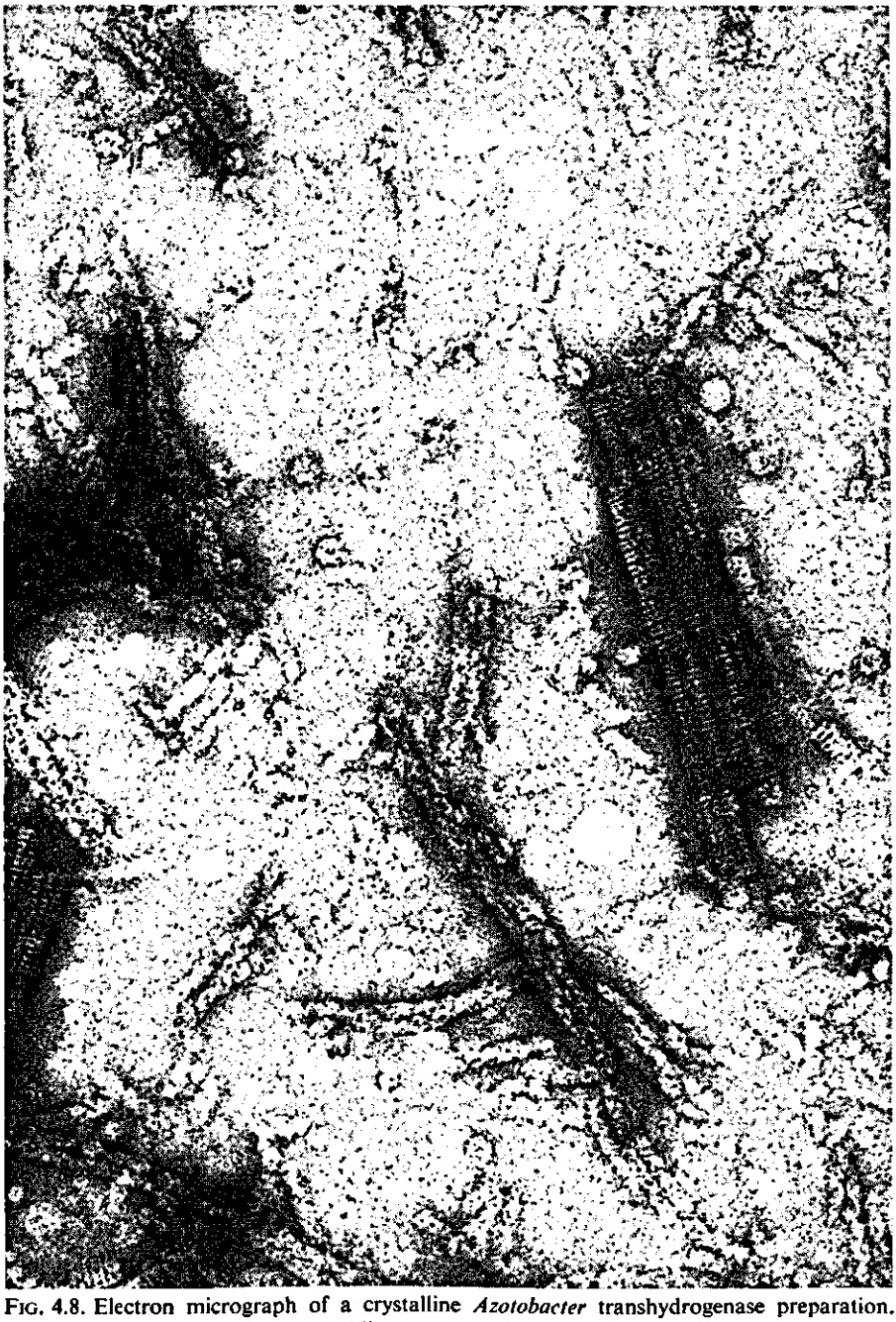

FIG. 4.8. Electron micrograph of a crystalline *Azotobacter* transhydrogenase preparation. Crystallization was performed by adding a saturated neutralized ammonium sulfate solution slowly at 4°; addition was stopped after a very slight cloudiness began to appear. The crystals were allowed to set at 4° and left in the mother liquor at 4°. One drop of this crystalline suspension was negatively stained with 0.5% uranyl acetate and extensively rinsed with contrast medium. × 130,000.

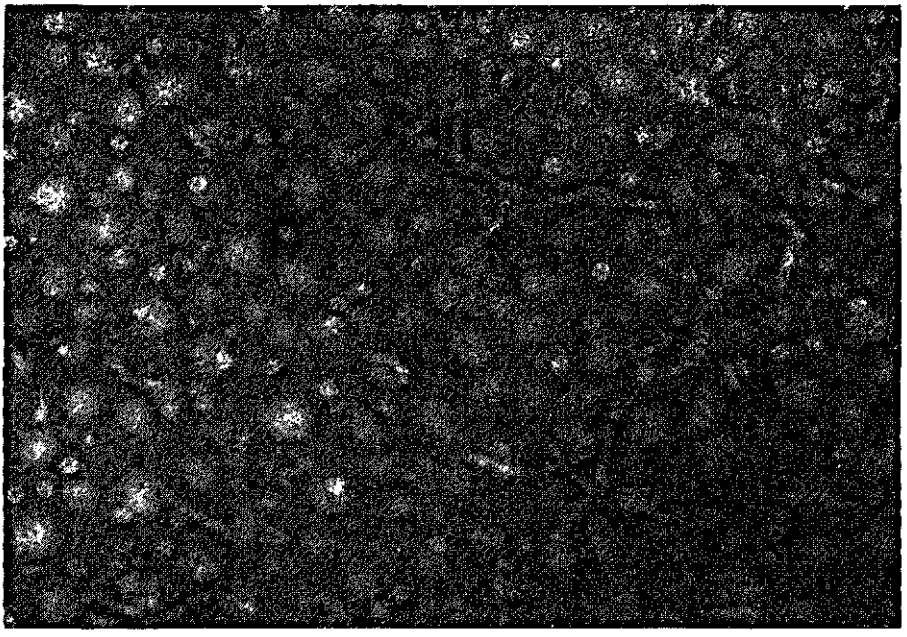

FIG. 4.9. Electron micrograph of the crystalline suspension of FIG. 4.8 after solubilization in Tris-HCl buffer (pH 7.5), containing 0.5 mM EDTA; negatively stained with 0.5% uranyl acetate. × 130,000.

in fact impossible, to determine whether one was dealing with real transhydrogenase structures or with cell membrane fragments.

Larger amounts of the typical transhydrogenase structures were observable in the calcium phosphate gel eluates. A correlation was found between the presence of PDC structures, the transhydrogenase structures and the specific activity of both enzymes. The higher the specific transhydrogenase activity the larger the number of long helical-like transhydrogenase structures, the lower the specific PDC activity the smaller the number of PDC tetrads. The eluates with the high transhydrogenase activity were also characterized by the presence of large amounts of rosette-like structures with a diameter of 115–145 Å, and 170–200 Å. Although concentration effects on the state of the association of the transhydrogenase cannot be excluded it is very attractive to correlate these findings with the problems met with in the purification procedure on DEAE-cellulose (cf. CHAPTER 3) and to postulate a direct connection between both enzymes. It seems possible that transhydrogenase and PDC form one complex, a conclusion supported by the ladder-like structure formed between transhydrogenase and transacetylase. Upon removal of the PDC activity and to a less extent the transacetylase activity, the state of aggregation of the transhydrogenase increases. A definite statement can only be given if the exact structure of both enzymes is known and after being able to demonstrate a direct complexing between transhydrogenase and PDC.

5. EFFECT OF $NADP^+$ ON THE SPECTRAL PROPERTIES OF *AZOTOBACTER* TRANSHYDROGENASE

5.1. INTRODUCTION

In CHAPTER 3 the isolation and purification of *Azotobacter* pyridine nucleotide transhydrogenase and several of its properties have been described. Transhydrogenases are able to catalyze the direct transfer of hydrogen from position 4 of a reduced to position 4 of an oxidized pyridine nucleotide. Studies with tritium-labeled pyridine nucleotides (LOUIE and KAPLAN, 1970b) have shown that the *Pseudomonas* enzyme is stereospecific for the 4B hydrogen atom with respect to both NADH and NADPH. According to LOUIE and KAPLAN (1970a) the hydrogen transfer should be less specific in the case of *Azotobacter* transhydrogenase than with the *Pseudomonas* enzyme. $NADP^+$ may play an important role in the mechanism of enzyme action, since the reduction of $NADP^+$ proceeds slower than the NAD^+ reduction, whereas $NADP^+$ is able to inhibit the different reactions catalyzed.

In studies with other flavoproteins (VEEGER et al., 1966; KOSTER and VEEGER, 1968; STAAL and VEEGER, 1969; ZEYLEMAKER, 1969) it was clearly shown that the oxidized products of a reaction, which act as competitive inhibitors, are able to show spectrally visible complexes with the oxidized enzyme. This technique has been successfully used in the study of the active sites of enzymes (MASSEY and GANTHER, 1965; DERVARTANIAN and VEEGER, 1964; VISSER et al., 1970; STAAL et al., unpublished results). Moreover several reports regarding spectral intermediates of reduced flavoproteins and pyridine nucleotides are known (STRITTMATTER, 1956; DOLIN, 1960, 1966; MASSEY, GIBSON and VEEGER, 1960; MASSEY and VEEGER, 1961, 1963; MASSEY and WILLIAMS, 1965; MASSEY et al., 1970).

In this respect it was of interest to study the effect of $NADP^+$ and other pyridine nucleotides on the spectral properties of oxidized and reduced transhydrogenase. The effect of $NADP^+$ on the spectral properties of the enzyme was especially of interest since the purification procedure (CHAPTER 3) and electron microscopic studies (CHAPTER 4), showed that $NADP^+$ causes a disaggregation or dissociation of the enzyme.

5.2. RESULTS

5.2.1. *Effect of $NADP^+$ on the absorption spectrum of oxidized transhydrogenase*

As already indicated in CHAPTER 3 the isolated transhydrogenase is greenish-yellow and highly fluorescent and shows a typical flavin absorption spectrum (cf. FIG. 3.5). After solubilization of the sedimented enzyme in the presence of $NADP^+$ the absorption spectrum is characterized by maxima at 438 nm,

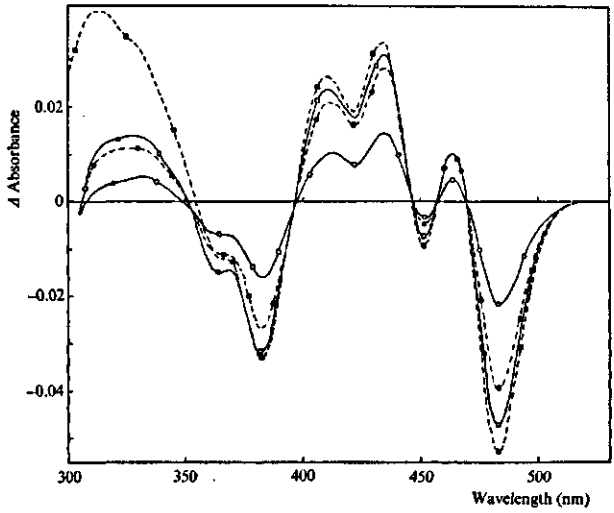

FIG. 5.1. Spectral titration of *Azotobacter* transhydrogenase with $NADP^+$ at 25°. Enzyme flavin, 40 μM, in 0.1 M potassium phosphate buffer (pH 7.5), containing 1 mM EDTA, in a final volume of 0.7 ml was titrated with $NADP^+$ in the same buffer. Experiments were carried out in tandem cells as described in CHAPTER 2 and difference spectra of enzyme plus $NADP^+$ minus enzyme recorded after mixing. $NADP^+$ additions per mole of flavin: o —— o, 0.6 mole; • —— •, 1.1 moles; □ —— □, 1.7 moles; ■ —— ■, 7.7 moles.

370–355 nm and 267 nm, minima at 390 nm and 320 nm, while marked shoulders are present at 464 nm and 420 nm. Upon dialysis spectral shifts to the red are observable. The dialysed transhydrogenase has its maxima at 442 nm, 368 nm and 269 nm and minima at 397 nm and 316 nm; the shoulders are less pronounced especially that at 464 nm. Both spectra have absorbance above 500 nm. Sometimes, however, extensive dialysis only was not sufficient to produce the maximal observable shifts in the spectrum. Removal of $NADP^+$ was facilitated by anaerobic treatment of the enzyme in the presence of glucose-6-phosphate and a trace of glucose-6-phosphate dehydrogenase, indicating that in the reduced state of the enzyme NADPH is loosely bound and can be more easily removed than $NADP^+$ from the oxidised state. In this respect it is of interest to refer to the stable $NADP^+$ complex of old yellow enzyme which also only dissociates by reducing the complex and dialysis under anaerobic conditions (EHRENBERG and LUDWIG, 1958).

Upon the addition of $NADP^+$ the reversal of the spectral shifts, as observed upon dialysis, can be induced. The difference spectrum obtained upon titration of a thoroughly dialysed transhydrogenase preparation with $NADP^+$ is shown in FIG. 5.1. The difference spectra obtained show negative maxima at 483 nm, 451 nm, 383 nm and 364 nm, positive maxima at 463 nm, 435 nm and 412 nm and isosbestic points at 468 nm, 457 nm and 398 nm. Formation of the intermediate difference spectra is complete before measurements can be made. The spectral shifts are independent of ionic strength and the formed $NADP^+$-

species has in contrast to the observation on ferredoxin-$NADP^+$ reductase (FOUST et al., 1969a) the same stability as the holo-enzyme. 70–80% of the maximal shift in the 370–500 nm region is obtained upon the addition of 1.0 mole $NADP^+$ per mole of enzyme flavin. A small positive band with a maximum at 330 nm is visible after the addition of 1.0–2.0 moles $NADP^+$/mole of flavin. The addition of larger amounts of $NADP^+$ causes only a very small increase in the difference spectrum in the 370–550 nm region, but in the 300–370 nm region a marked spectral change is observed. The difference spectrum shows a band with a maximum at 315 nm and a shoulder around 330 nm while the absorbances at 383 nm and 364 nm are influenced by the new spectral band. The titration curves for the absorbance changes at 325 nm are clearly biphasic. This behaviour clearly indicates the existence of at least two different binding sites for $NADP^+$. The first one, with a dissociation constant (K_D) in the order of 2–3 μM at 25° (value from five independent experiments), causes the spectral shifts in the visible region of the spectrum, while the second one with a dissociation constant $>$ 100 μM is reponsible for the spectral changes in the 300–360 nm region (FIG. 5.2).

It is of interest to recall the similarity of this latter band with the NAD^+-complex of glyceraldehyde-3-phosphate dehydrogenase (CHANCE, 1955; KIRSCHNER et al., 1966) and the existence of a NAD^+-complex with the reduced NADH-cytochrome b_5 reductase in which an SH-group participates and which has a maximum at 315 nm as demonstrated by STRITTMATTER (1959). Spectrally visible complexes were also demonstrated for NAD^+ and lipoamide dehydrogenase (VISSER et al., 1970), $NADP^+$ and glutathione reductase (STAAL et al., unpublished), for $NADP^+$ and ferredoxin-$NADP^+$ reductase (FOUST et al., 1969a). Sometimes, the absorbance change in the visible region developed upon the addition of larger amounts of $NADP^+$. From extrapolation of the linear

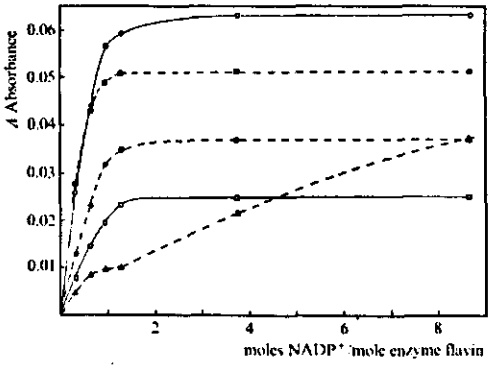

FIG. 5.2. Titration of *Azotobacter* transhydrogenase with $NADP^+$ at 25°. 39 μM Transhydrogenase flavin in 0.1 M phosphate buffer (pH 7.5), containing 1 mM EDTA, was titrated with $NADP^+$ at the concentrations indicated and the positive or negative absorbance changes at 483 nm (o —— o), 435 nm (● —— ●), 410 nm (□ —— □), 383 nm (■ —— ■) and 330 nm (△ —— △) were measured and plotted as a function of the $NADP^+$ addition per mole of enzyme flavin.

part of the titration curve it could be calculated in those cases that 1.4 to 1.6 moles $NADP^+$ per mole of flavin were necessary to give full saturation in the 370–500 nm region. The maximal absorbance change per mole of flavin, however, is of the same order as observed in the other cases where 0.9–1.2 moles $NADP^+$ are sufficient. The differences observed are probably due to small amounts of bound $NADP^+$, which is difficult to remove by dialysis. In this respect it is comparable with glyceraldehyde-3-phosphate dehydrogenase where charcoal treatment is necessary for an effective removal of NAD^+ (CONWAY and KOSHLAND, 1968). In the case of the *Azotobacter* transhydrogenase charcoal treatment for removing bound $NADP^+$, however, will possibly be hampered by the structural changes occurring in the absence and presence of $NADP^+$. The idea of the presence of bound $NADP^+$ responsible for partial dissociation is supported by the electron microscopic studies; preparations treated with the glucose-6-phosphate dehydrogenase system are more homogeneous in structure in comparison with the dialyzed ones and contain practically no smaller units (cf. CHAPTER 4).

No spectral shifts are obtained upon the addition of NAD^+, $TNAD^+$ and 2'AMP.

5.2.2. *Effect of $NADP^+$ and thio-$NADP^+$ on the flavin fluorescence*

The dialyzed transhydrogenase is characterised by a flavin fluorescence with an emission maximum at 506–508 nm, much lower than the maxima for free FAD or FMN at 526 nm, or FAD bound to *Azotobacter* and pig heart lipoamide dehydrogenase at 520 nm. The emission spectrum of the dissociated transhydrogenase flavin, however, is identical with that of the dissociated flavin for lipoamide dehydrogenase.

Upon the addition of $NADP^+$ and thio-$NADP^+$ the flavin fluorescence is quenched and the emission maximum is shifted to lower wavelengths. $NADP^+$ induces a shift of the emission maximum from 506–508 nm to 498 nm with a concomittant quenching of the flavin fluorescence (FIG. 5.3) upon excitation

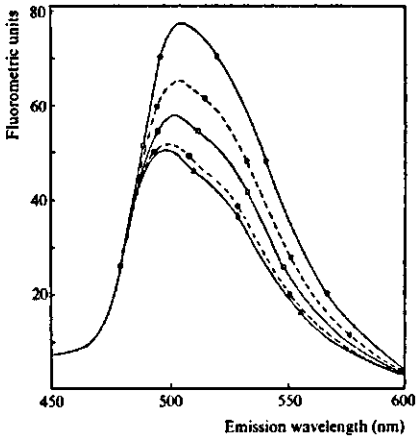

FIG. 5.3. Fluorometric titration of *Azotobacter* transhydrogenase with $NADP^+$ at 25°. 11 μM Enzyme flavin in 0.1 M phosphate buffer (pH 7.5), containing 1 mM EDTA, titrated with $NADP^+$ in the same buffer and emission spectra (excitation at 398 nm) recorded. Spectra corrected for dilution and scatter of the solvent. $NADP^+$ additions per mole of flavin: ○ —— ○, none; ● —— ●, 0.35 mole; □ —— □, 0.7 mole; ■ —— ■, 1.3 moles; △ —— △, 1.7–6 moles.

at 398 nm, the isosbestic point in the spectra of enzyme and its $NADP^+$-complex. At the same time a shoulder at 520 nm becomes visible. Maximal quenching obtained in three independent experiments was about 35–40%; this value was obtained at about 1.0 mole $NADP^+$/mole of flavin. Thio-$NADP^+$ induces the same type of quenching and a similar shift in the emission maximum, but much higher concentrations are necessary. Only 10–12% quenching is observed at a $TNADP^+$ concentration of 0.2 mM.

The dissociation constants calculated for the $NADP^+$ and $TNADP^+$ complex are about 5 μM and 90 μM, respectively, indicating a much lower affinity for thio-$NADP^+$ than for $NADP^+$. The difference in affinity is an explanation for the stronger inhibitory effects of $NADP^+$ than of $TNADP^+$, as observed in the kinetic experiments (cf. CHAPTER 6). From the results it may be concluded that the $NADP^+$-complex with the lower dissociation constant, which is responsible for the shifts in the visible region of the absorption spectrum, also induces the flavin emission shift and the fluorescence quenching. The fluorescence characteristics are not influenced by NAD^+, thio-NAD^+ and 2'AMP, neither do they compete with $NADP^+$.

5.2.3. *Effect of $NADP^+$ on the optical rotatory dispersion and circular dichroism*

The optical rotatory dispersion and circular dichroism absorption curves of *Azotobacter* transhydrogenase in the absence and presence of $NADP^+$ and of its apoenzyme are shown in FIG. 5.4 and FIG. 5.5.

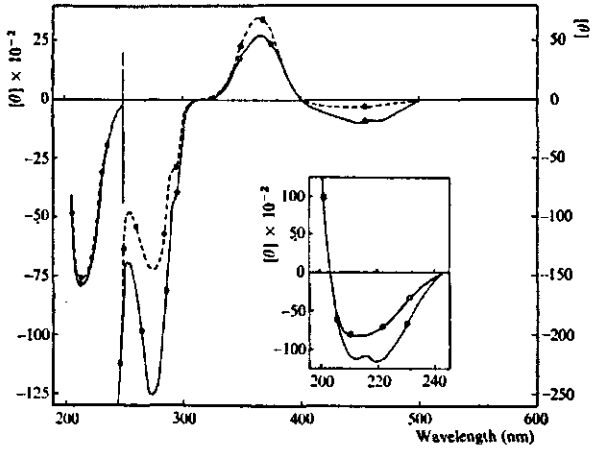

FIG. 5.4. Effect of $NADP^+$ on the Circular Dichroism of *Azotobacter* transhydrogenase at 25°. Enzyme in 0.1 M potassium phosphate buffer (pH 7.5) containing 1 mM EDTA. Measurements performed at 2.6 mg/ml in cells of 0.5, 0.1 and 0.05 cm pathlength. Spectra corrected for the presence of free $NADP^+$. o —— o, no additions; • —— •, in the presence of 3.4 moles $NADP^+$/mole flavin. Inset: CD curve of *Azotobacter* apoenzyme (■ —— ■) prepared as described in CHAPTER 2, together with the $NADP^+$ free enzyme (o —— o). Protein concentration of apoenzyme 0.03 mg/ml. Measurements with the apoenzyme performed at 10° in cells of 0.1 cm pathlength.

The CD spectrum of the enzyme in the absence of $NADP^+$ is characterized in its 200–500 nm region by four major ellipticity extrema at about 450 nm, 365 nm, 273 nm, and 212 nm, with mean residue molar ellipticities [θ] of −20, +55, −250 and −8900 degrees cm^2/dmole, respectively. A marked shoulder is present at 295 nm. The apoprotein, which shows no obvious bands at wavelengths longer than 250 nm, is characterized by a well defined negative helix band in the 210–220 nm region, indicating that the other bands for the holoenzyme could be attributed to flavin-flavin and flavin-protein interactions.

The CD spectrum obtained for the enzyme is totally different from that of free FAD (HESP et al., 1969) and resembles that of free FMN (EDMONDSON and TOLLIN, 1970). Free FAD has negative bands at 375 nm and 275 nm, positive bands at 340 nm and 255 nm, while a marked shoulder is present at 310 nm; no CD band is present at 450 nm. Free FMN has a positive band at 340 nm and a negative band at 450 nm. With respect to free and bound FAD the reversal of the 375 nm band and the presence of the 450 nm band is characteristic. The 375 nm band may be related to an open form of the enzyme bound flavin, resulting in properties similar to those of FMN (*MILES and URRY, 1968*). The presence of the 450 nm band may, according to EDMONDSON and TOLLIN (1970) be the result of specific protein – FAD interactions which break up the complexing of the isoalloxazine ring with the adenine ring and position the ribityl side chain and the isoalloxazine ring in such a manner that the 450 nm band can be observed. In FAD the ribityl side chain is not able to interact strongly with the isoalloxazine ring as a result of steric limitations caused by the complexing with the adenine ring resulting in the absence of the 450 nm band. In this respect the transhydrogenase closely resembles the FAD containing flavoproteins *p*-hydroxybenzoate hydroxylase from *Pseudomonas putida* (HESP et al., 1969) and ferredoxin-$NADP^+$ reductase from Spinach (EDMONDSON and TOLLIN, 1970), but differs from *Azotobacter* (cf. CHAPTER 7) and pig heart lipoamide dehydrogenase (VEEGER and VOETBERG, to be published). In the latter case also no optical activity above 400 nm can be observed, indicating that the side chain interactions may be very weak. The CD spectrum of the transhydrogenase is just the reverse of several FMN-containing flavoproteins, e.g. flavodoxin from *Pseudomonas elsdenii*, *Clostridium pasteurianum* and *Rhodospirillum rubrum* and Shetna flavoprotein, indicating that the flavin environment of transhydrogenase is similar to that in the other proteins except that opposite polarizations in the flavin transitions are induced (EDMONDSON and TOLLIN, 1970). The spectrum is, however, quite different in shape from those of the FAD-containing oxidases as D-amino acid oxidase (AKI et al., 1966), glucose oxidase and L-amino acid oxidase (EDMONSON and TOLLIN, 1970), which are characterized by positive dichroic bands at 380 nm and in the case of L-amino acid oxidase also at longer wavelengths.

In the presence of $NADP^+$ no drastic changes in overall shape of the CD curve are observed, only the molar ellipticities of several bands change. The 450 nm dichroic band is considerably lowered and the 365 nm band has a somewhat higher ellipticity indicating that either the enzyme-bound flavin is

directly involved in the binding of $NADP^+$ or that other groups in the vicinity of the flavin exert their influence upon binding. The most striking changes, however, are observed in the 250–300 nm region. Upon the addition of increasing amounts of $NADP^+$ the 273 nm band is considerably lowered and flattened while the shoulder at 290 nm becomes more pronounced; the 365 nm band is slightly widened in the region 310–340 nm. Only very small changes are obtained in the α-helix region of the spectrum. These results might suggest that $NADP^+$ binding results in conformational changes of the enzyme-bound flavin since the changes observed can be related to the specific flavin dichroic band. The decrease of the 450 nm band thus indicates a weakening or changing of the side chain interactions and complexing of the isoalloxazine ring with the adenine ring (EDMONDSON and TOLLIN, 1970) or $NADP^+$, resulting in a decrease in fluorescence of the bound FAD as observed in the fluorescence experiments. Protein conformational changes due to dissociation may be responsible for the changes at 273 nm. On the other hand a different conformation of bound flavin due to $NADP^+$ binding can also be responsible for the changes, because flavin has CD bands in this region, a conclusion supported by the fact that hardly any changes are observed in the α-helix region. Local changes, however, do not need to result in a large effect on the α-helix content.

Addition of $NADP^+$ to the apoenzyme does not result in changes of the CD characteristics.

The ORD curves for the transhydrogenase in the absence and presence of $NADP^+$, as given in FIG. 5.5, are characterized by minima at about 233 nm, maxima at about 200 nm, and a slight shoulder at 210–220 nm. Both curves are anomalous and do not conform to the MOFFIT-YANG equation. The 300–600 nm region of the curves is very similar to that of D-amino acid oxidase (AKI et al., 1966) and the anomaly of the ORD curves is evidently the consequence of the superposition of Cotton effects of the chromophores of the bound coenzyme and these of the protein moiety.

In the absence of $NADP^+$ a clear-cut Cotton effect is found in the absorption band at 280 nm. Upon the addition of $NADP^+$ the Cotton effect at 280 nm disappears, while the magnitudes at 233 nm and 200 nm are hardly influenced. The fact that incomplete removal of $NADP^+$ already resulted in a partial disappearance of this Cotton effect points to a close relationship with the changes in the CD absorption curves at 275 nm, and is thus the result of the same effects. The results also indicate that the far ultraviolet rotatory dispersion is virtually useless as an indicator for events occurring at the active site and that the ultraviolet to visible part of the dispersion curve is very sensitive to changes occurring at the active site. A similar situation was found for alcohol dehydrogenase (LI et al., 1962) where rotatory dispersion titrations were introduced for the investigation of mechanisms of enzyme action and of binding of nucleotides to the enzyme.

Semiquantitative values for the helix content could be calculated from the ORD and CD magnitudes at 233 nm and 222 nm, respectively by using poly-α-L-glutamic acid (PGA) as a reference standard. For the holo-enzyme and its

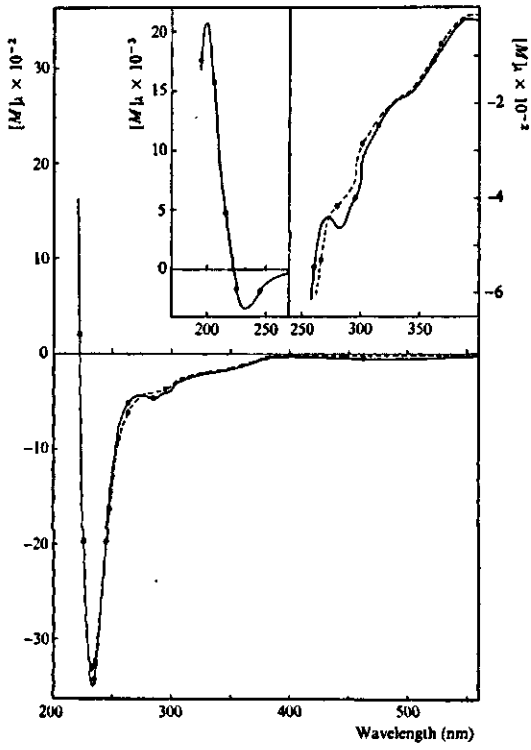

FIG. 5.5. Effect of $NADP^+$ on the optical rotatory dispersion of *Azotobacter* transhydrogenase in 0.1 M potassium phosphate buffer (pH 7.5), containing 1 mM EDTA, at 25°. Measurements performed at 2.6 mg/ml and 0.52 mg/ml (dilution had no effect on the dissociation) in cells of 1.0, 0.5, 0.2 and 0.05 cm path length. The maximum at 200 nm was determined at a protein concentration of 0.24 mg/ml. Molar rotation expressed as mean residue molar rotation in degrees cm^2/dmole. o — o — o, no additions; • — • — •, in the presence of 3.4 moles $NADP^+$/mole of flavin. Inset: the same curves with a different scale.

$NADP^+$-complex these data have no significance, due to the contribution of the prosthetic group at these wavelengths, which might give the CD band at 210–220 nm its peculiar shape. Furthermore URRY an LI (1969) have shown that large shifts at 210 nm occur, when the size of the macromolecule exceeds the wavelength. It is in our opinion a coincidence that the ORD spectrum shows a 232 nm minimum. The apoenzyme spectrum shows characteristics of an α-helix and a content of 22% can be calculated. On the other hand no significance can be attributed to this value. Not only because of uncertainties in the method of calculation but mainly because of the observation that the apoenzyme can be reconstituted to about 50% activity (cf. CHAPTER 3), which indicates the presence of a large amount of altered protein.

5.2.4. *Effect of $NADP^+$ and NAD^+ on the chemical reduction of transhydrogenase*

When the *Azotobacter* transhydrogenase was titrated anaerobically with NADH, NADPH and sodium dithionite, upon a small addition of reductant the decline of the absorbance over the region 300–500 nm was followed by an increase of the absorbance to the initial level when NADH or dithionite was used or to a level typical for the intermediate stages of the $NADP^+$-complex formation in the case of NADPH as reductant. The rate of re-oxidation could

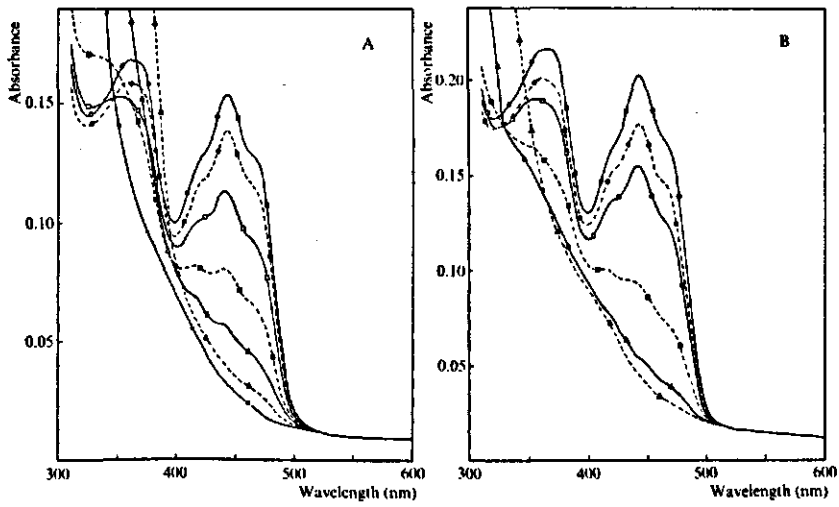

FIG. 5.6. Anaerobic reduction of *Azotobacter* transhydrogenase at 25°. Enzyme in 0.1 M potassium phosphate buffer (pH 7.5), containing 1 mM EDTA in a final volume of 2.25 ml. NADPH and dithionite dissolved in the same buffer. Spectra recorded after mixing and corrected for dilution and traces of oxygen present. A. Titration with NADPH in the presence of *Neurospora* NADase. Cell contained 13 μM transhydrogenase flavin. o —— o, oxidized enzyme, in the absence and presence of NAD-nucleosidase; • —— •, 0.3 mole NADPH/mole flavin; □ —— □, 0.75 mole NADPH/mole flavin; ■ —— ■, 1.4 moles NADPH/mole flavin; △ —— △, 2.6 moles NADPH/mole flavin; ▲ —— ▲, 7.3 moles NADPH/mole flavin; × —— × —— ×, spectrum of dithionite-reduced enzyme. B. Anaerobic titration with sodium dithionite. The concentration of sodium dithionite, made up in the same buffer under anaerobic conditions, was determined by simultaneously titrating lumiflavin under identical conditions. The cuvette contained 16 μM transhydrogenase flavin. o —— o, oxidized enzyme; • —— •, 0.3 mole dithionite/mole flavin; □ —— □, 0.55 mole dithionite/mole flavin; ■ —— ■, 1.3 moles dithionite/mole flavin; △ —— △, 1.8 moles dithionite/mole flavin; ▲ —— ▲, 2.5 moles dithionite/mole flavin.

be increased by shaking. The lag-period observed, varied from experiment to experiment. Since it was also present when lumiflavin was titrated with dithionite, it was concluded that the lag-period was due to about 10–40 nmoles of residual oxygen. For this reason all calculations were corrected for the lag-periods observed. Because of the fact the oxygen contamination was of the same order as the amounts of enzyme used, control experiments in the absence of product had to be performed in the presence of *Neurospora* NADase, which hydrolyses only the oxidized form of the pyridine nucleotides.

Upon anaerobic titration with NADPH in the presence of *Neurospora* NADase the results shown in FIG. 5.6, A were obtained. After addition of up to 0.9 mole of NADPH per mole of flavin a linear decline in absorbance is found at 440 nm. Above this ratio the absorbance in the 400–500 nm region still gradually declines upon the addition of NADPH but the absorbance at 330 nm starts to increase likewise. The presence of unreacted NADPH is indicated by the deviations from linearity observed in the titration curves at

440 nm and the appearance of an absorption band at 340 nm. The addition of even 4 moles of NADPH per mole of total flavin does not yield the typical spectrum of the fully reduced enzyme as observed in the sodium dithionite titration. The maximal absorbance change at 440 nm is in the order of 70–72% of the initial absorbance. Extrapolation of the linear part of several titration curves reveals that 2 moles of NADPH per mole of flavin are necessary for complete reduction. The dissociation constant calculated from the non-linear part of the titration curve, $K_D = 1.6-1.9\ \mu M$, which is the value for the second molecule of NADPH. In the presence of NADase no long wavelength band (VAN DEN BROEK and VEEGER, 1970) is observable. Air re-oxidation of the fully reduced enzyme is rapid and the original oxidized enzyme spectrum is obtained. The intermediate stages with respect to the 340 nm and 440 nm absorbances are completely identical with those obtained upon titration with NADPH.

In contrast to the results obtained for the *Pseudomonas* transhydrogenase (COHEN, 1967; COHEN and KAPLAN, 1970) the reduction of *Azotobacter* transhydrogenase by NADH proceeds without any activator. When the transhydrogenase is titrated anaerobically with NADH in the presence of NADase an identical picture is obtained as for the NADPH reductions, e.g. no long wavelength band, and up to 0.9 mole of NADH per mole of flavin no deviation from linearity in the titration curve is found. Also in this case high concentrations of NADH are necessary to obtain full reduction. It can be calculated that 2 moles of NADH per mole of flavin are necessary for complete reduction; the K_D for the second NADH molecule is 1.2–1.5 μM. The original spectrum of the oxidized enzyme is re-obtained after re-oxidation by air.

The requirement of four electrons per flavin molecule could be confirmed by sodium dithionite titrations. The results of such a titration are summarized in FIG. 5.6, B. Up to about 1.8 moles of dithionite per mole of flavin a linear decrease in absorbance at 440 nm occurs. Reduction is complete at about 2.0–2.2 moles of dithionite per mole of total flavin and no further changes in the visible spectrum are obtained upon the addition of more dithionite; the presence of unreacted dithionite is indicated by an increase in absorbance at about 315 nm. The titration curve for the dithionite reduction is completely linear and from extrapolation it may be concluded that about 2 moles of dithionite per mole of flavin are necessary for complete reduction. Maximum reduction obtained with dithionite is 78–80% of the initial absorbance at 440 nm, a value which is higher than finally obtained upon titration with NADH and NADPH in the presence of *Neurospora* NADase. After air re-oxidation the original spectrum is obtained. From the fact that between 0.3 and 1.8 moles of dithionite per mole of enzyme flavin an isosbestic point is found at 330 nm, which is not isosbestic with the spectrum of the oxidized enzyme, it might be concluded that the enzyme contains a small amount of impurity. A similar effect can be seen in the early stages of titration with NADPH.

In the presence of NAD^+ and $NADP^+$ the anaerobic reduction of the transhydrogenase proceeds considerably different from the patterns in the absence of these nucleotides, the results depend on the concentration of the product

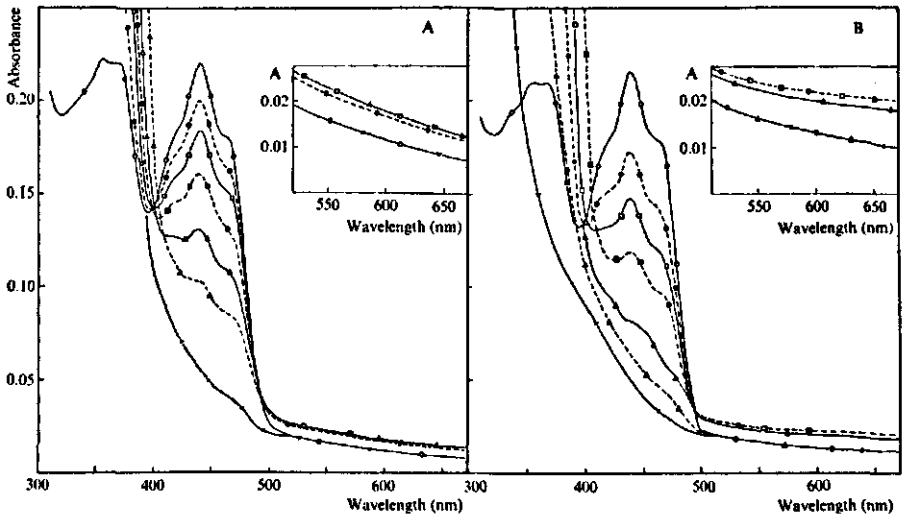

FIG. 5.7. Anaerobic reduction of *Azotobacter* transhydrogenase in the presence of high concentrations of $NADP^+$ at 25°. Enzyme and pyridine nucleotides in 0.1 M potassium phosphate buffer, containing 1 mM EDTA. Spectra recorded after mixing and corrected for dilution and traces of oxygen present. A. Titration with NADPH. The anaerobic cuvette contained 17 μM enzyme flavin and 180 μM $NADP^+$. o —— o, oxidized enzyme in the presence of $NADP^+$; ● —— ●, 1.5 moles NADPH/mole flavin; □ —— □, 3.4 moles NADPH/mole flavin; ■ —— ■, 5.8 moles NADPH/mole flavin; △ —— △, 11.3 moles NADPH/mole flavin; ▲ —— ▲, 27 moles NADPH/mole flavin; × —— × —— ×, enzyme reduced with NADPH in the presence of NADase. B. Titration with NADH. The cuvette contained 17 μM enzyme flavin and 190 μM $NADP^+$. o —— o, oxidized enzyme in the presence of $NADP^+$; ● —— ●, 7.3 moles NADH/mole flavin; □ —— □, 15.5 moles NADH/mole flavin; ■ —— ■, 44 moles NADH/mole flavin; △ —— △, enzyme reduced with NADH in the presence of NADase; ▲ —— ▲, enzyme reduced with NADH in the presence of NAD^+; × —— ×, enzyme reduced with sodium dithionite.

present at the beginning of the titration. In the presence of product all reduction stages are characterized by the presence of a long wavelength band above 500 nm indicating a specific interaction between reduced flavin and NAD^+ or $NADP^+$ which is possibly of the charge-transfer type (MASSEY and PALMER, 1962). Because of its very low extinction coefficient it is very difficult to determine the ratio of reductant to flavin at which the band is optimal. It is surprising, however, that the 500–600 nm band does not increase in magnitude, upon progression of the decline of the 400–500 nm band. This indicates that we are dealing with two reductive processes.

FIG. 5.7, A shows the effect of high concentrations of $NADP^+$ on the absorbance changes upon anaerobic titration of the enzyme with NADPH. Strong retardation of the flavin reduction occurs as indicated by the high absorbances at 340 nm of unreacted NADPH. Very high concentrations of NADPH are necessary to obtain partial reduction of the flavin. At lower $NADP^+$ concentrations similar pictures are obtained, although the reduction is less retarded.

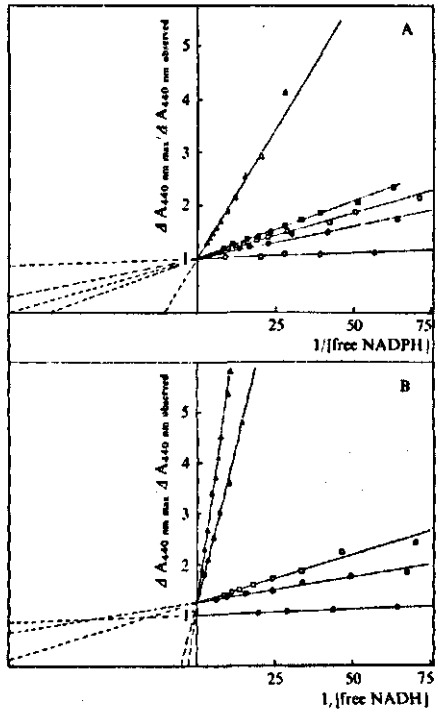

FIG. 5.8. BENESI-HILDEBRAND plots for the reduction of *Azotobacter* transhydrogenase in the absence and presence of products. Reciprocal of relative absorbance change at 440 nm plotted vs. reciprocal of free reductant (mM^{-1}). Anaerobic reduction experiments performed at 25° under the conditions indicated. Enzyme and additions in 0.1 M potassium phosphate buffer (pH 7.5), containing 1 mM EDTA in a total volume of 2.5 ml. Spectra recorded after mixing and corrected for dilution and traces of oxygen present. A. Titration with NADPH in the absence and presence of different amounts of $NADP^+$. o —— o, no $NADP^+$ + *Neurospora* NADase; • —— •, 1.2 moles of $NADP^+$ per mole of flavin; □ —— □, 1.7 moles of $NADP^+$ per mole of flavin; ■ —— ■, 2.4 moles of $NADP^+$ per mole of flavin; △ —— △, 10 moles of $NADP^+$ per mole of flavin. B. Titration with NADH in the absence and presence of NAD^+ and $NADP^+$. o —— o, no NAD^+ or $NADP^+$, in the presence of *Neurospora* NADase; • —— •, 0.8 mole of NAD^+ per mole of flavin; □ —— □, 1.0 and 1.5 moles NAD^+ per mole of flavin; △ —— △, 11.3 moles of $NADP^+$ per mole of flavin; ▲ —— ▲, 17 moles of $NADP^+$ per mole of flavin.

From BENESI-HILDEBRAND plots (BENESI and HILDEBRAND, 1949), relating the reciprocals of the absorbance change at 440 nm to unreacted NADPH it could be derived that at infinite NADPH concentrations the same reduction levels should be obtained in the presence and absence of $NADP^+$ (FIG. 5.8, A). Thus $NADP^+$ competes with the second NADPH molecule in preventing full reduction. The calculated dissociation constant of $NADP^+$ for this process is 3–4 μM. $NADP^+$ interferes with the reduction of the oxidized enzyme by the first molecule of NADPH in a non-competitive way. Unfortunately no infor-

mation could be obtained on the number of $NADP^+$ molecules involved in this latter process.

At low concentrations of NAD^+ the reduction of the enzyme by NADH is more retarded than that by NADPH in the presence of low concentrations of $NADP^+$. In the presence of high concentrations of $NADP^+$ the reduction of the enzyme by NADH is retarded very strongly and much larger amounts of NADH are necessary (FIG. 5.7, B). Even compared with the system NADPH-$NADP^+$ the reduction proceeds more retarded.

BENESI-HILDEBRAND plots of FIG. 5.8 show that in the presence and absence of $NADP^+$ the same reduction can be obtained at infinite NADPH concentration. On the other hand the NADH reduction proceeds less extensively in the presence of either NAD^+ or $NADP^+$ as compared with the system NADH + NADase (FIG. 5.7, B and FIG. 5.8, B). This difference is thus dependent on the presence of NAD^+, and thus must be due to different intermediates in the reduction process. Due to the reaction, in the experiment with $NADP^+$ also NAD^+ is present in large quantities. From the plots of FIG. 5.8, B it is clear that NAD^+ and $NADP^+$ interfere with the reduction to the NAD^+-dependent 4-equivalent reduced intermediate in a competitive way. Assuming a K_D for NADH of 1.8 μM, dissociation constants for NAD^+, $K_D = 0.7$ μM and for $NADP^+$, $K_D = 1.3$ μM, can be calculated. The latter value has to be corrected for the presence of NAD^+ and is actually higher, cf. 3–4 μM as calculated for FIG. 5.8, A. From the experiment of FIG. 5.7, B, it can be shown that NAD^+ prevents the reduction of the oxidized enzyme by the first molecule of NAD^+ in a non-competitve way. Here also no information could be obtained on the actual number of NAD^+ molecules involved.

The re-oxidation by air of the enzyme reduced in the presence of NAD^+ and $NADP^+$ differs completely from the picture obtained with enzymes reduced in the absence of these oxidized nucleotides. The absorbance at 440 nm has already completely regained its original level before all NADH or NADPH is oxidized by the transhydrogenase. The rate of re-oxidation of the reduced nucleotides is completely determined by the concentration of NAD^+ or $NADP^+$ present, the higher the concentration the lower the rate of oxidation. In case NAD^+ is present the spectrum of the original enzyme is regained, in the case of $NADP^+$ the typical spectrum of the $NADP^+$-complex is obtained.

The reduction of the enzyme flavin by dithionite is also influenced by the presence of $NADP^+$. Depending on the $NADP^+$ concentration present at the beginning of the titration the amount of dithionite needed for complete reduction is increased by about the amount of $NADP^+$ present. The titration curves for the dithionite reduction at different levels of $NADP^+$ are still linear and maximal reduction levels obtained are the same as in the control, in the absence of $NADP^+$. The spectra are characterized by the presence of a small absorption band above 500 nm, which points to the interaction of reduced flavin and $NADP^+$ and by the presence of an isosbestic point at 365 nm. The appearance of a 340 nm band, which is especially pronounced when high $NADP^+$ concentrations are present, indicates that the reduced flavin is easily

re-oxidized by $NADP^+$, with the formation of NADPH. On the other hand the possibility of direct reduction of $NADP^+$ by dithionite cannot be exluded. The following section, however, shows that the dithionite-reduced enzyme can be rapidly oxidized by $NADP^+$.

5.2.5. *Effect of $NADP^+$ on reduced transhydrogenase*

In the foregoing anaerobic reduction experiments it is clearly demonstrated that $NADP^+$ strongly influences the chemical reduction of the transhydrogenase, the level obtained being completely dependent on the $NADP^+$/donor ratio. It was of interest to know whether typical spectral intermediates were produced upon anaerobic titration of reduced enzyme with $NADP^+$ or if the fully oxidized enzyme was regained.

From the literature several reports regarding spectral intermediates of reduced flavoproteins and pyridine nucleotides are known. VEEGER and MASSEY (1963) showed that the spectrum of the 2-equivalent reduced lipoamide dehydrogenase is considerably modified in the presence of NAD^+, the major spectral changes occurring immediately, followed by further slow changes, which are accompanied by the slow development of an EPR-signal (MASSEY et al., 1966). Recent stopped flow experiments (VEEGER et al., 1970) point to the fact that the 2-equivalent-reduced-lipoamide dehydrogenase-NAD^+ complex is the catalytically active species of the overall reaction. Kinetically active enzyme-substrate complexes of dithionite-reduced NADH-peroxidase and several pyridine nucleotide analogues were demonstrated by DOLIN (1960, 1966); the spectra formed on the addition of NAD^+ or NADH to dithionite-reduced enzyme were almost identical to the spectrum formed on the addition of NADH to oxidized enzyme. Conflicting reports have appeared regarding spectral intermediates of old yellow enzyme and pyridine nucleotides (HAAS, 1937; EHRENBERG and LUDWIG, 1958; BEINERT and SANDS, 1960; NAKAMURI et al., 1965). MASSEY et al., (1970) were able to determine the spectrum of the rapidly produced intermediate enzyme form upon reduction of old yellow enzyme with NADPH and to calculate the spectrum obtained upon titration of reduced enzyme with $NADP^+$. It was shown that both spectra had characteristics in common, but differed significantly in extinction coefficients, particularly in the wavelength region above 500 nm. From these results the authors concluded that the intermediates were not identical with the simple flavin semiquinones, but possibly represented partially reduced forms of the enzyme.

Upon the addition of $NADP^+$ to NADPH-reduced transhydrogenase the spectrum of the partially or totally reduced enzyme disappears immediately and a return of the visible absorbance is obtained, the level of absorbance depending on the concentration of $NADP^+$. Formation of the different intermediate spectra is complete before measurements can be made and under the anaerobic conditions the spectra do not change for the next fifteen hours, indicating that the intermediates obtained after each addition of $NADP^+$ are quite stable. BENESI-HILDEBRAND plots (BENESI and HILDEBRAND, 1949) were drawn for the wavelength region 400–500 nm to calculate the spectrum at

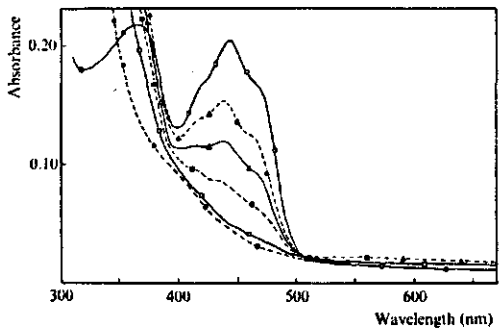

FIG. 5.9. Titration of *Azotobacter* transhydrogenase with $NADP^+$ after reduction with sodium dithionite. 16 μM Transhydrogenase flavin in 0.1 M phosphate buffer (pH 7.5), containing 1 mM EDTA was reduced with 3.1 moles of sodium dithionite per mole of flavin and titrated anaerobically with $NADP^+$. Spectra recorded after mixing and corrected for dilution and traces of O_2 present. o —— o, oxidized flavin; • —— •, after reduction with dithionite; □ —— □, 1.1 moles $NADP^+$/mole flavin; ■ —— ■, 2.2 moles $NADP^+$/mole flavin; △ —— △, 3.8 moles $NADP^+$/mole flavin; ▲ —— ▲, 6.8 moles $NADP^+$/mole flavin.

infinite $NADP^+$ concentration. The calculated spectrum is almost identical with that obtained after re-oxidation e.g. with the $NADP^+$-complex.

When the NADH-reduced enzyme is oxidized by $NADP^+$, the spectra obtained after each addition are almost identical with those obtained in the titration experiment with NADPH-reduced enzyme. The only difference being the more pronounced disappearance of the long wavelength band in the case of the NADPH-reduced enzyme. The level of absorbance of the re-oxidized enzyme at infinite $NADP^+$ concentration as calculated from BENESI-HILDEBRAND plots is, however, not identical with that of the re-oxidized enzyme. The spectral characteristics of the oxidized enzyme-$NADP^+$ complex are present at infinite $NADP^+$ concentrations, but the absorbance is about 8% too low.

When enzyme was reduced with sodium dithionite the amount of $NADP^+$ needed to reconstitute the visible absorbance depended on the concentration of unreacted dithionite. In the absence of the latter, as indicated by the lack of the typical absorbance band at 315 nm, the additions of $NADP^+$ resulted in a direct return of the visible absorbance and the spectrum of the oxidized $NADP^+$-complex could be calculated at infinite $NADP^+$ concentration from BENESI-HILDEBRAND plots. A dissociation constant for the reduced enzyme-$NADP^+$ complex of about 10 μM could be calculated. When the enzyme was reduced with excess dithionite, the initial addition of $NADP^+$ only resulted in the disappearance of the dithionite absorbance at 315 nm which was replaced by an absorbance at 340 nm indicating that NADPH was formed from dithionite and $NADP^+$. At the same time only slight changes in the visible absorption region occurred, of which the appearance of a slight absorbance at longer wavelengths was most striking. As soon as the amount of added $NADP^+$ was

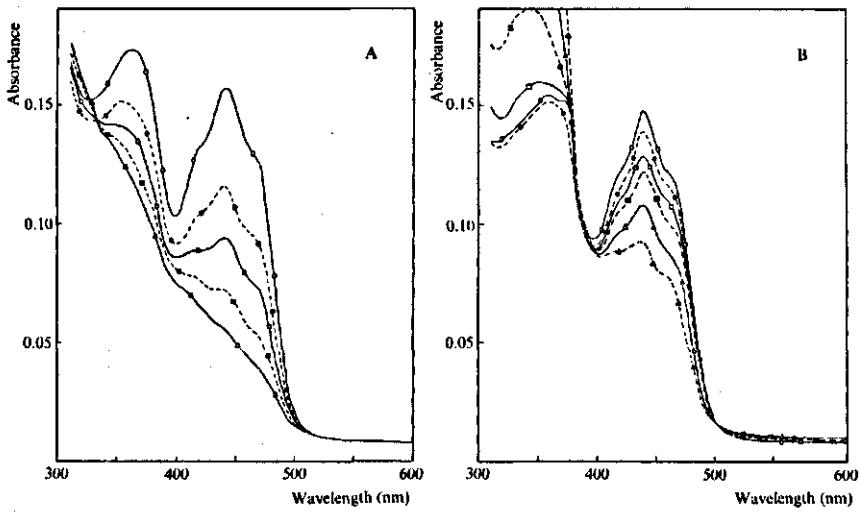

FIG. 5.10. The effect of light on the spectrum of *Azotobacter* transhydrogenase in the absence and presence of $NADP^+$. 13 μM Enzyme flavin in 0.1 M potassium phosphate buffer (pH 7.5), containing 25 mM EDTA in a final volume of 2.25 ml was, after removal of O_2, illuminated with visible light (> 390 nm) from a 500 W Xenon lamp at 16°. At the times indicated spectra were recorded; corrections were made for the observed lag period due to residual oxygen. A. No $NADP^+$. o —— o, oxidized enzyme. Time of irradiation: ● —— ●, 2 min; □ —— □, 4 min; ■ —— ■, 7.5 min; △ —— △, 14 min. B. In the presence of 14 moles $NADP^+$ per mole of flavin. o —— o, oxidized enzyme-$NADP^+$ complex. Time of irradiation: ● —— ●, 3 min; □ —— □, 6 min; ■ —— ■, 12 min; △ —— △, 25 min; ▲ —— ▲, 50 min.

equivalent to that of unreacted dithionite the spectrum of the reduced enzyme disappeared and was replaced by intermediate oxidation reduction stages, characterized by an increase of absorbance over the whole wavelength range from 400 to 700 nm (FIG. 5.9). The calculated dissociation constant (K_D) was in the order of 40 μM.

5.2.6. *Effect of $NADP^+$ on the photoreduction of transhydrogenase*

In common with many other flavoproteins (MASSEY and PALMER, 1966; MCCORMICK et al., 1967; ZANETTI et al., 1968; MAYHEW and MASSEY, 1969) *Azotobacter* transhydrogenase can be reduced anaerobically by irradiation with visible light in the presence of high concentrations of EDTA, the rate and extent of reduction depending on the presence of $NADP^+$.

FIG. 5.10 summarizes the results obtained upon photochemical reduction in the absence and presence of $NADP^+$. After an initial lag period of about 1.5 min, due to residual oxygen, a regular decline in absorbance is observed. In the absence of $NADP^+$ the first reduction stage is characterized by a decrease in absorbance in the wavelength region 320–500 nm, while the different stages of reduction have an isosbestic point at 335 nm. The spectrum of the

oxidized enzyme is not isosbestic at this wavelength. Thus it can be concluded, that we are dealing with the same reduction stages as obtained upon titration with sodium dithionite (FIG. 5.6, B). No long wavelength absorbance is observable. Maximal reduction is about 70% of the initial absorbance at 440 nm. Addition of NADH or NADPH to the photoreduced species does not lead to further changes in absorbance in the visible region. The possibility, however, that the produced species is unreactive with NADH or NADPH cannot be excluded; the latter type of behaviour has been observed for several flavoproteins (ZANETTI et al., 1968; MASSEY and GIBSON, 1964; MASSEY et al., 1966). When air was re-admitted the spectrum returned to that of the original, oxidized enzyme immediately via identical intermediate stages. Irradiation of enzyme partially reduced with NADH or NADPH resulted in a somewhat accelerated formation of the ultimate reduction stage; the spectra observed, however, are completely identical to those given in FIG. 5.10, A. The slightly increased absorbance at wavelength $>$ 500 nm, present after the initial reduction with NAD(P)H, indicative for the interaction between reduced enzyme and $NAD(P)^+$, did not change upon irradiation. Re-oxidation occurred very rapidly and when NADPH was used for the initial reduction the typical spectrum of the $NADP^+$-complex was obtained. In the presence of a high concentration of $NADP^+$ the photochemical reduction is delayed considerably; after 50 minutes of irradiation only a 35% decline of the initial absorbance is obtained. The results obtained in the presence of 14.5 moles of $NADP^+$ per mole of enzyme flavin are summarized in FIG. 5.10, B. The figure is characterized by the presence of a slightly increased absorbance at wavelength $>$ 500 nm and by the presence of a 340 nm band. As soon as a slight decrease in absorbance over the wavelength region below 500 nm has occurred, this 340 nm band starts to develop as a consequence of the oxidation of the reduced enzyme by $NADP^+$, resulting in the formation of NADPH. Upon further irradiation the absorbance at 440 nm decreases regularly, but the time course indicates that a very long irradiation period would be needed to obtain the same reduction level as in the absence of $NADP^+$.

5.3. DISCUSSION

From the results shown it may be concluded that $NADP^+$ strongly influences the redox properties and thus the spectral properties of the *Azotobacter* transhydrogenase. The spectral titrations indicate that two $NADP^+$-complexes, with totally different dissociation constants, exist. The $NADP^+$-complex with the highest affinity is mainly responsible for the absorbance changes in the visible region of the spectrum, the quenching of the flavin fluorescence and the shift of its maximum; moreover it is responsible for the changes in the ORD and CD curves since it was observed that incomplete removal of $NADP^+$ upon dialysis already results in a decrease of the maximal effects obtainable. The $NADP^+$-complex with the lowest affinity causes the spectral differences in the 300–360 nm region of the spectrum. The existence of similar complexes of

$NADP^+$ and glutathione reductase (STAAL et al., unpublished), $NADP^+$ and ferredoxin $NADP^+$-reductase (FOUST et al., 1969) and NAD^+ and lipoamide dehydrogenase from pig heart (VISSER et al., 1970) is of great interest, because some of these enzymes are closely related. In the latter case the existence of 2 NAD^+-complexes was demonstrated and the spectral differences were shown to be pH and temperature dependent (VEEGER et al., 1970). It was concluded that the spectral shifts in lipoamide dehydrogenase are probably due to changes in polarity of the flavin (cf. VISSER et al., 1970).

Shifts in the absorption spectra have been observed upon binding flavin nucleotides to protein (PENZER and RADDA, 1967); the 375 nm band shifts to shorter wavelengths, and the 447 nm band to longer whereas in most flavoproteins shoulders are present at 430 nm and 480 nm (MASSEY and GANTHER, 1965). The splitting of the latter band might be the result of a non-polar environment (PENZER and RADDA, 1967). Several explanations are given for the shifts in absorbance: interaction of the isoalloxazine ring with dipolar groups in the protein (THEORELL et al., 1960), interaction of a protein tyrosyl group with flavin (EDMONDSON and TOLLIN, 1970), interaction of a protein tryptophan group with flavin (VEEGER and VOETBERG, to be published) or changes in polarity (VEEGER et al., 1966). In the majority of flavoproteins the maximum of flavin absorbance in the visible part of the spectrum is at wavelengths larger than 447 nm. Transhydrogenase is an exception in this respect, because of its maximum absorbance at 442 nm (438 nm for the enzyme-$NADP^+$ complex). The only other flavoprotein known which shows this type of spectrum is the electron transport flavoprotein (ETF), acting in fatty acid and sarcosine oxidation (CRANE and BEINERT, 1954; FRISELL and MACKENZIE, 1962). Until now, no explanation can be offered for this phenomenon. From studies on the relation between flavin interaction and protein structures, DE KOK (1970) postulated that upon binding of FAD to the apoenzyme of lipoamide dehydrogenase either the interaction with adenine is completely broken and substituted by protein interactions or that the complex with adenine is partially opened upon binding of FAD to the apoenzyme, resulting in a quenching of protein fluorescence and an increase in flavin fluorescence intensity (cf. VISSER, 1970). According to EDMONDSON and TOLLIN (1970), the flavin adenine complex prevents the interaction of the ribityl hydroxyl groups with the isoalloxazine ring. Upon binding of flavin to protein the latter interaction will greatly increase, because specific protein-FAD interactions will break up the flavin-adenine complex and position the ribityl side chain and the isoalloxazine ring for their interaction. In the transhydrogenase the latter type of interaction might be present, because the flavin fluorescence of the protein bound flavin is higher than that of the dissociated flavin and the CD absorption curve shows the typical 450 nm optical activity.

Addition of $NADP^+$ influences the flavin fluorescence by quenching and lowers the magnitude of rotational strength of the long wavelength CD-band. This could possibly mean that interaction between isoalloxazine and $NADP^+$ occurs, or that the ribityl-isoalloxazine interaction is weakened. However,

the influence of other groups in the vicinity of the flavin cannot be excluded. Moreover, protein conformational changes are also very likely, because $NADP^+$ causes dissociation of the enzyme, while pronounced changes in the CD and ORD behaviour are found in the 250–300 nm region.

The anaerobic titration experiments with NADH and NADPH in the presence of *Neurospora* NAD^+-nucleosidase show that 2 moles of reductant (4 electron equivalents) are required to reduce one mole of enzyme bound flavin; this requirement was confirmed by sodium dithionite titrations. Since full reduction of one mole FAD requires only 2 electron equivalents, it seems very likely that groups other than FAD in the *Azotobacter* transhydrogenase are reduced by reduced pyridine nucleotides and dithionite. Three examples of flavoproteins are known, i.e. lipoamide dehydrogenase (MASSEY and VEEGER, 1961), glutathione reductase (MASSEY and WILLIAMS, 1965) and thioredoxin reductase (ZANETTI and WILLIAMS, 1967; THELANDER, 1968), in which a redox active disulfide is present in addition to its flavin prosthetic group and is involved in the catalytic mechanism. In the case of the *Azotobacter* transhydrogenase no clear-cut evidence is still available, but there are indications that disulfide groups may be involved in the reduction of the enzyme. In this respect, the recent observation of ORLANDO (1970) on the activating effect of reduced lipoamide on both the energy-linked and the non-energy-linked transhydrogenase, active in photosynthesis, is of great interest. Especially in view of our observation that *Azotobacter* transhydrogenase and the pyruvate dehydrogenase complex are in close interaction (CHAPTER 3 and 4).

Studies of the absorption spectra during the titration of the enzyme with NADH, NADPH and dithionite did not result in the detection of any stable two-equivalent reduced intermediate, similar to that observed in flavoproteins like lipoamide dehydrogenase (MASSEY et al., 1960) and glutathione reductase (COLMAN and BLACK, 1965). In this respect the spectra show many similarities with those obtained after reduction of thioredoxin reductase with NAD(P)H and reduced thioredoxin (THELANDER, 1968; ZANETTI and WILLIAMS, 1967); in contrast to the latter enzyme, however, no blue semiquinone form of the transhydrogenase could be produced by photo-irradiation in the presence of EDTA (ZANETTI et al., 1968). Anaerobic reduction with all 3 types of reductant and anaerobic photo-irradiation simply resulted in the reduction of the flavin; only in the presence of $NADP^+$ and NAD^+ a weak absorption band above 500 nm without a specific maximum, is observed, probably due to a specific interaction of the oxidized pyridine nucleotides with the reduced flavin. Furthermore the results point to the fact that the long wavelength absorbance band belongs to the two-equivalent reduced enzyme-oxidized pyridine nucleotide complex.

Assuming a reducible group X, like in lipoamide dehydrogenase, the following series of reactions can be visualized (cf. MASSEY and VEEGER, 1961).

$$1.\ H^+ + E - FAD - X + PNH \rightleftharpoons E - FADH_2 - X - PN^+$$
$$2.\ E - FADH_2 - X - PN^+ \rightleftharpoons E - FADH_2 - X + PN^+$$

3. $E - FADH_2 - X \rightleftharpoons E - FAD - XH_2$
4. $H^+ + E - FAD - XH_2 + PNH \rightleftharpoons E - FADH_2 - XH_2 - PN^+$
5. $E - FAD - X + NADP^+ \rightleftharpoons E - FAD - X - NADP^+$

where PNH and PN^+ are the reduced and oxidized pyridine nucleotides respectively.

In this scheme $E - FADH_2 - X - PN^+$ shows the long-wavelength absorbance and $E - FAD - X - NADP^+$ the spectral characteristics of the oxidized enzyme-$NADP^+$ complex.

The question arises as to why the formation of the species $E - FADH_2 - XH_2 - PN^+$ is the last step in the reduction process and if it were, why it does not show absorbance beyond 500 nm. The latter question cannot be answered, but the following evidence points to the existence of this species as last step. The experiments in the presence of NADase, which should exclude the possibility of an equilibrium, show titration curves with a striking deviation from linearity after the addition of the first mole of reductant; when reduction is performed with dithionite linear titration curves are obtained even in the presence of $NADP^+$. The results suggest that upon reduction in the presence of NADase no complete release of products occurs and that in the bound state the oxidized pyridine nucleotide is responsible for the deviation in the titration curve. This is presumably not the first molecule oxidized pyridine nucleotide formed because,

1. the titration curve is linear up to 1 mole of donor
2. no 500–600 nm absorbancy is present.

Furthermore, the observation that the total absorbance change obtained at 440 nm after reduction with dithionite is larger ($\sim$ 80%) than that found upon reduction with either NADH or NADPH in the presence of NADase ($\sim$ 70%), favours the idea and points to the existence of reaction (4) in the scheme above.

The reductive mechanism outlined above, is supported by the titration studies. The better conclusions can be drawn from the end point towards the 4-equivalent reduced state. If reaction (4) were followed by a dissociation of the oxidized pyridine nucleotide (actually an unreasonable assumption in view of the titration in the presence of NADase) NAD^+ and $NADP^+$ would show a non-competitive retardation of the reduction by NADH and NADPH, respectively. The competitive retardation of the reduction is thus due to the effects of NAD^+ and $NADP^+$ on the back reaction (2).

Similarly non-competitive retardation of the reduction by the first molecule of donor is observed as expected from reaction (1) and (2) (cf. Addendum). Unfortunately the first part of the titration curve does not allow a reliable BENESI-HILDEBRAND plot to be made to conclude whether 2 $NADP^+$ molecules are counteracting the reduction of the oxidized enzyme by NADPH as would be expected if $NADP^+$ is bound to the oxidized enzyme, on the NADPH-binding site (reaction 5). Some indirect evidence shows this to be the case. From the NADPH-$NADP^+$ titration curve it can be calculated that for the

retardation of the reduction, $K_D \sim 3$–4 μM, which is much lower than $K_D \sim 10$ μM, for the reduced enzyme-$NADP^+$ complex as calculated from the dithionite-$NADP^+$ titration experiment, but equal to the dissociation constant of the oxidized enzyme-$NADP^+$ complex.

Thus it is clear from these experiments that NAD^+ and $NADP^+$ interact in a different way with the different forms of the enzyme, e.g. $NADP^+$ has a higher affinity for the oxidized enzyme, while NAD^+ has a higher affinity for the reduced enzyme. The consequences of this difference will be discussed in connection with the kinetic behaviour of this enzyme.

It is clear that the reduction level of the enzyme bound flavin is determined by the ratio of the reduced and oxidized forms of the pyridine nucleotides. It is surprising, however, that the spectrum calculated at infinite donor concentration of the systems NADH-$NADP^+$ and NADH-NAD^+ differs from that obtained for the system NADH-NADase. Similarly the spectrum at infinite acceptor concentration of the system NADH-$NADP^+$ differs from that of the oxidized enzyme. Since the corresponding spectra calculated for the system NADPH-$NADP^+$ at infinite donor and acceptor concentrations are identical with the enzyme reduced by NADPH-NADase and the oxidized enzyme-$NADP^+$ complex respectively, it means that the method of approach is correct and thus the differences are real.

The difference of the titration systems, NADH + NAD^+ and NADH + $NADP^+$ with the system NADPH + $NADP^+$ is the presence of NAD^+. Thus the difference is due to binding of NAD^+ to the reduced enzyme. Accepting the scheme outlined above, it means that this species of 4-equivalent reduced enzyme contains an extra molecule of NAD^+; the titration curves show that NAD^+ has a high affinity for the reduced enzyme, $K_D \sim 0.7$ μM. It can be expected, that this extra NAD^+ molecule will be in interaction with the flavin. The extrapolated spectrum seems to indicate long wavelength absorbance; the differences in the 500–600 nm region are too small, however, to allow any accurate extrapolation, and thus any definite conclusion concerning this point. It is of course of great importance to know whether such a charge transfer band is present, since it would indicate close positions between the flavin and this extra NAD^+ molecule. The existence of such a species is consistent with the kinetic studies (CHAPTER 6) which indicate a ternary complex mechanism.

The observation that the species $E\text{-}FADH_2\text{-}XH_2\text{-}PN^+$ has no absorbance beyond 500 nm excludes positioning of the pyridine nucleotide in direct interaction with the isoalloxazine ring thus giving rise to charge transfer interaction (DE KOK et al., 1970; HEMMERICH et al., 1970). On the other hand it is questionable whether oxidized pyridine nucleotide is present, because one would expect at least dissociation of this product, followed by degradation by NADase and formation of the fully reduced enzyme. Since N-5 adduct of flavin has an absorption spectrum in the visible region very similar to that of leuco-flavin, an adduct between C-4A-nicotinamide-N-5-isoalloxazine (schematically given as $E\text{-}FADH\text{-}NADH\text{-}XH_2$) gives a better description of this species.

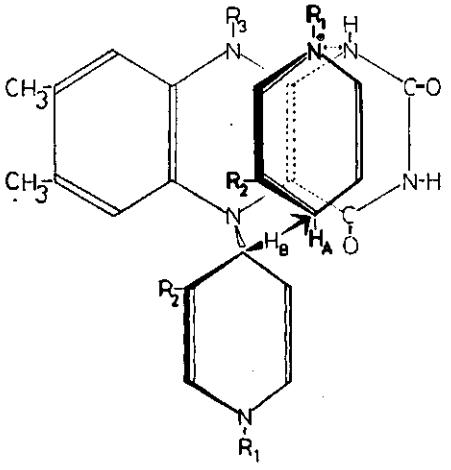

FIG. 5.11. Proposed model for a specific 4B-4B hydrogen transfer.

Accepting a ternary complex mechanism, the following proposals for the active site of the enzyme can be derived. When the extra NAD^+ molecule is bound to the reduced enzyme in the same position as $NADP^+$ to the oxidized enzyme, it can be expected that the N-atom of the pyridine ring will be in close interaction with N-1 of the isoalloxazine ring. This can be derived from the shift of the fluorescence emission towards shorter wavelength upon binding of $NADP^+$. ELEY et al. (1970) have shown that N-1 protonated flavins have an emission around 490 nm. The shift of the emission can thus be explained by close proximity of the positively charged N-1 of the nicotinamide ring and N-1 of the isoalloxazine ring. The following structure gives a model for the specific B-B transfer of hydrogen atom, as observed with the *Pseudomonas* transhydrogenase (LOUIE and KAPLAN, 1970b).

Addendum

Some general reductive mechanisms may be proposed in connection with the observations in this chapter, and they can be related to a BENESI-HILDEBRAND plot.

$$\text{A.} \quad E + S \underset{k_2}{\overset{k_1}{\rightleftharpoons}} ES$$

$$E + P \underset{k_4}{\overset{k_3}{\rightleftharpoons}} E - P$$

The enzyme is able to react with reductant S, but dissociation of the oxidized product does not occur; in the presence of P complex formation with oxidized enzyme occurs. The BENESI-HILDEBRAND relation

$$\frac{[ES]}{[E]} = \frac{1}{1 + \frac{k_2}{k_1[S]}\left(\frac{k_3 + k_4[P]}{k_3}\right)} = \frac{1}{1 + \frac{K_D}{[S]}\left(1 + \frac{[P]}{K_P}\right)}$$

predicts that P will inhibit competitively with respect to S.

B. $$E + S \underset{k_2}{\overset{k_1}{\rightleftharpoons}} ES \underset{k_4}{\overset{k_3}{\rightleftharpoons}} EH_2 + P$$

Dissociation of oxidized product occurs, but the product is not able to bind to the oxidized enzyme. The BENESI-HILDEBRAND relation predicts a non-competitive retardation of reduction, linear in $[P]$

$$\frac{[EH_2]}{[E]} = \frac{1}{1 + \frac{[P]}{K_P}\left(1 + \frac{K_D}{[S]}\right)}$$

When P is able to form a complex with the oxidized enzyme, mechanism B is extended by the following step: $E + P \underset{k_6}{\overset{k_5}{\rightleftharpoons}} EP$. The BENESI-HILDEBRAND relation is modified by an additional term:

$$\frac{[EH_2]}{[E]} = \frac{1}{1 + \frac{[P]}{K_P}\left\{1 + \frac{K_D}{[S]}\left(1 + \frac{[P]}{K_I}\right)\right\}},$$

but it still predicts non-competitive retardation of reduction; a quadratic dependency in $[P]$ is obtained.

In the equations: $K_D = \frac{k_2}{k_1}$, $K_P = \frac{k_3}{k_4}$ and $K_I = \frac{k_6}{k_5}$

6. KINETIC STUDIES ON *AZOTOBACTER* TRANSHYDROGENASE

6.1. INTRODUCTION

Azotobacter pyridine nucleotide transhydrogenase catalyzes the transfer of hydrogen from the reduced pyridine nucleotide to the oxidized form (KAPLAN et al., 1952), according to the basic reaction

$$NADPH + NAD^+ \rightleftharpoons NADP^+ + NADH \qquad (I)$$

Coenzyme analogues although not all, can be used (cf. CHAPTER 3). For the *Pseudomonas* transhydrogenase (COHEN, 1967; COHEN and KAPLAN, 1970a,b) it was found that the reversal of reaction (I) proceeds at a negligible rate, but is greatly accelerated by the addition of 2'AMP. In the case of the *Azotobacter* enzyme this type of activation was not obtained, unless the buffer and pH of the assay system were changed (cf. CHAPTER 3 and VAN DEN BROEK and VEEGER, 1970). The rate of the reaction from right to left seems to be dependent on the ratio $NADP^+/NADPH$, although other factors may be involved.

In order to obtain some information about the catalytic mechanism of the transhydrogenase, kinetic studies were performed. The systems studied included both the naturally occurring coenzymes and their thio-analogues; they are summarized in reaction (I) and (II).

$$NAD(P)H + TNAD(P)^+ \rightleftharpoons NAD(P)^+ + TNAD(P)H \qquad (II)$$

The results obtained are compared with those given for the *Pseudomonas* transhydrogenase.

6.2. RESULTS

The enzyme preparations used in parts of this study were not completely pure, but experiments with pure enzyme showed the same kinetic picture.

6.2.1. $NADPH + TNAD^+ \rightarrow NADP^+ + TNADH$

FIG. 6.1 shows the effect of varying the concentration of NADPH and $TNAD^+$ on the enzyme activity. The plots $1/v$ vs. 1/[NADPH] at variable $TNAD^+$ concentrations tend to be parallel at lower NADPH concentrations; at high NADPH concentrations inhibition is found, especially at low acceptor concentrations. The extent of inhibition diminishes upon increasing the $TNAD^+$ concentrations.

In the $1/v$ vs. $1/[TNAD^+]$ plots only at the lower NADPH concentrations parallel lines are obtained. At higher NADPH concentrations ($> 40\ \mu M$) the

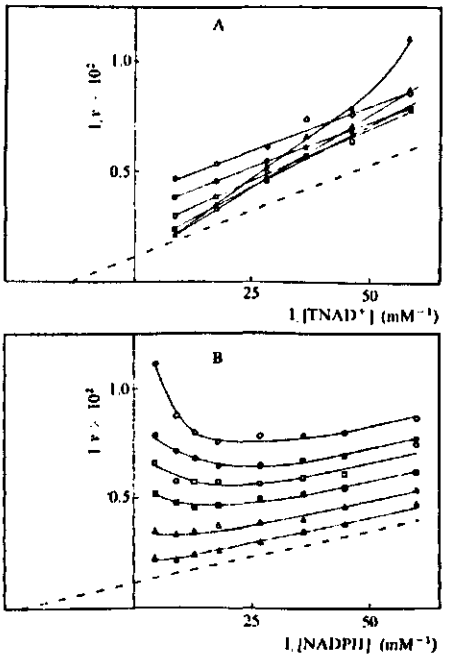

FIG. 6.1. TNAD$^+$ reduction with NADPH. A. $1/v$ vs. $1/$ [TNAD$^+$] plots at different concentrations of NADPH: ○ —— ○, 17 μM; ● —— ●, 22 μM; □ —— □, 37 μM; ■ —— ■, 78 μM; △ —— △, 111 μM; ▲ —— ▲, 222 μM, and - - - - - -, at infinite NADPH concentration. B. $1/v$ vs. $1/$ [NADPH] plots at different TNAD$^+$ concentrations: ○ —— ○, 17 μM; ● —— ●, 22 μM; □ —— □, 27 μM; ■ —— ■, 35 μM; △ —— △, 57 μM; ▲ —— ▲, 114 μM; - - - - -, at infinite concentration. v expressed as μmoles NADPH oxidized per min per mg of protein.

slopes of the lines increase, and also V_{max}. At very low TNAD$^+$ concentrations an upward deflection of the line is observed. As a consequence the v vs. [TNAD$^+$] curve becomes s-shaped at high NADPH concentrations. Similar s-shaped curves were obtained for the NAD$^+$ reduction by NADPH. In contrast to the results of COHEN (COHEN, 1967; COHEN and KAPLAN, 1970b) the rate of the reaction is not dependent on [NADPH]^2.

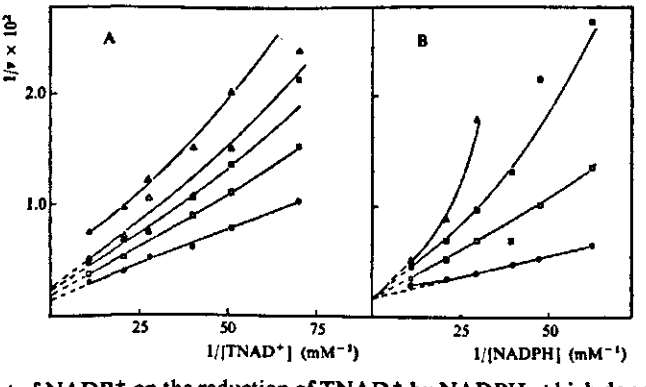

FIG. 6.2. Effect of NADP$^+$ on the reduction of TNAD$^+$ by NADPH at high donor and acceptor concentrations. A. $1/v$ vs. $1/$ [TNAD$^+$] plots at constant NADPH concentration (97 μM) and varying NADP$^+$ concentrations. B. $1/v$ vs. $1/$ [NADPH] plots at constant TNAD$^+$ concentration (90 μM) and different NADP$^+$ concentrations. [NADP$^+$]: ● —— ●, none; □ —— □, 29 μM; ■ —— ■, 58 μM; △ —— △, 90 μM; ▲ —— ▲, 120 μM. v expressed as μmoles NADPH oxidized per min per mg of protein.

By extrapolation to infinite substrate concentrations, from FIG. 6.1 values for K_m for TNAD$^+$ of about 75 μM and a K_m for NADPH of about 40 μM are calculated. The catalytic centre activity calculated for this reaction at infinite substrate concentrations is 53,000 min^{-1}.

NADP$^+$ strongly inhibits the reduction of TNAD$^+$. The inhibition pattern obtained is complex and determined absolutely by both donor and acceptor concentrations. The LINEWEAVER-BURK plots obtained for donor and acceptor in the presence of NADP$^+$ are non-linear; also non-linear $1/v$ vs. [NADP$^+$] plots are found at low donor and acceptor concentrations. FIG. 6.2 shows LINEWEAVER-BURK plots in the presence of different NADP$^+$ concentrations at high donor and acceptor concentrations and variable acceptor and donor concentrations, respectively. The general pattern is that at higher NADPH concentrations the plots become more linear; upon increasing the acceptor concentrations lower donor concentrations are necessary to give linear plots. The inhibition at low NADP$^+$ concentrations is non-competitive with respect to NADPH at low TNAD$^+$ concentrations, but no linear $1/v$ vs. 1/[NADPH] plot is obtained. At higher acceptor concentrations the $1/v$ vs. 1/[NADPH] plots at these NADP$^+$ concentrations become linear and tend towards competitive inhibition. The inhibition of NADP$^+$ with respect to TNAD$^+$ tends to be non-competitive at all NADPH concentrations, although it is very difficult to be sure about this at low NADP$^+$ concentrations.

From the LINEWEAVER-BURK plots shown in FIG. 6.3 in the presence of about 60 μM NADP$^+$ it can be seen that the curves become dependent on [NADPH]^2 and are convergent. Surprisingly, no substrate inhibition is observed at low TNAD$^+$ concentrations.

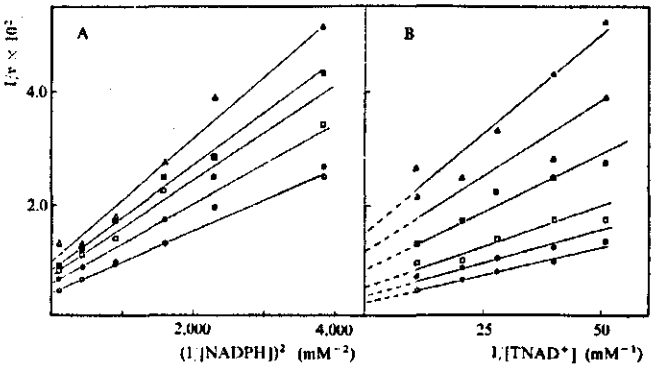

FIG. 6.3. Effect of NADP$^+$ on the reduction of TNAD$^+$ by NADPH. A. $1/v$ vs. $(1/[NADPH])^2$ plots at different TNAD$^+$ concentrations and constant NADP$^+$ concentration (= 58 μM). Top to bottom: 20, 25, 36, 49 and 90 μM TNAD$^+$. B. $1/v$ vs. 1/ [TNAD$^+$] plots at different NADPH concentrations and constant NADP$^+$ concentration (= 58 μM). Top to bottom: 16, 21, 25, 34, 48 and 97 μM NADPH. v expressed as μmoles NADPH oxidized per min per mg of protein.

6.2.2. *NADH + TNAD$^+$ → NAD$^+$ + TNADH*

In the reduction of TNAD$^+$ by NADH a similar set of parallel LINEWEAVER-BURK plots is obtained in the absence of inhibitors; the substrate inhibition, however, is less pronounced. The $1/v$ vs. 1/[NADH] plots remain reasonably linear and parallel; this is also the case in the $1/v$ vs. 1/[TNAD$^+$] plots, but at high donor concentrations (> 100 μM) a crossing of the lines is observed. The K_m values obtained upon extrapolation to infinite substrate concentrations are about 60 μM for both NADH and TNAD$^+$. The catalytic centre activity calculated at infinite substrate concentrations is 30,000 min^{-1}.

Both NAD$^+$ and NADP$^+$ are able to inhibit the reduction of TNAD$^+$ by NADPH. The inhibition of NAD$^+$ is purely non-competitive towards NADH and linear $1/v$ vs. 1/[NADH] plots and $1/v$ vs. [NAD$^+$] plots are obtained. FIG. 6.4 summarizes the inhibitory effects of NAD$^+$ with respect to NADH. An inhibition constant K_i (NAD$^+$) of about 130 μM can be calculated from these plots. The inhibition of NAD$^+$ with respect to TNAD$^+$ is competitive (CHUNG, 1970).

NADP$^+$ is a very strong inhibitor of this reaction. Although acceptor in the reaction with NADH, it can be used as inhibitor, because under the conditions of the experiments, the rate of formation of NADPH is negligible in the absence of added NADPH (cf. CHAPTER 3). NADP$^+$ inhibition is non-competitive with respect to NADH at high acceptor concentrations; at low acceptor con-

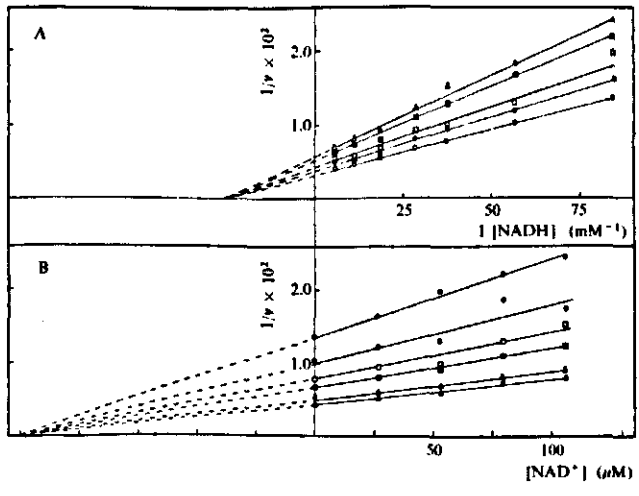

FIG. 6.4. Effect of NAD$^+$ on the reduction of TNAD$^+$ by NADH. A. $1/v$ vs. 1/ [NADH] plots at different NAD$^+$ concentrations and constant TNAD$^+$ concentration (50 μM). NAD$^+$ concentration: o —— o, none; ● —— ●, 26.5 μM; □ —— □, 53 μM; ■ —— ■, 80 μM; △ —— △, 106 μM. B. $1/v$ vs. [NAD$^+$] plots at different NADH concentrations and constant TNAD$^+$ concentration (50 μM). Top to bottom: 12 μM, 18 μM, 27 μM, 36 μM, 53 μM, and 89 μM NADH, respectively. v expressed as μmoles NADH oxidized per min per mg of protein.

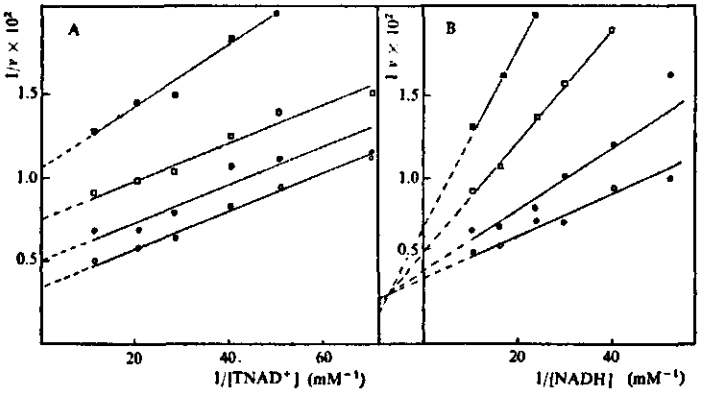

FIG. 6.5. Effect of $NADP^+$ on the reduction of $TNAD^+$ by NADH. $1/v$ vs. 1/ [substrate] plots at high donor and acceptor concentrations. $NADP^+$ concentrations: ○ —— ○, none; ● —— ●, 9.7 μM; □ —— □, 19.4 μM; ■ —— ■, 38.8 μM. A. $1/v$ vs. 1/ [$TNAD^+$] plots at constant NADH concentration (95 μM) and different $NADP^+$ concentrations. B. $1/v$ vs. 1/ [NADH] plots at constant $TNAD^+$ concentration (95 μM) and different $NADP^+$ concentrations. v expressed as μmoles NADH oxidized per min per mg of protein.

centrations the $1/v$ vs. 1/[NADH] plots become non-linear and, although difficult to estimate, have at low $NADP^+$ concentrations a tendency towards competitive inhibition. At higher $NADP^+$ concentrations a mixed type of non-competitive inhibition is observed.

At low $NADP^+$ concentrations there is a tendency to uncompetitive inhibition towards $TNAD^+$, but at higher $NADP^+$ concentrations the inhibition becomes non-competitive. FIG. 6.5 shows the LINEWEAVER-BURK plots in the presence and absence of $NADP^+$ at high donor and acceptor concentrations. The $1/v$ vs. [$NADP^+$] plots are non-linear at low donor and acceptor concentration, but upon raising these concentrations they tend to become straight.

6.2.3. *NADH + $TNADP^+$ → NAD^+ + TNADPH*

The reduction of $TNADP^+$ by NADH proceeds directly without the addition of any activator. Inhibition of the enzyme activity occurs at high acceptor concentrations and can be overcome by raising the donor concentration. FIG. 6.6 shows the effect of varying the concentrations of both $TNADP^+$ and NADH. In the $1/v$ vs. 1/[$TNADP^+$] plot a series of lines is obtained which tends to be parallel in the non-inhibitory concentration range. A similar set of parallel lines is found in the $1/v$ vs. 1/[NADH] plot at different acceptor concentrations, although at high acceptor concentrations a crossing of the lines is obtained. This behaviour is just the opposite of that found in the reduction of $TNAD^+$ or NAD^+ by NADPH. From extrapolation to infinite substrate concentrations a K_m for NADH of 83 μM and a K_m for $TNADP^+$ of 32 μM was calculated from FIG. 6.6. The catalytic centre activity for this reaction calculated at infinite substrate concentrations is 30,000 min^{-1}.

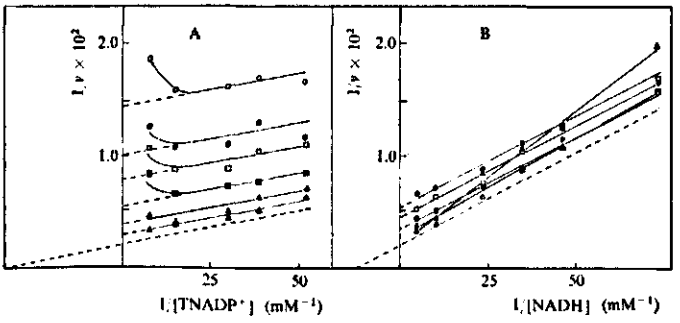

FIG. 6.6. Reduction of TNADP$^+$ by NADH. A. $1/v$ vs. 1/ [TNADP$^+$] plots at different NADH concentrations: o —— o, 14 μM; ● —— ●, 22 μM; □ —— □, 29 μM; ■ —— ■, 42 μM; △ —— △, 96 μM; ▲ —— ▲, 192 μM; dotted line extrapolated to infinite NADH concentration. B. $1/v$ vs. 1/ [NADH] plots at different TNADP$^+$ concentrations: ● —— ●, 19 μM; □ —— □, 26 μM; ■ —— ■, 33,5 μM; △ —— △, 67 μM; ▲ —— ▲, 134 μM, dotted line, extrapolated to infinite TNADP$^+$ concentration. v expressed as μmoles NADH oxidized per min per mg of protein.

NADP$^+$ also inhibits this reaction under conditions that it is not reduced by NADH. The inhibition with respect to both TNADP$^+$ and NADH is non-competitive (FIG. 6.7).

The effect of NADP$^+$ on the enzyme activity is also clearly demonstrated in the LINEWEAVER-BURK plots at variable donor and acceptor concentrations in the presence of 50 μM NADP$^+$ (FIG. 6.8); instead of a series of parallel lines or curves a series of lines, converging on or close to the negative abscissa is obtained. The $1/v$ vs. [NADP$^+$] plots are non-linear at low donor and acceptor concentrations, but tend to straighten at higher substrate concentrations.

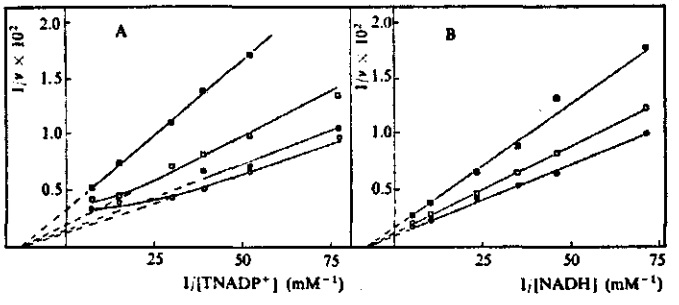

FIG. 6.7. Effect of NADP$^+$ on the reduction of TNADP$^+$ by NADH at high donor and acceptor concentrations. A. $1/v$ vs. 1/ [TNADP$^+$] plots at constant NADH concentration (192 μM) and different NADP$^+$ concentrations. B. $1/v$ vs. 1/ [NADH] plots at constant TNADP$^+$ concentration (134 μM) and different NADP$^+$ concentrations. NADP$^+$ concentrations: o —— o, none; ● —— ●, 12 μM; □ —— □, 24 μM; ■ —— ■, 49 μM; v expressed as μmoles NADH oxidized per min per mg of protein.

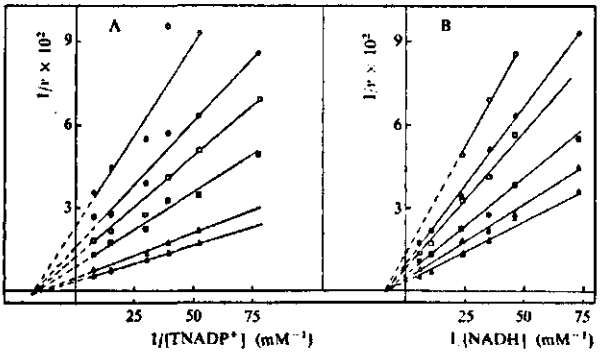

FIG. 6.8. Effect of $NADP^+$ on the reduction of $TNADP^+$ by NADH. A. $1/v$ vs. $1/[TNADP^+]$ plots of different NADH concentrations and constant $NADP^+$ concentration (50 μM). Top to bottom: 14(○), 22(●), 29(□), 42(■), 95(△) and 192(▲) μM NADH. B. $1/v$ vs. $1/[NADH]$ plots at different $TNADP^+$ concentrations and constant $NADP^+$ concentration (50 μM). Top to bottom: 13(○), 19(●), 26(□), 33(■), 57(△) and 134(▲) μM $TNADP^+$. v expressed as μmoles NADH oxidized per min per mg of protein.

6.2.4. *NADPH + TNADP⁺ → NADP⁺ + TNADPH*

The reduction of $TNADP^+$ by NADPH is inhibited by both high donor and acceptor concentrations; the inhibition can be overcome by raising the concentration of the acceptor and donor, respectively. A set of these LINEWEAVER-BURK plots is shown in FIG. 6.9. The complexity of the relation does not allow an extrapolation to infinite substrate concentrations.

The pattern of inhibition of this reaction by $NADP^+$ is very complex (FIG. 6.10). In the first place the $1/v$ vs. $[NADP^+]$ plots are linear at high con-

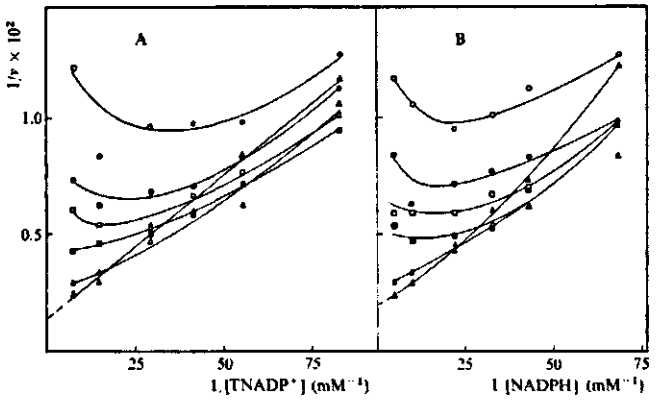

FIG. 6.9. $TNADP^+$ reduction by NADPH. A. $1/v$ vs. $1/[TNADP^+]$ plots at different NADPH concentrations: ○ —— ○, 15μM; ● —— ●, 23μM; □ —— □, 31 μM; ■ —— ■, 45 μM; △ —— △, 100 μM; ▲ —— ▲, 200 μM. B. $1/v$ vs. $1/[NADPH]$ plots at different $TNADP^+$ concentrations: ○ —— ○, 12 μM; ● —— ●, 18 μM; □ —— □, 24 μM; ■ —— ■, 34 μM; △ —— △, 68 μM; ▲ —— ▲, 136 μM. v expressed as μmoles NADPH oxidized per min per mg of protein.

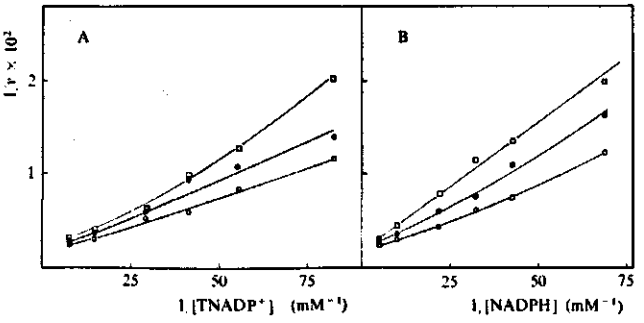

FIG. 6.10. Effect of $NADP^+$ on the $TNADP^+$ reduction by NADPH. A. $1/v$ vs. $1/[TNADP^+]$ plots at constant NADPH concentration (200 μM) and different $NADP^+$ concentrations. B. $1/v$ vs. $1/[NADPH]$ plots at constant $TNADP^+$ concentration (136 μM). $NADP^+$ concentration: o —— o, none; • —— •, 50 μM; □ —— □, 100 μM. v expressed as μmoles NADPH oxidized per min per mg of protein.

centrations of both donor and acceptor. On the other hand at low concentrations of acceptor a marked deviation from linearity is observed. Secondly substrate inhibition is present to some extent and its contribution is difficult to estimate. The results seem to indicate that $NADP^+$ inhibits with respect to both $TNADP^+$ and NADPH either non-competitively with a point of intersection close to the ordinate, or competitively. It is difficult to distinguish between the two possibilities due to the non-linearity on both sides of the L-B plot in the absence of $NADP^+$ (cf. FIG. 6.10).

No catalytic centre activity at infinite substrate concentrations could be calculated for this reaction; the maximal rate obtained at the highest substrate concentrations is in the order of 30,000–40,000 min^{-1}.

6.2.5. *NADPH + NAD^+ → $NADP^+$ + NADH*

The direct transfer of hydrogen from NADPH to NAD^+ can be measured by keeping the donor concentration at a constant level by using a regenerating system in the assay; the absorbance change at 340 nm is thus only due to the formation of NADH and may be taken as a measure for the activity of the transhydrogenase in this system. Both substrates are inhibitory at high concentrations, although the inhibition can be overcome by raising the concentration of the second substrate. The LINEWEAVER-BURK plots for this reaction are comparable with those found for the reduction of $TNAD^+$ by NADPH, although the inhibition of NADPH in the reaction with NAD^+ is much more pronounced. The upward deflection at low NAD^+ and high NADPH concentrations in the LINEWEAVER-BURK plot also points to an s-shaped v vs. $[NAD^+]$ curve (FIG. 6.11).

The inhibition obtained at the different substrate concentrations is more pronounced at lower temperatures. Parallel curves or lines are not even obtained in the $1/v$ vs. $1/[NAD^+]$ plot at variable NADPH concentrations at 8°; the slopes of the lines increase with increasing donor concentrations. This donor

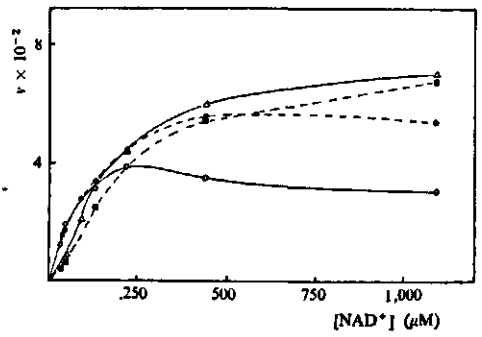

FIG. 6.11. Effect of NADPH and NAD^+ concentration on the velocity of the reduction of NAD^+ by NADPH. Initial velocity expressed as μmoles NADPH oxidized per min. v plotted vs. $[NAD^+]$ at different concentrations of NADPH: o —— o, 45 μM; ● —— ●, 90 μM; △ —— △, 220 μM; □ —— □, 440 μM.

TABLE 6.1. Kinetic parameters calculated for the different transhydrogenase reactions at 25°. The values of K_m and V_{max} are calculated at infinite substrate concentrations from LINEWEAVER-BURK plots. Velocity based upon flavin content of the enzyme (1 mole FAD per 60,000 g of protein) and expressed as catalytic centre activity.

Reaction	K_m values (μM)		Catalytic centre activity (min^{-1})
NADPH—$TNAD^+$	K_m (NADPH)	40	53,000
(From FIG. 6.1)	K_m ($TNAD^+$)	75	
NADH—$TNAD^+$	K_m (NADH)	60	
	K_m ($TNAD^+$)	50	30,000
	K_i (NAD^+)	125	
NADPH—NAD^+	K_m (NADPH)	15	40,000
	K_m (NAD^+)	110	
NADPH—$TNADP^+$	K_m (NADPH)	—	30,000–40,000
(From FIG. 6.9)			
NADH—$TNADP^+$	K_m (NADH)	83	30,000
(From FIG. 6.6)	K_m ($TNADP^+$)	32	
NADH—$NADP^+$	K_m (NADH)	25	8,500
no $MgCl_2$	K_m ($NADP^+$)	10	
(From FIG. 6.13)	K_m (NADH)	18	11,500
4 mM $MgCl_2$	K_m ($NADP^+$)	14	

inhibition is also clearly demonstrated in the $1/v$ vs. 1/[NADPH] plot. On raising the temperature a greater tendency towards parallel plots is obtained and the substrate inhibition becomes less pronounced. The Arrhenius plot is reasonably linear and an activation energy of about 14 Kcal/mole could be calculated. The catalytic centre activity calculated at infinite substrate concentrations is 40,000 min^{-1}. The K_m values obtained are 15 μM and 110 μM for NADPH and NAD^+, respectively.

ATP has a remarkable inhibitory effect on the reduction of NAD^+ by NADPH. The extent of inhibition is completely determined by the concentration of both substrates. Upon raising the ATP concentration the inhibition at high concentrations of NAD^+ becomes much more pronounced. The inhibition towards NADPH tends to be NAD^+ dependent. The ATP effect at low NADPH and variable NAD^+ concentrations is summarized in FIG. 6.12. A similar effect was found with GTP. The inhibitory effects of ATP and GTP are

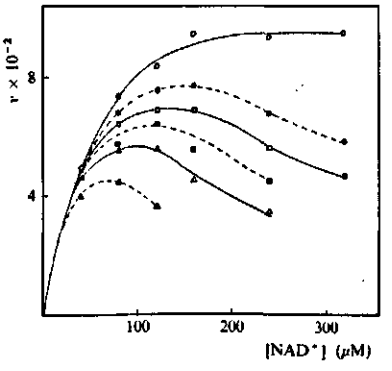

FIG. 6.12. Effect of ATP on the reduction of NAD^+ by NADPH at low NADPH concentration (33 μM) and variable NAD^+ concentrations: o —— o, none; ● —— ●, 48 μM; □ —— □, 96 μM; ■ —— ■, 192 μM; △ —— △, 288 μM; and ▲ —— ▲, 720 μM ATP, respectively. v expressed as μmoles NADPH oxidized per min.

counteracted by $MgCl_2$. No clear inhibitory effects were shown with ADP, GDP, 5'AMP and 3'5'AMP.

6.2.6. *NADH + NADP⁺ → NAD⁺ + NADPH*

As already indicated in CHAPTER 3 the reduction of $NADP^+$ by NADH proceeds only under special conditions. It was shown that the course of the reaction is evidently determined by the concentration of both donor and acceptor and by the presence of $MgCl_2$ and the product, NADPH. In the absence of the latter compounds a lag period in the activity curve is observed. The length of this lag period was dependent on the concentration of $NADP^+$ and NADH, the initial NADPH concentration, the amount of transhydrogenase used in the assay and the type of preparation tested. In the presence of $MgCl_2$ smaller amounts of NADPH are necessary to overcome the lag period; $MgCl_2$ can be replaced by $CaCl_2$, $MgSO_4$, $MnSO_4$ or KCl, although with varying but smaller effectivity. The activating effect of NADPH is in turn counteracted by ATP, the effective ATP concentration depending on the concentration of $MgCl_2$; in its absence, ATP concentrations as low as 10–40 μM are already strongly inhibitory in the reaction.

Upon varying the concentrations of the two substrates and that of NADPH, typical s-shaped relations were found between the enzyme activity and the concentration of both $NADP^+$, NADH and NADPH (VAN DEN BROEK and VEEGER, 1968). These results suggest that the transhydrogenase activity is regulated by the ratio $NADP^+$/NADPH (VAN DEN BROEK and VEEGER, 1970).

This ratio is not the only factor determining the lag period. At higher enzyme concentrations hardly any lag period is observed, due to autocatalytic acceleration of the rate of reaction by rapid NADPH production, which overcomes the lag period within 10 seconds, needed in spectrophotometric assays. Thus it is possible to perform kinetic studies in this direction, provided one works at constant enzyme concentrations in order to prevent induction of the lag period at lower enzyme concentrations. The disadvantages of the rather large absorbance changes (0.1–0.2 per min) is overcome by the reasonably good linearity of the initial rate recorder tracings, by working with a high speed

recorder (Honeywell, Model Elektronik 16) and thus obtaining reliable data. The data of such an experiment can be interpreted on an indicative and not on an absolute basis.

In all these determinations the NADH regenerating system consisted of excess alcohol, semicarbazide and rather high concentrations of yeast alcohol dehydrogenase (ADH), according to COLOWICK et al. (1952) to be sure that the produced NAD^+ was immediately reconverted into NADH; in this way the NADH level was kept constant and the absorbance change at 340 nm was only due to the formation of NADPH. It was therefore necessary for each series of experiments to determine optimal conditions, with respect to transhydrogenase, alcohol dehydrogenase, $MgCl_2$ and substrates.

The enzymatic activity of a preparation with a specific activity of about 160 units per mg was analysed at variable donor and acceptor concentrations, in the absence and presence of $MgCl_2$, while inhibition studies were performed with NADPH. All initial velocity measurements were performed in 0.1 M Tris-HCl, pH 7.6, with 0.15 M alcohol and 22 μg ADH, at all concentrations of the pyridine nucleotides.

Both in the absence and presence of $MgCl_2$ the reciprocal plots $1/v$ vs. 1/[substrate] at variable donor and acceptor concentrations do not show the characteristic tendency to a parallel line relationship as observed for the other reactions. The LINEWEAVER-BURK plots differ also from those obtained in the

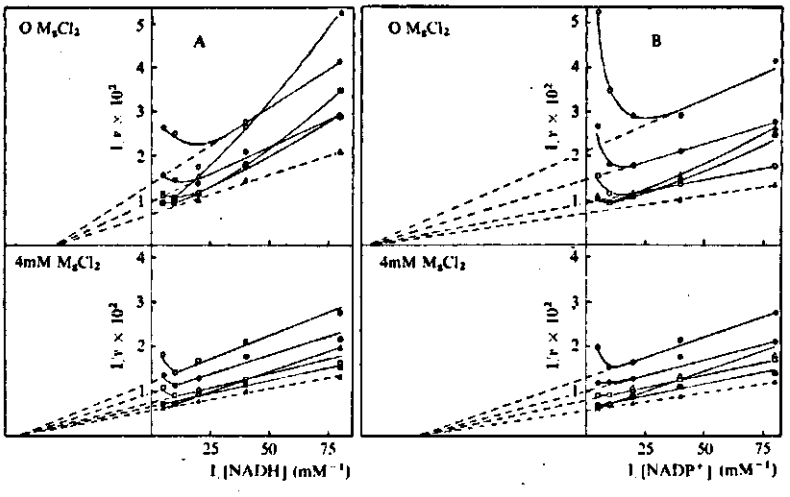

FIG. 6.13. Reduction of $NADP^+$ by NADH in the absence and presence of $MgCl_2$. A. $1/v$ vs. 1/ [NADH] plots at variable acceptor concentrations. $NADP^+$ concentration: ○ —— ○, 12.5 μM; ● —— ●, 25 μM; □ —— □, 50 μM; ■ —— ■, 100 μM; △ —— △, 200 μM; ▲ —— ▲, obtained by extrapolating to infinite $NADP^+$ concentration. B. $1/v$ vs. 1/ [$NADP^+$] plots at different donor concentrations. NADH concentration: ○ —— ○, 12.5 μM; ● —— ●, 25 μM; □ —— □, 50 μM; ■ —— ■, 100 μM; △ —— △, 200 μM; ▲ —— ▲, obtained by extrapolating to infinite NADH concentration. Top and bottom, in the absence and presence of 4 mM $MgCl_2$, respectively. v expressed as μmoles NADH oxidized per min per mg of protein.

reaction with NADH and TNADP$^+$, but show the same tendency as observed for this reaction in the presence of NADP$^+$ (FIG. 6.8). All reciprocal plots show converging lines; from extrapolation of the plots in the non-inhibitory region it may be concluded they tend to converge to one point on the abscissa. The reaction is inhibited by high concentrations of both substrates; the inhibiting effect of NADP$^+$ is somewhat more pronounced. By raising the concentration of the second substrate the inhibition diminishes, but does not disappear completely. The inhibiting effects of both substrates are less pronounced in the presence of $MgCl_2$. Because both substrates are inhibitory at high concentrations, the plots at high substrate concentrations have increased slopes, although V_{max} still tends to increase. FIG. 6.13 shows the effect of variable donor and acceptor concentrations on the enzyme activity in the absence and presence of $MgCl_2$. The K_m values calculated from these plots at infinite substrate concentrations differ slightly in the absence and presence of $MgCl_2$; K_m for NADP$^+$ 10 and 14 μM, K_m for NADH 25 and 18 μM, respectively. The catalytic centre activities calculated for this reaction at infinite substrate concentrations in the absence and presence of $MgCl_2$ are 8,500 min^{-1} and 11,500 min^{-1}, respectively.

The inhibition pattern of this reaction is very complex, but it can be generally stated, that it is of the mixed-inhibitory type (FIG. 6.14). From these graphs, which are also very much complicated by the substrate inhibition, which both donor and acceptor show, it can be concluded that the LINEWEAVER-BURK plots with both substrates in the presence of NADPH have no mutual point of intersection.

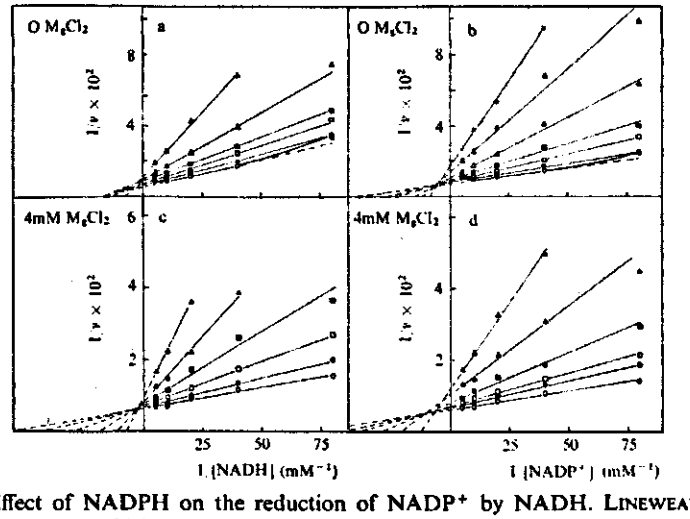

FIG. 6.14. Effect of NADPH on the reduction of NADP$^+$ by NADH. LINEWEAVER-BURK plots at high donor (NADH = 100 μM, in b and d) and high acceptor concentrations, (NADP$^+$ = 100 μM, in a and c), in the absence and presence of $MgCl_2$ (4 mM). NADPH concentrations: o —— o, none; • —— •, 12.5 μM; □ —— □, 25 μM; ■ —— ■, 50 μM; △ —— △, 100 μM; ▲ —— ▲, 200 μM; × —— ×, 300 μM. v expressed as μmoles NADH oxidized per min per mg of protein.

6.3. Discussion

For several flavoproteins, e.g. yeast and erythrocyte glutathione reductase (Scott et al., 1965; Massey and Williams, 1965; Icén, 1967), lipoamide dehydrogenase (Massey et al., 1960), and D-amino acid oxidase (Dixon and Kleppe, 1965), reaction mechanisms have been proposed, based on the formation and decomposition of binary complexes of the two substrates with the enzyme. A binary ping-pong bi-bi mechanism (Cleland, 1963) was accepted as a general mechanism, but studies with these flavoproteins (Koster and Veeger, 1968; Staal and Veeger, 1969; Visser et al., 1970; Veeger et al., 1970) and also with succinate dehydrogenase (Zeylemaker et al., 1969) showed that instead of this type of mechanism, Theorell-Chance or ordered bi-bi mechanisms are operating. With these enzymes it was found that the oxidized products act as competitive inhibitors of the donating substrates and that they are able to show spectrally visible complexes with the oxidized enzyme. In the light of the isolated N-5 adducts of flavin and substrate (De Kok and Veeger, 1967; De Kok et al., 1970) it was even questioned by Staal and Veeger (1969) whether all flavoproteins are acting with an ordered bi-bi or ternary complex mechanism. Hemmerich, Nagelschneider and Veeger (1970) even questioned whether the flavin is redox active rather than group-transfer active in redox reactions.

Several observations suggest that the *Azotobacter* transhydrogenae might be operating with a ping-pong bi-bi mechanism. The Lineweaver-Burk plots of the reactions NADPH → NAD$^+$, NADPH → TNAD$^+$ and NADH → TNAD$^+$ show a family of parallel lines at not too high donor concentrations. The K'_m vs. V'_m plot (Slater, 1955), made from the values of the apparent K_m and V_{max} which were obtained from extrapolation of the linear parts of the L-B plots, passes through the origin, supporting the possibility of a ping-pong mechanism. As outlined in the literature (Koster and Veeger, 1968; Zeylemaker et al., 1969; Staal and Veeger, 1969), however, this criterion is not sufficient since an ordered bi-bi mechanism or Theorell-Chance mechanism can also give a parallel line relationship, providing the dissociation constant of the first substrate (K_S^A) is much smaller than the limiting Michaelis constant for the second substrate (K_m^B). It is thus recommended (cf. DerVartanian, 1965; DerVartanian et al., 1966; Koster and Veeger, 1968) to use a competitive inhibitor towards the first substrate in order to increase the term $K_{AB} = K_S^A K_m^B$ in the equation

$$\frac{V_{max}}{v} = 1 + \frac{K_A}{[A]} + \frac{K_B}{[B]} + \frac{K_{AB}}{[A][B]} \qquad (1)$$

by multiplying it with a factor $(1 + [I]/K_I)$, thus making the plots convergent. In these mechanisms the K'_m vs. V'_m plot does not pass through the origin, although the line can intersect with the K'_m-axis close to the origin, making it difficult to distinguish clearly between the two mechanisms.

Cohen (Cohen, 1967; Cohen and Kaplan, 1970 b) could not distinguish

between the two mechanisms for the *Pseudomonas* transhydrogenase, but favoured the ping-pong bi-bi mechanism. In later studies (LOUIE and KAPLAN, 1970 b) it was suggested, however, that the Theorell-Chance mechanism might give a better description. Assuming either a ping-pong mechanism or an ordered bi-bi mechanism, lacking the last term in the rate equation, the substrate inhibition of the donor could be easily explained at high donor concentrations by the formation of a 4-equivalent reduced enzyme which is partially active or inactive (cf. CHAPTER 5). The existence of complexes of oxidized enzyme with $NADP^+$ and $TNADP^+$ (cf. CHAPTER 5) could explain the inhibition of the reactions $NAD(P)H \rightarrow TNADP^+$ and $NADH \rightarrow NADP^+$ at high acceptor concentrations. The fact that this is not observed with NAD^+ or $TNAD^+$ is consistent with the finding that similar complexes of these nucleotides with the oxidized enzyme, do not exist.

The general equation derived for both mechanisms for the reactions $NADPH \rightarrow TNAD^+$, $NADH \rightarrow TNAD^+$ and $NADPH \rightarrow NAD^+$ would be

$$\frac{V_{max}}{v} = 1 + \frac{K_m^A}{[A]} + \frac{K_m^B}{[B]}\left(1 + \frac{[A]}{K_{SS}^A}\right) \qquad (2)$$

in which K_{SS}^A is the dissociation constant of the donor from the 4-equivalent reduced enzyme. The equation would explain the substrate inhibiton at high donor concentration, which diminishes at high acceptor concentration, while at low donor concentrations the L-B plots are parallel.

For the systems $NADPH \rightarrow TNADP^+$ and $NADH \rightarrow TNADP^+$ the rate equation derived, would be

$$\frac{V_{max}}{v} = 1 + \frac{K_m^A}{[A]}\left(1 + \frac{[B]}{K_S^B}\right) + \frac{K_m^B}{[B]}\left(1 + \frac{[A]}{K_{SS}^A}\right) \qquad (3)$$

in which K_S^B is the dissociation constant of the oxidized enzyme-$TNADP^+$ complex. The equation would explain the inhibiton at high donor and acceptor concentrations and its counteraction by acceptor and donor, respectively. It is clear that large deviations from linearity are observed in the plots.

The studies in the presence of inhibitor are extremely complicated by the occurence of substrate inhibition and are inconsistent with the proposed ping-pong bi-bi mechanism. This mechanism can lead to competitive inhibition by the product of the first substrate (NAD^+) with respect to the acceptor ($TNAD^+$) (CHUNG, 1970), but cannot lead to pure non-competitive inhibition by NAD^+ with respect to NADH (cf. FIG. 6.4), unless a complicated relation, which varies with the concentration of $TNAD^+$, exists between the kinetic constants. For an ordered bi-bi mechanism the same is valid, but there is an additional possibility. Pure non-competitive inhibition of NAD^+ with respect to NADH can be obtained when $TNAD^+$ is the first substrate, NAD^+ being the last product, to dissociate from the enzyme (for which no experimental evidence is available) and in the special case that the dissociation constant for $TNAD^+$ is equal to

its Michaelis constant (MAHLER and CORDES, 1969); however, in this case no parallel line relationship can be obtained.

It was demonstrated (VAN DEN BROEK and VEEGER, 1970), that inhibition of the reactions NADPH → TNAD$^+$ and NADH → TNAD$^+$ occurs with 1 or 2 moles of NADP$^+$, depending on the concentrations of the donor. At high donor concentrations, where only one mole of NADP$^+$ is involved in the inhibition of the enzyme, non-competitive inhibition with respect to TNAD$^+$ and competitive inhibition with respect to NADPH is observed in the NADPH → TNAD$^+$ reaction (FIG. 6.2). Thus the totally opposite effects of product inhibition with respect to donor and acceptor indicate a different mechanism for the two reactions.

Furthermore in the presence of higher NADP$^+$ concentrations the order of the reaction changes. The relation with [NADPH]^2 is a consequence of the inhibition by two NADP$^+$ molecules, since in the absence of NADP$^+$ a linear relation with [NADPH] is observed. The relation with [TNAD$^+$] remains linear, although at low concentrations a deviation is visible to a higher order reaction. The possibility exists that the relation of the rate of the *Pseudomonas* enzyme with [NADPH]^2 and [TNAD$^+$] as observed by COHEN (COHEN, 1967; COHEN and KAPLAN, 1970 b) is due to contamination with NADP$^+$. 2'AMP should counteract this inhibitory effect, since these authors obtained a linear relationship with respect to NADPH in the presence of 2'AMP.

Although the inhibition pattern by NADP$^+$ in the NADPH → TNAD$^+$ system can be explained by both the ping-pong bi-bi and the ordered bi-bi mechanism, these mechanisms also do not provide an explanation for the dependency of the rate on [NADPH]^2 under these conditions. Due to the presence of 2'AMP, COHEN (COHEN, 1967; COHEN and KAPLAN, 1970 b) neglected this point in his proposals for the *Pseudomonas* enzyme.

The question arises as to what kind of mechanism is operating under these conditions. The dependency of the rate on [NADPH]^2 in the presence of NADP$^+$ suggests that the reductive step leads to an active 4-equivalent reduced enzyme. Therefore it is reasonable to assume a similar step in the absence of NADP$^+$, which is cancelled out in the rate equation.

The following two mechanisms are possible for the reaction NADPH → TNAD$^+$:

MECHANISM I

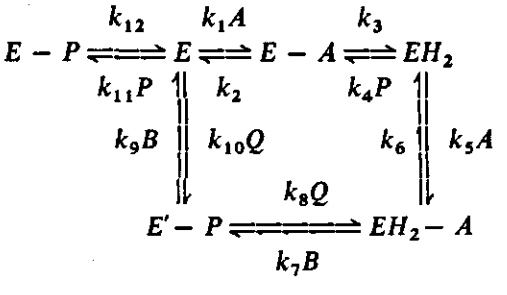

MECHANISM I,A

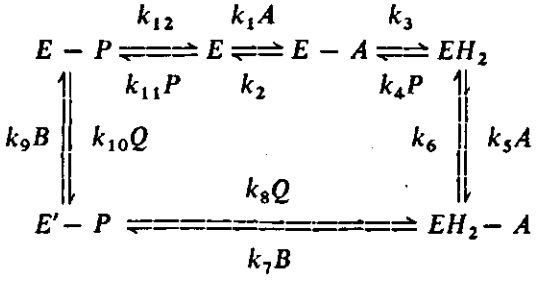

The initial velocity equations under the conditons $[Q] = 0$ and $[P] \neq 0$ are:

MECHANISM I

$$\frac{k_3[E_0]}{v} = 1 + \frac{(k_2 + k_3)(1 + [P]/K_p)}{k_1[A]} + \frac{(k_3 + k_4[P])}{k_5[A]} +$$

$$+ \frac{(k_3 + k_4[P])k_6}{k_5[A]k_7[B]} + \frac{k_2k_4[P](1 + [P]/K_p)}{k_1[A]k_5[A]} +$$

$$+ \frac{k_2k_4[P]k_6(1 + [P]/K_p)}{k_1[A]k_5[A]k_7[B]} + \frac{k_3(k_7 + k_9)}{k_7k_9[B]} \qquad (4)$$

MECHANISM I,A

$$\frac{\frac{k_3k_{12}}{k_3 + k_{12}}[E_0]}{v} = 1 + \frac{k_{12}(k_2 + k_3)(1 + [P]/K_p)}{k_1[A](k_3 + k_{12})} +$$

$$+ \frac{k_{12}(k_3 + k_4[P])}{k_5[A](k_3 + k_{12})} + \frac{(k_3 + k_4[P])k_6k_{12}}{k_5[A]k_7[B](k_3 + k_{12})} +$$

$$+ \frac{k_2k_4[P]k_{12}(1 + [P]/K_p)}{k_1[A]k_5[A](k_3 + k_{12})} + \frac{k_3k_{12}(k_7 + k_9)}{k_7k_9[B](k_3 + k_{12})} \qquad (5)$$

E_o is the total enzyme concentration and $K_P = k_{12}/k_{11}$; A is the donor (NADPH), B the acceptor (TNAD$^+$), P the first product (oxidized A = NADP$^+$) and Q the second product (reduced B = TNADH).
In MECHANISM I P inhibits competitively with respect to NADPH.
In MECHANISM I,A this is only possible if $k_{12} \gg k_3$; under these conditions MECHANISM I,A becomes identical to MECHANISM I.

In the absence of inhibitor P rate equation (4) is reduced to equation (6)

$$\frac{k_3[E_0]}{v} = 1 + \frac{k_5(k_2 + k_3) + k_1k_3}{k_1k_5[A]} + \frac{k_3k_6}{k_5[A]k_7[B]} + \frac{k_3(k_7 + k_9)}{k_7k_9[B]} \quad (6)$$

From this equation it can be derived, that the velocity is linearly dependent on $[A]$ and $[B]$. In the case of $k_6/k_5\,[A] \ll 1 + k_7/k_9$, a parallel line relationship can be obtained as observed in FIG. 6.1; this is very reasonable, since k_6/k_5, the dissociation constant of the second NADPH molecule from the 4-equivalent reduced enzyme is very small, 2 μM (cf. CHAPTER 5).

In the presence of inhibitor P the velocity is dependent on $[A]^2$ (cf. FIG. 6.3) and $[B]$ and the inhibition on $[P]^2$ at low concentrations of A and B. At increasing concentrations of A the terms in the denominator of the rate equation which contain $[A]^2$ tend to zero faster than the other terms, making the relation linear in $[A]$ and $[B]$ under conditions that the inhibition is linearly dependent on $[P]$ (cf. VAN DEN BROEK and VEEGER, 1970). The inhibition remains competitive towards A (NADPH) and non-competitive with respect to B (TNAD$^+$). This equation, however, does not provide an explanation for the observed inhibition by NADPH, but abortive complexes of the type *EH_2-NADP$^+$-NADPH* or *EH_2-(NADPH)$_2$*, with NADP$^+$ bound at an a-specific site, e.g. the NAD$^+$ binding site, can explain this phenomenon. The inhibition of the reaction NADPH $\rightarrow$ TNADP$^+$ by TNADP$^+$ might be explained by the affinity of the latter for the oxidized enzyme.

MECHANISM I does not provide an explanation for the inhibition patterns of NAD$^+$ in the reaction NADH $\rightarrow$ TNAD$^+$. Assuming that NAD$^+$ does not form the *E-P* complex, the rate equation predicts that NAD$^+$ will inhibit competitively towards both NADH and TNAD$^+$ and that the velocity will be dependent on [NADH]^2. This however, is not observed.

By changing the sequence of addition of the acceptor molecule and the second donor molecule, a slightly modified MECHANISM II can be given

MECHANISM II

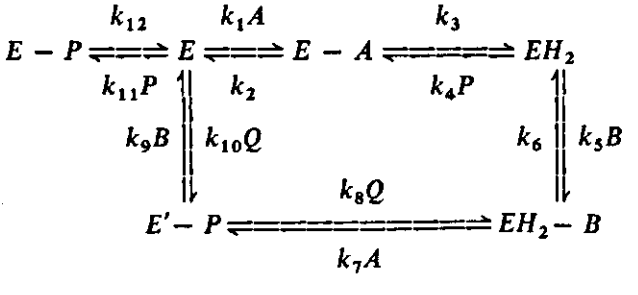

with the following initial velocity rate equation

$$\frac{k_3[E_0]}{v} = 1 + \frac{k_7(k_2 + k_3)(1 + [P]/K_p) + k_1k_3}{k_1k_7[A]} +$$

$$+ \frac{k_9(k_3 + k_4[P]) + k_3k_5}{k_5k_9[B]} +$$

$$+ \frac{k_1k_6(k_3 + k_4[P]) + k_2k_4[P]k_7(1 + [P]/K_p)}{k_1k_7[A]k_5[B]} +$$

$$+ \frac{k_2k_4[P]k_6(1 + [P]/K_p)}{k_1[A]k_5[B]k_7[A]} \qquad (7)$$

Assuming NAD^+ does not form the *E-P* complex, i.e. $[P]/K_p = 0$, the equation predicts for the NADH → $TNAD^+$ reaction competitive inhibition by NAD^+ with respect to $TNAD^+$ and NADH, while the rate of the reaction will be dependent on $[NADH]^2$, which is not observed. Equation (7) also does not explain the inhibition patterns of $NADP^+$ in the reaction NADPH → $TNAD^+$. However, when an irreversible binding of $TNAD^+$ to the reduced enzyme is assumed, i.e. $k_6 = 0$, the rate equation is simplified to the form given in eq. (8)

$$\frac{k_3[E_0]}{v} = 1 + \frac{k_7(k_2 + k_3) + k_1k_3}{k_1k_7[A]} + \frac{k_9(k_3 + k_4[P]) + k_3k_5}{k_5k_9[B]} +$$

$$+ \frac{k_2k_4[P]}{k_1[A]k_5[B]} \qquad (8)$$

Under these conditions the equation predicts that the velocity is linearly dependent on $[A]$, $[B]$ and $[P]$, while the inhibition of P (= NAD^+) will be competitive with respect to B (= $TNAD^+$) and non-competitive towards A (= NADH). Furthermore it can be derived that a parallel line relationship is obtained in the absence of NAD^+, but in its presence the L-B plots are convergent. The observed substrate inhibition is not explained by this mechanism, but the existence of abortive complexes can explain this phenomenon. The inhibition by $NADP^+$ will be non-competitive with respect to A and B (FIG. 6.5) as can be derived from eq. (7) with $k_6 = 0$ and P = $NADP^+$, due to the existence of the two complexes *E-NADP*$^+$ and EH_2-*NADP*$^+$.

According to the relations proposed and the kinetic patterns obtained it is very reasonable to assume that the reactions NADPH → $TNAD^+$ and NADH → $TNAD^+$ will proceed along different pathways, which, however, are closely related. Evidence for this comes from the spectral studies (cf. CHAPTER 5) where it was found that the reaction of the two donors with the

oxidized enzyme does not follow the same pattern; at infinite donor concentration the absorption spectrum of the system NADPH-$NADP^+$ is different from that of the system NADH-NAD^+. The existence of two complexes *NADPH-EH_2* and *NADH-EH_2-NAD^+* was proposed. A complex of the type *E-$TNAD^+$-NADH* could be involved in the reaction with NADH, although it has not been taken up in the scheme in order to make the equation as simple as possible. Taking these complexes into consideration the overall kinetic picture will not change, only a few more constants are added to eq. (8).

The question arises whether the reactions NADPH → $TNADP^+$, NADH → $TNADP^+$ and NADH → $NADP^+$ follow similar patterns as outlined above. The substrate inhibition, observed in the reaction NADH → $TNADP^+$ can be explained by the formation of the abortive oxidized enzyme-$TNADP^+$ complex. In the presence of $NADP^+$ the inhibition is non-competitive with respect to both donor and acceptor, which can only be explained by eq. (7) with $P = NADP^+$. The linearity of the $1/[TNADP^+]$ plots indicates that the formation of the oxidized-$TNADP^+$ complex is largely prevented by $NADP^+$ due to its higher affinity for the oxidized enzyme. It is difficult to make a definite statement about the actual inhibition pattern of $NADP^+$ in the reaction NADPH → $TNADP^+$, especially whether the inhibitor is competitive towards both substrates (FIG. 6.10). Competitive inhibition would be consistent with the kinetic picture of FIG. 6.8, where for the NADH → $TNADP^+$ reaction it was shown that in the presence of $NADP^+$ the mechanism could be of the rapid equilibrium random bi-bi type (CLELAND, 1963). In such a mechanism both products inhibit competitively.

A rapid equilibrium type of mechanism is also consistent with the data of the reaction NADH → $NADP^+$ (FIG. 6.13) and is attractive for several reasons. A direct transfer of hydrogen from the 4B position of the nicotinamide ring of NADH to the 4B position of that of $NADP^+$ without exchange of protons of the medium, as observed by LOUIE and KAPLAN (1970 b) for the *Pseudomonas* transhydrogenase is less likely in a ping-pong mechanism than in an ordered bi-bi or rapid equilibrium random bi-bi mechanism, in which both substrates are simultaneously bound on the enzyme. The direct hydrogen transfer might proceed via N-5 of the isoalloxazine ring without actually reducing the flavin (HEMMERICH et al., 1970).

A rapid equilibrium random bi-bi mechanism does not exclude MECHANISMS I and II as pathways in the reduction of $TNAD^+$. MECHANISM II is a consequence of the irreversible binding of $TNAD^+$ to the reduced enzyme; the mechanism becomes random when reversible substrates like $NADP^+$ and $TNADP^+$ are involved. The assumption of reversible and irreversible binding of the acceptor is justified by the observation (cf. CHAPTER 5) that NAD^+ has a five-fold higher affinity for the reduced enzyme than $NADP^+$.

The remaining question is the reaction NADH → $NADP^+$. The activating effect of NADPH in this reaction can be explained in terms of competition of $NADP^+$ and NADPH for the oxidized enzyme. Due to its higher affinity for the oxidized enzyme, NADPH can more readily reduce the enzyme than NADH

and convert it into the reactive 2-equivalent reduced enzyme. At high concentrations of NADH the lag period is less than at low concentrations, supporting the view that this donor is less effective in this respect (VAN DEN BROEK and VEEGER, 1968, 1970). The observation that an equimolar amount of NADPH is sufficient for maximum activity suggests that the actual physiological pathway will be a shuttling between the 2-equivalent and the 4-equivalent reduced enzyme.

It must be mentioned that the '*allosteric*' type of kinetic picture obtained with this enzyme (viz. s-shaped velocity vs. substrate curves, FIG. 6.11) does not need to be explained by the different theories developed for such cases (cf. MONOD et al., 1965; KOSHLAND JR., et al., 1966). Actually it was pointed out earlier (SWEENY and FISHER, 1968), that complex kinetic mechanisms could give a similar picture. Even the strong influence of ATP and GTP on the kinetic picture of the reaction NADH → $NADP^+$ could be explained in these terms. By being bound at a non-catalytic site these compounds could enhance the binding of $NADP^+$ to the oxidized enzyme or lower the affinity of NADPH, thus effecting only the kinetic parameters. The question is whether the influence of these trinucleotides should be called *allosteric* since they have a direct influence on a different site.

On the basis of these s-shaped curves the occurrence of a preferred order mechanism was proposed (VAN DEN BROEK and VEEGER, 1970), as described by FERDINAND (1966) for phosphofructokinase. At that time, however, the complexing with $TNADP^+$ and the occurrence of the reaction to the 4-equivalent reduced enzyme were not known.

The demonstration that the reversal of reaction (I) may vary from preparation to preparation suggests that this is a $NADP^+$ inhibition phenomenon, which might be explained in terms of bound $NADP^+$ from endogeneous origin (KAPLAN et al., 1952). Upon purification this $NADP^+$ will be removed. The 2'AMP activation experiments (LOUIE and KAPLAN, 1970 a), our electron microscopic investigations (CHAPTER 4) and the studies of JONES and REDFEARN (1967) on endogeneous $NADP^+$ strongly support this suggestion and they indicate that the site with its high affinity for $NADP^+$ will be involved in the reaction. No answer can be given about the possible involvement of different protein conformations, induced by $NADP^+$. In this respect, however, it is of interest to recall the recently published suggestion of RYDSTRÖM et al. (1970) of the possibility of an energy-linked conformational change of mitochondrial transhydrogenase, involving a conversion of the enzyme from an inactive to an active state.

7. STUDIES ON *AZOTOBACTER* LIPOAMIDE DEHYDROGENASE AND ITS APOPROTEIN

7.1. INTRODUCTION

Lipoamide dehydrogenase (E.C.1.6.4.3.) catalyzes the re-oxidation of dihydrolipoic acid and derivatives by NAD^+ and functions in the oxidative decarboxylation of α-ketoglutaric acid and pyruvate as part of a multi-enzyme complex. The enzyme is widely spread in nature and has been isolated from several types of organisms, including bacteria e.g. *Escherichia coli* (KOIKE et al., 1960), *Mycobacterium tuberculosis* (GOLDMAN, 1960), *Streptococcus faecalis* (DOLIN, unpublished results), baker's yeast (MISAKA and NAKANISHI, 1963; WREN and MASSEY, 1965), higher plants e.g. *Spinacea oleracea* (BASU and BURMA, 1960; MATTHEWS and REED, 1963; JACOBI and ÖHLERS, 1968) and higher organisms e.g. pig heart (STRAUB, 1939; SAVAGE, 1957; MASSEY et al., 1960), beef liver (LUSTY, 1963), human liver (IDE et al., 1967) and identified in several other tissues and organisms. The enzyme has been previously known as Straubs diaphorase, catalyzing the oxidation of NADH by artificial electron acceptors, but it was shown by MASSEY (1958, 1960) to be identical with lipoamide dehydrogenase.

In the course of our investigations on succinic dehydrogenase and non-heme iron proteins from *Azotobacter vinelandii* it was found that relative high amounts of free and pyruvate dehydrogenase-complex-bound lipoamide dehydrogenase were present in this bacteria in the log-phase of the growth. Our interest was called to the enzyme by the presence of the NAD^+-dependent NADPH-lipoate activity in different extracts. As shown (cf. CHAPTER 3) this type of activity was due to a complexing of the free and pyruvate-complex-bound lipoamide dehydrogenase activity with the *Azotobacter* transhydrogenase. The large scale procedure developed for the isolation and purification of *Azotobacter* transhydrogenase yielded side fractions suitable for the isolation of lipoamide dehydrogenase.

This study deals with some of the properties of the *Azotobacter* lipoamide dehydrogenase and its apoprotein. The data presented in this study are compared with those given for lipoamide dehydrogenase from pig heart and *E. coli*.

7.2. RESULTS

7.2.1. *Spectral properties*

The isolated *Azotobacter* lipoamide dehydrogenase exhibited the typical spectrum of a flavoprotein, as shown in FIG. 7.1. Maxima occur at 456–457 nm, 350–370 nm and 260–270 nm, minima at 394 nm, 325 nm and 240 nm, while a marked shoulder at 485 nm and a less marked one at about 430 nm are observable. Some preparations, however, characterized by a similar specific activity,

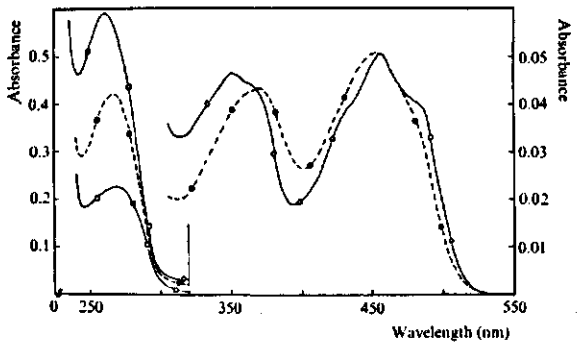

FIG. 7.1. Absorption spectra of *Azotobacter* lipoamide dehydrogenase. Enzyme in 0.03 M potassium phosphate buffer (pH 7.4) containing 0.3 mM EDTA. Spectra recorded versus buffer. o —— o, Holoenzyme as isolated according to the method of MASSEY (MASSEY, 1960; MASSEY et al., 1960), 0.35 mg of protein per ml. • —— •, Apoenzyme-FAD complex, 0.30 mg of protein per ml. Apoenzyme prepared according to the method of KALSE and VEEGER (1968) and solubilized in 0.3 M phosphate buffer (pH 7.5), containing 3 mM EDTA. Apoenzyme incubated with FAD (200 μM) at 25° for 2 hours and extensively dialysed against 3 times 200 ml 0.03 M phosphate buffer (pH 7.4), containing 0.3 mM EDTA, after which difference spectrum recorded. □ —— □, Apoenzyme, 0.17 mg of protein per ml.

did not show appreciable shoulders around the peak at 457 nm. The absorbance ratios at the different maxima, $A_{350}/A_{457} = 0.90$ and $A_{457}/A_{392} = 2.7$, are in good agreement with those given in the literature for lipoamide dehydrogenase from different sources (SAVAGE, 1957; LUSTY, 1963; KOIKE et al., 1960; MATTHEWS and REED, 1963; WREN and MASSEY, 1965). The ratio $A_{280}/A_{457} = 7.5$ is on the average somewhat higher, possibly due to high nucleic acid contamination.

The prosthetic group of the bright yellow, highly fluorescent enzyme was separated by heat treatment at 100° in sealed vessels or by precipitating the apoprotein with cold 5% trichloracetic acid (MAYHEW and MASSEY, 1969); it is characterised by maxima at 262 nm, 375 nm and 448 nm. Extrapolation of the heat treatment data revealed an extinction coefficient at 455 nm of 11,300 $M^{-1}cm^{-1}$ for the protein-bound flavin. An extinction coefficient identical with that of free FAD was also obtained from the TCA treatment. The prosthetic group was identified as FAD by thin layer chromatography (KILGOUR et al., 1957) with three different solvent systems.

The optical rotatory dispersion and circular dichroism absorption curves of *Azotobacter* lipoamide dehydrogenase are shown in FIG. 7.2 and FIG. 7.3.

The CD spectrum in the 200–500 nm region is characterized by three major ellipticity extrema at about 370 nm, 282 nm and 208–222 nm, with mean residue molar ellipticities, $[\theta]$, of + 43, + 62 and − 15,000 degrees cm^2 $dmoles^{-1}$, respectively. The negative band corresponds to a well defined double helix and has minima at 208 nm and 220–222 nm. In contrast to several other FAD

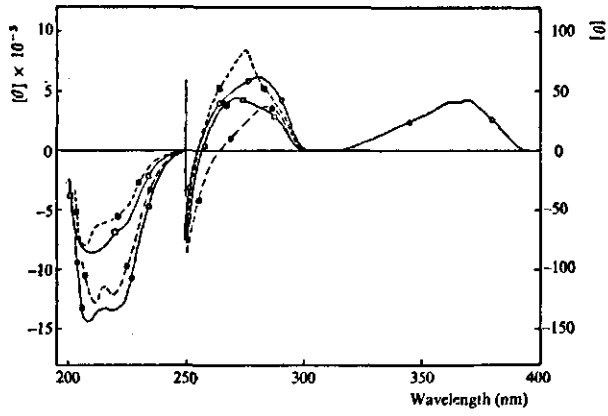

FIG. 7.2. Circular Dichroism spectra of *Azotobacter* lipoamide dehydrogenase and its apoproteins. Enzymes in 0.03 M potassium phosphate buffer (pH 7.4), containing 0.3 mM EDTA. Measurements were performed at 10° in cells of 1–10 mm pathlength. ○ —— ○, holoenzyme as isolated, 1.15 mg of protein per ml; ● —— ●, apoenzyme, (1,33 mg/ml) prepared according to the method of KALSE and VEEGER (1968) by treating the holoenzyme two times with acid ammonium sulfate in the presence of KBr. □ —— □, apoenzyme (1.75 mg of protein/ml) prepared according to the method of BRADY and BEYCHOK (1968, 1969) by dialysis of the holoenzyme against 1.5 M guanidine-HCl in 0.03 M phosphate buffer (pH 7.6) containing 1 mM EDTA in the presence of FMN (FMN concentration equal to that of FAD in the enzyme solution); ■ —— ■, apoenzyme (0.53 mg of protein/mg) prepared according to the method of BRADY and BEYCHOK (1968, 1969) by dialysis of the holoenzyme against 1.5 M guanidine-HCl in the absence of FMN.

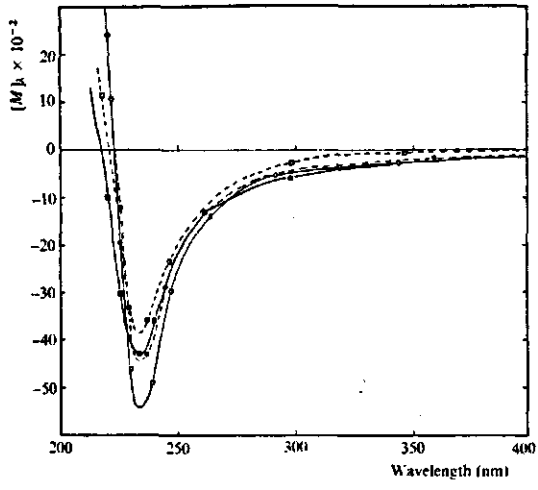

FIG. 7.3. Optical Rotatory Dispersion curves of *Azotobacter* lipoamide dehydrogenase and its apoproteins. Conditions and preparations as described in FIG. 7.2. ○ —— ○, Holoenzyme as isolated (1.15 mg of protein/ml); ● —— ●, apoenzyme (1.33 mg of protein/ml), prepared by the acid ammonium sulfate treatment; ■ —— ■, apoenzyme (1.75 mg of protein/ml), prepared by the guanidine-HCl treatment in the presence of FMN; □ —— □, apoenzyme (0.53 mg of protein/ml), prepared by the guanidine-HCl treatment in the absence of FMN.

containing flavoproteins no optical activity can be observed above 400 nm (cf. CHAPTER 5); the overall shape, however, is rather similar. A characteristic difference from the CD spectrum of the pig heart lipoamide dehydrogenase (VEEGER et al., 1969) is the reversal of the 280 nm band and the absence of the small shoulder at 300–320 nm.

The ORD spectrum of the enzyme is characterized by a minimum at 233 nm with a mean residue rotation of about $-5{,}500$ degrees $cm^2\ dmole^{-1}$. The shape of this curve is identical to that for the pig heart enzyme, although the mean residue rotation at 233 nm in our case is higher.

Semiquantitative values for the helix content can be calculated from the CD magnitudes at 222 nm using poly - α - L-glutamic acid or poly - L - lysine - HCl as a reference standard (GREENFIELD and FASMAN, 1969). The helix content calculated from $[\theta]_{222}$ is about 35%.

7.2.2. *Ultracentrifugal studies*

The enzyme sediments as a single symmetrical peak in the analytical ultracentrifuge. A sedimentation coefficient ($s_{20,w}$) was determined according to SVEDBERG and PEDERSON (1940) and found to be 6.15 S at a protein concentration of 8.1 mg/ml.

From gel filtration with Sephadex G-200 columns, of which the effective pore radius was determined with alcohol dehydrogenase (ACKERS, 1964), a Stokes radius of 39.7 Å for the lipoamide dehydrogenase can be calculated. This permits the determination of the diffusion constant according to the method of SIEGEL and MONTY (1965, 1966), $D_{20,w} = 5.36 \times 10^{-7}\ cm^2 sec$. Combination of the different constants reveals a molecular wight of 103,000 daltons (SIEGEL and MONTY, 1965, 1966). From these results a frictional ratio of the holoenzyme, $f/f_o = 1.28$, was also calculated.

By application of the sucrose gradient method of MARTIN and AMES (1961) and assuming molecular weights of the markers used of 150,000 daltons for yeast alcohol dehydrogenase and 250,000 daltons for catalase, a molecular weight for the native enzyme of 101,000 daltons (average value of 4 independent experiments) was calculated using the approximation

$$R = \left(\frac{\text{mol.wt. of unknown sample}}{\text{mol.wt. of marker}}\right)^{2/3}$$

where R is the ratio of distance from the meniscus travelled by the unknown protein sample to the distance from the meniscus travelled by the marker. The results obtained are in good agreement with those given for lipoamide dehydrogenase from pig heart (VISSER and VEEGER, 1968). TABLE 7.1 summarizes the results.

7.2.3. *Reactivity of the enzyme*

Compared with the pig heart enzyme (MASSEY et al., 1960; VISSER, 1970) the *Azotobacter* lipoamide dehydrogenase is characterized by higher lipoate and

TABLE 7.1. Comparison of different molecular constants of lipoyl dehydrogenase from *Azotobacter*, pig heart and *E.coli*. The values for the apoenzyme of the *Azotobacter* and pig heart enzyme are also given. Conditions as described in: 'METHODS AND MATERIALS'.

Preparation	*Azotobacter*		Pig heart		*E.coli*
Molar constant	native enzyme	apoenzyme	native enzyme	apoenzyme	native enzyme
Stokes radius(Å)	40	30	42*	31*	
$D_{20,w}$ ($cm^2sec^{-1} \times 10^7$) Sephadex G-200	5.36	7.10	5.07*	6.86*	
$s_{20,w}$	6.0	3.8	5.8*	4.2*	6.24****
$D_{20,w}$ ($cm^2sec^{-1} \times 10^7$) Ultracentrifuge	—	7.15	4.63**	6.92* 6.08***	5.01****
$M_{S,D}$ (*D*-Sephadex)	103,600	48,000	102,800*	55,000*	
$M_{S,D}$ (*D*-Ultracentrifuge)	—	51,500	81,000*** 114,000**	54,500*	112,000****
*M*sucrose gradient	101,000	57,000			
f/f_o	1.28	1.22	1.35*	1.25*	

* ref. VISSER and VEEGER, 1968
** ref. MASSEY et al., 1962
*** ref. SAVAGE, 1957
**** ref. KOIKE et al., 1963

DCIP-activities, as measured under standard conditions of donor and acceptor. Representative enzyme preparations show the following activities: lipoate activity, 25 (± 3) μmoles mg^{-1} min^{-1} and DCIP activity, 5 (± 1) μmoles mg^{-1} min^{-1} (cf. pig heart: lipoate activity ± 20 μmoles/min/mg and DCIP activity 0.7–0.8 μmoles/min/mg; VISSER, 1970). The relatively high diaphorase activity is not due to metal contamination, since the same precautions were taken in the purification procedures as for the pig heart enzyme, e.g. 0.5–1 mM EDTA was included at all stages. In contrast to the pig heart enzyme (KALSE and VEEGER, 1968; VISSER, 1970) dilution of the enzyme to protein concentrations of 0.01 mg/ml in 0.03 M phosphate buffer (pH 7.5) does not result in significant changes in activity for the next 48 hours.

The reaction with lipoic acid is strongly determined by the type and concentration of buffer used; lipoate activity is optimal at pH 6.5 in 1 M tri-sodium citrate-phosphoric acid buffer; at lower citrate concentrations and in the presence of potassium ions the activity measured is much lower.

Depending on the concentration of donor and acceptor the oxidation of lipoate shows a pronounced lag period. The lag is eliminated by the addition of NAD^+ to the reaction mixture (cf. MASSEY and VEEGER, 1960; KAWAHARA et al., 1968; KOIKE et al., 1960; MATTHEWS and REED, 1963; LUSTY, 1963; IDE et al., 1967). The lipoate reduction is strongly inhibited by NADH non-competitively with respect to lipoic acid (FIG. 7.4). Because NAD^+, a product-inhibitor of the reaction, is included as an activator no conclusions can be drawn

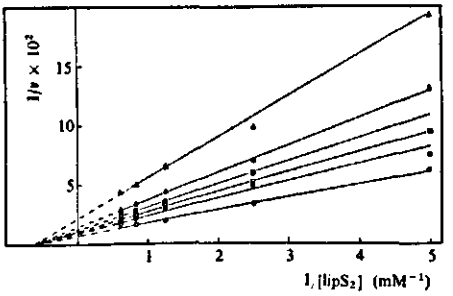

FIG. 7.4. Effect of NADH on the reduction of $lipS_2$ by NADH in the presence of NAD^+. $LipS_2$ activity determined at 25° as described in CHAPTER 2 and corrected for blank rates without $lipS_2$. The reaction was started by the addition of 3 μg lipoamide dehydrogenase. v expressed as μmoles NADH oxidized per min per mg of protein. The results are plotted according to the method of LINEWEAVER and BURK (1934). Concentration of NADH: o —— o, 19 μM; • —— •, 38 μM; □ —— □, 57 μM; ■ —— ■, 76 μM; △ —— △, 95 μM; ▲ —— ▲, 187 μM.

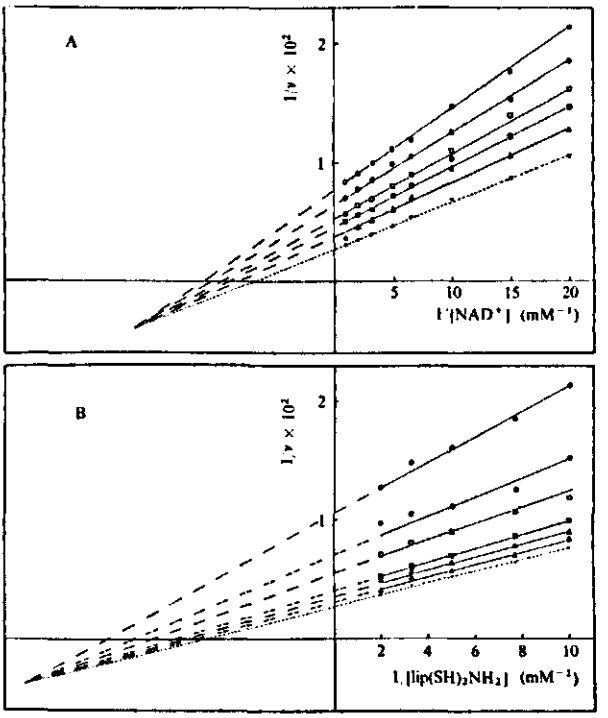

FIG. 7.5. Reduction of NAD^+ by $lip(SH)_2NH_2$. Assays were carried out spectrophotometrically at 340 nm at 25° as described in CHAPTER 2. The reaction was started by the addition of 1 μg of *Azotobacter* lipoamide dehydrogenase. Velocities expressed as μmoles NAD^+ reduced per min per mg of protein. A. $1/v$ vs. $1/[NAD^+]$ plots at different $lip(SH)_2NH_2$ concentrations: o —— o, 100 μM; • —— •, 133 μM; □ —— □, 200 μM; ■ —— ■, 300 μM; △ —— △, 400 μM. The dotted L-B plot (•-•-•) is obtained by extrapolating to infinite $lip(SH)_2NH_2$ concentration. B. $1/v$ vs. $1/[lip(SH)_2NH_2]$ plots at different NAD^+ concentrations: o —— o, 50 μM; • —— •, 100 μM; □ —— □, 150 μM; ■ —— ■, 300 μM; △ —— △, 500 μM; ▲ —— ▲, 1 mM. The dotted L-B plot (• – • – •) is obtained by extrapolating to infinite NAD^+ concentration.

TABLE 7.2. The relation between kinetic parameters calculated with NAD^+ and $lip(SH)_2NH_2$ as substrates at 25°, according to the simplified ternary complex mechanism outlined by VISSER (VISSER et al., 1970; VISSER, 1970). The figures are based upon the flavin content of the *Azotobacter* enzyme and expressed per catalytic centre. The data for the pig heart enzyme are also given (from ref. VISSER et al., 1970).

Kinetic parameter	*Azotobacter* enzyme	Pig heart enzyme
V_{max}	18,500	17,300
$K_m(NAD^+)$	180 μM	250 μM
$K_m(lip(SH)_2NH_2)$	145 μM	360 μM
k_1	2×10^6 M^{-1} sec^{-1}	1.25×10^6 M^{-1} sec^{-1}
k_{-1}	200 sec^{-1}	500 sec^{-1}
$\frac{1 + k_{-2}/k_3}{k_2}$	6.5×10^{-7} M sec^{-1}	50×10^{-7} M sec^{-1}
$K_D(NAD^+)$	100 μM	400 μM

from the complicated kinetic patterns. The activity (moles NADH oxidized per minute per mole of enzyme flavin) calculated at infinite lip S_2 and 19 μM NADH in the presence of 108 μM NAD^+ is 8,500.

The reaction lip $(SH)_2$ NH_2 + NAD^+ → lip S_2NH_2 + NADH + H^+ was studied at variable donor and acceptor concentrations. The series of LINEWEAVER-BURK plots at varying concentrations are non-parallel (cf. MASSEY et al., 1960), but converge to one point in the third quadrant (FIG. 7.5). No activation is observed at low donor and acceptor concentrations as with the pig heart enzyme (cf. VISSER et al., 1970). This type of kinetics is found in studies with several other flavoproteins (cf. KOSTER and VEEGER, 1968; ZEYLEMAKER et al., 1969; ZEYLEMAKER, 1969; STAAL and VEEGER, 1969) and points to an 'ordered bi-bi' mechanism (CLELAND, 1963). No definite statement concerning the mechanism of the *Azotobacter* lipoamide dehydrogenase can be given, since no inhibition studies were performed. From the plots given K_m values are calculated; K_m for NAD^+ at infinite $lip(SH)_2NH_2$ is 180 μM; K_m for $lip(SH)_2NH_2$ at infinite NAD^+ is 145 μM. The value of V_{max} calculated at infinite substrate concentrations is 370 μmoles NAD^+ reduced min^{-1} mg^{-1}, equivalent to a catalytic center activity of 18,500 min^{-1}. The calculated K_m values are about half those of the pig heart enzyme (VISSER et al., 1970; MASSEY, 1963), but the catalytic center activity is in rather good agreement with the value given by VISSER (VISSER et al., 1970). Assuming a ternary complex mechanism some velocity constants are calculated according to the simplified mechanism outlined by VISSER et al., (1970). A survey of the calculations in comparison with the data from the pig heart enzyme are given in TABLE 7.2.

7.2.4. *Preparation of the apoenzyme and recombination with FAD*

Removal of the flavin was accomplished by the acid ammonium sulfate treatment as described by KALSE and VEEGER (1968) for the pig heart enzyme. The precipitated apoenzyme was not dissolved in 1 M Tris-acetic acid buffer (pH 8.1) containing 3 mM EDTA, but in 0.3 M potassium phosphate buffer (pH 7.2), containing 3 mM EDTA at room temperature and diluted with 0.03 M

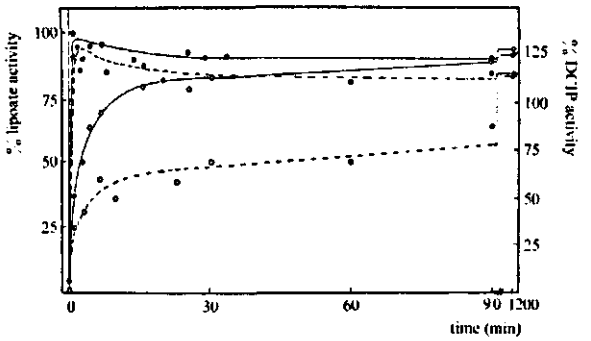

FIG. 7.6. Effect of temperature on the recombination of *Azotobacter* lipoamide dehydrogenase apoenzyme with FAD. Apoenzyme, prepared according to the method of KALSE and VEEGER (1968), (4 μM) was incubated with FAD (200 μM) in 0.1 M phosphate buffer (pH 7.4), containing 1 mM EDTA at 0° and 25°. Samples were withdrawn at the times indicated and lipoate (o —— o) and DCIP (• —— •) activities were determined as described in CHAPTER 2. Full and dotted lines, incubation at 25° and 0°, respectively. Activities expressed as % of original activity.

phosphate buffer (pH 7.2) to a concentration of 0.2 M. When the apoenzyme was dissolved in Tris-buffer an instant flocculation occurred and the capability to recombine with FAD was considerably lowered. The residual activity of the apoenzyme was on the average 3 to 4% of the original lipoate and DCIP activities. After a second treatment the residual activities had decreased to about 0.5% without appreciable loss of protein and ability to recombine with FAD, unless buffers other than 0.3 M phosphate buffer (pH 7.2) were used for solubilisation.

The enzymatic activity is only restored by FAD and not by FMN. The recombination is a time and temperature dependent process (FIG. 7.6). The restoration of the lipoate activity with FAD is considerably retarded at 0° and maximal activity obtained after an incubation period of 3 hours is only about 50–60% of the original activity, but after 24–48 hours incubation a level of 80–90% is obtained. Remarkable is that at 0° a relatively rapid increase in lipoate activity to about 40–50% of the original value is followed by a much slower increase. At 25° 80–90% of the original activity is already regained within an incubation period of 30 min and a biphasic process does not occur. No gross differences are obtained for the DCIP activity at both temperatures. Maximum DCIP activity is already obtained after about 1–2 min, but in contrast to the pig heart enzyme (KALSE and VEEGER, 1968) the activity is not much higher than that of the holoenzyme and it hardly decreases with time.

The spectrum of the reconstituted FAD enzyme is shown in FIG. 7.1. It is characterized by small shifts of maxima and minima and by changes in the characteristic ratios. Maxima occur at 453–456 nm, 370 nm and 265 nm, minima at 403 nm, 312 nm and 245 nm, while no shoulders are observable at 430 nm and 485 nm. The ratios A_{370}/A_{456}, A_{456}/A_{493} and A_{280}/A_{456}, are 0.85, 1.92 and 6.0 respectively for the reconstituted FAD-enzyme. In this respect it is of interest to

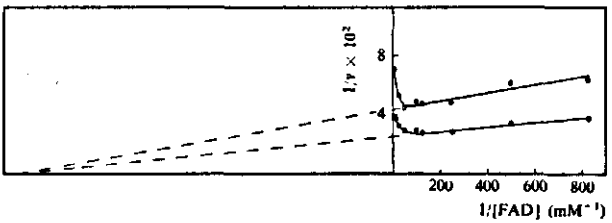

FIG. 7.7. Effect of FAD on the reactivation of *Azotobacter* lipoamide dehydrogenase apoenzyme by FAD. Apoenzyme, prepared according to the method of KALSE and VEEGER (1968), was incubated at 25° with FAD at the concentrations indicated. After an incubation period of 30 min samples were withdrawn and $lipS_2$ activities (o —— o) measured; the DCIP activities (• —— •) were measured after an incubation period of 2 hours. Velocity expressed as μmoles NADH oxidized per min per mg.

recall the similarity of this spectrum with the spectrum of lipoamide dehydrogenase apoenzyme-FMN complex form pig heart (VISSER and VEEGER, 1970), although in the latter case the maximum was at 445 nm. FIG. 7.7 shows the effect of the FAD concentration on the reactivation of the apoenzyme. High concentrations of FAD are inhibitory both on the restoration of lipoate and DCIP activity. This inhibitory effect complicates the exact determination of the K_m value for FAD. From three independent experiments an average apparent K_m for FAD of about 6×10^{-7}M was calculated and assuming the K_D is equal to K_m a K_{ass} for FAD of 1.6×10^{6}M can be calculated. This value obtained is about 10-fold higher than that of the pig heart enzyme (VISSER and VEEGER, 1970), but quite similar to that of glutathione reductase (STAAL et al., 1969).

FMN does not restore any activity, but as found by VISSER and VEEGER (1970) for pig heart lipoamide dehydrogenase and by STAAL et al. (1969) for glutathione reductase, FMN can affect the binding of FAD. In the first case FMN is a competitive inhibitor of FAD binding. Pre-incubation of the *Azotobacter* apoenzyme wit FMN at 25° and subsequent incubation with FAD lowers the activity restored considerably, although 80–90% of the maximum level of recombination obtained is reached within a period of about 5 min. Addition of FMN alter full restoration by FAD results in a slow decline in

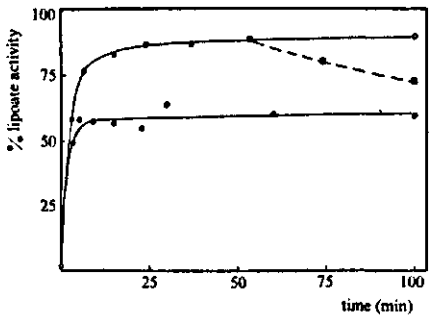

FIG. 7.8. Influence of FMN on the restoration of lipoate activity. Apoenzyme of *Azotobacter* lipoamide dehydrogenase was prepared according to the method of KALSE and VEEGER (1968). • —— •, 0.1 mg apoenzyme preincubated with 230 μM FMN at 25° during 30 min, 130 μM FAD added and activities determined at the times indicated. o —— o, control, not preincubated with FMN, but left at 25° for 30 min, before 130 μM FAD was added. ■ —— ■, 120 μM FMN added after nearly full restoration of activity by FAD. The activities are expressed as % of the original lipoate activity.

activity. The results are shown in FIG. 7.8.

In their studies on lipoamide dehydrogenase from pig heart BRADY and BEYCHOK (1968, 1969) distinguished between two conformations of apoenzyme by preparing their apoenzyme with 1.5 M guanidine-hydrochloride in the absence and presence of FMN. In the presence of thiol derivatives the authors were able to bring about complete recombination of the apoenzyme with FAD. Although it was shown in our laboratory that the pig heart apoenzyme prepared by the method of KALSE and VEEGER (1968) differed from that prepared with guanidine-HCl (VOETBERG, unpublished) it was of interest to compare both methods for the *Azotobacter* enzyme.

Preparation of the apoenzyme by dialysis against 1.5 M guanidine-hydrochloride in potassium phosphate buffer (pH 7.6) in the absence or presence of FMN results only in very small losses of protein (about 10%), in contrast to BRADY and BEYCHOK (1969) who lost about 60% of the protein in the absence of FMN. The apoenzyme prepared in the absence of FMN had a residual activity of about 2–3% of the original lipoate and DCIP activity. In the absence of thiol derivatives both at 0° and 25°, only 6% of the original lipoate activity and 15% of the original DCIP activity is regained even after several days. Addition of 0.1 M β-mercaptoethanol raises the restored lipoate activity to about 25–30%, a slightly higher activity (30–35%) is obtained after an incubation period of 24 to 48 hours on ice. In the presence of dithiothreitol (0.1 mM or higher) only 8–10% of the original lipoate activity can be obtained. The DCIP activities are difficult to determine due to the presence of the thiol compounds. The apoenzyme prepared in the presence of FMN shows a somewhat higher residual activity, 7–8%, with respect to both the lipoate and DCIP activities. This preparation, however, is able to give partial recombinaation with FAD in the absence of any thiol. After an incubation period of 30 min with FAD about 20% of the original lipoate activity is obtained, which does not significantly increase during the next 24 hours; on the other hand the DCIP activity regained after one hour is about 80–90% of the original DCIP activity. In this case, however, addition of thiol, at low and high FAD concentrations, does not result in an increased level of restored lipoate activity.

7.2.5. *Some properties of the apoenzyme*

The *Azotobacter* apoenzyme as prepared by the acid ammonium sulfate treatment is rather stable. On standing on ice at a protein concentration of 1.0 mg per ml for a period of 14 days about 50% of the original lipoate activity can still be regained; freezing at −15° for a same period only results in a very small decline in the ability to restore the lipoate activity. Dialysis of the apoenzyme for 2–24 hours against 30 mM potassium phosphate buffer (pH 7.5) containing 0.5–1 mM EDTA does not affect the capability to recombine with FAD. In general the stability of the *Azotobacter* apoenzyme is higher than that of pig heart (cf. VISSER and VEEGER, 1970).

From ultracentrifugation studies and gel filtration with Sephadex G-200, performed at a lower protein concentration than for the native enzyme, data

concerning molecular weight, diffusion and sedimentation coefficients, and frictional ratio were obtained. The data are summarized in TABLE 7.1 with the values for the holoenzyme. The results are almost equivalent to those of the pig heart apoenzyme and it is reasonable to conclude that the *Azotobacter* apoenzyme has also a molecular weight of about 52,000 daltons (average value) indicating the holoenzyme is a dimer.

The absorption spectrum of the apoenzyme obtained after a second acid ammonium sulfate treatment, as expected, is characterized by the absence of any absorbance above 320 nm; the maximum is located at 265–270 nm. The concentration of the apoenzyme can be measured at 280 nm taking $A = 1{,}1$ (cm $mg^{-1}ml^{-1}$), a value obtained by comparing the absorbance with the protein content found by the biuret method (GORNALL et al., 1949; ITZHAKI and GILL, 1964). Similar characteristics are observed for the apoenzyme preparations prepared according to the method of BRADY and BEYCHOK (1968, 1969), although the preparation obtained in the presence of FMN still shows some absorbance in the wavelength region above 320 nm. The extinction coefficient at 280 nm is in rather good agreement with that found by KALSE and VEEGER (1968) but differs considerably with the value of 0.48 as given by BRADY and BEYCHOK (1969) for the pig heart apoenzyme.

The ORD and CD curves of the three types of *Azotobacter* apoenzyme are given in FIG. 7.2 and FIG. 7.3. The ORD spectra of the three types of apoprotein are characterized by their minima around 233 nm; the shapes of the curves are almost identical to that of the native enzyme, although the mean residue rotation of the apoproteins at this wavelength is lower than that for the holoenzyme. The apoprotein prepared by dialysis against guanidine-HCl in the absence of FMN has the lowest mean residue rotation which is about 20–25% less than for the native enzyme. More pronounced differences are observed in the CD curves of the three apoproteins. All three curves are characterized by the absence of any dichroism above 300 nm and by the presence of a maximum between 270 and 285 nm and a minimum in the region 208–220 nm; great differences, however, are obtained in the mean residue molar ellipticities with respect to the native enzyme (cf. FIG. 7.2) at these characteristic wavelengths. The most striking changes are observable in the apoenzyme prepared by dialysis against guanidine-HCl in the absence of FMN. The molar ellipticity is slightly increased in the 280 nm region with respect to the native enzyme but is drastically lowered at 220 nm while the shape of the 208–220 nm band suggests that the α-helix structure has disappeared to a great extent. These differences point to different enzyme conformations which are not only caused by loss of flavin but are also induced by the method of preparation used. The fact that the acid ammonium sulfate-treated preparation shows a much higher ability to recombine with FAD is consistent with the observation that much less dramatic conformational changes were induced by this method than in the guanidine-HCl-treated apoenzyme. From the results it can also be concluded that through FMN-binding and dissociation the protein is kept in a less denaturated state.

7.3. Discussion

The data presented show that the *Azotobacter* lipoamide dehydrogenase has several properties in common with the enzyme from other sources (Koike et al., 1963; Lusty, 1963; Matthews and Reed, 1963; Wren and Massey, 1965; Visser and Veeger, 1968). The results obtained with gel filtration, sedimentation, diffusion and sucrose gradient centrifugation clearly point to a molecular weight of 102,000 daltons for the holoenzyme and 52,000 daltons for the apoenzyme. The physical characteristics for the *Azotobacter* enzyme, listed in Table 7.1, are in good agreement with those given in the literature for the pig heart enzyme (Visser and Veeger, 1968), for the *E. coli* enzyme (Koike et al., 1963) and for the yeast enzyme (Wren and Massey, 1963). They also support the idea of the existence of a monomer-dimer system (Visser and Veeger, 1968).

The isolated enzyme, characterised by the relative high lipoate and DCIP activities, as measured under standard conditions, is very stable, even upon dilution to rather low protein concentrations. The lipoate activity is NAD^+-dependent and is strongly inhibited by NADH (Fig. 7.4) in a non-competitive manner with respect to lipoic acid.

The enzyme is highly reactive in the reduced lipoamide-NAD^+ system, due to a high substrate affinity as concluded from the K_m values, calculated from the plots in Fig. 7.5. The maximum velocity obtained at infinite substrate concentrations, however, is of the same order as that for the pig heart enzyme (cf. Visser et al., 1970; Visser, 1970). The kinetics of the reaction in the absence of inhibitor (Fig. 7.5) clearly points to an ordered bi-bi mechanism (Cleland, 1963), supporting the kinetic studies on the pig heart enzyme (Visser et al., 1970; Visser, 1970). No definite statement can be given in our case, since no inhibition studies were performed, but assuming a similar mechanism as for the pig heart enzyme the kinetic constants, as far as calculated, are of the same order of magnitude (Table 7.2).

Removal of the flavin from the *Azotobacter* enzyme by the acid ammonium sulfate treatment according to the method of Kalse and Veeger (1968) proceeds in a very reproducible manner; a second treatment does not even alter the properties of the apoenzyme. The apoenzyme is rather stable and can be easily reconstituted with FAD. This behaviour indicates that the treatment does not result in irreversible changes in the protein structure precluding the rebinding of FAD, as proposed by Williams (1965) for the *E. coli* enzyme. Nevertheless, changes occur as can be concluded from changes in physical properties like sedimentation coefficient, diffusion constant, molecular weight, and changes in frictional coefficient (Table 7.1). Furthermore solubilisation of the precipitated apoenzyme has to be performed in phosphate buffers of high ionic strength and ageing of the apoenzyme decreases its ability to recombine with FAD, although the latter process in our case is less pronounced as for the pig heart enzyme (Visser and Veeger, 1970). Moreover, the CD and ORD experiments (Fig. 7.2 and Fig. 7.3) indicate that conformational changes occur; the helix content might decrease although bound FAD might have some

influence as concluded form the small shift of the maximum from 208 nm to 212 nm. The differences obtained in the restoration of the lipoate and DCIP activities upon incubation with FAD at 0° and 25° also point to sequential alterations in the protein. The changes in DCIP-activity, however, are less pronounced than for the pig heart enzyme (KALSE and VEEGER, 1968). The effects in our case are probably masked by the relatively high DCIP activity of the *Azotobacter* holoenzyme. The spectrum of the reconstituted enzyme (FIG. 7.1) is also indicative of an altered structure in the reconstituted enzyme. The absence of the splitting of the '450' nm band may be due to a more polar environment of the flavin (VEEGER et al., 1966; PENZER and RADDA, 1967). The spectrum of the reconstituted enzyme is rather similar to that calcultaed by WILLIAMS (1965) for *E. coli*, assuming a mixture of 65% FAD and 35% native mutant *E. coli* lipoamide dehydrogenase. The activities of the reconstituted *Azotobacter* FAD-apoprotein complex are identical with those of the original holoenzyme. It is of interest to mention that sometimes holoenzymes were isolated which were characterised by an absorption spectrum almost identical with that of the reconstituted enzyme.

As outlined for the pig heart enzyme (VISSER and VEEGER, 1968; VISSER, 1970) and supported by our observations, the bound flavin molecule plays an important role in the stabilisation of the tertiary protein structure. Upon recombination the original structure is not completely restored as concluded from the spectral differences and from the differences in sensitivity towards FMN between the holoenzyme and the reconstituted enzyme. The effect of FMN on the apoprotein-FAD-complex, replacing the loosely bound FAD, points to a series of conformational changes of the protein in the recombination process, positively induced by FAD and partially counteracted by FMN.

The different methods of preparing the apoenzyme lead to different types of apoenzyme as can be concluded from the recombination experiments with FAD and the CD absorption curves. The results indicate that not only removal of FAD is responsible for the differences observed. The acid ammonium sulfate treatment according to KALSE and VEEGER (1968) appears to be the mildest method; only small changes are observed in the ORD and CD characteristics of these apoproteins with respect to the original holoenzyme. Moreover almost complete restoration of the original activity is obtained upon incubation with FAD, within a very short incubation period at 25°. In contrast to the pig heart enzyme (VEEGER et al., 1969) no increase in helix content could be observed in the apoenzyme with respect to the holoenzyme; the helix content is even slightly decreased. The method of BRADY and BEYCHOK (1968, 1969) results in a more drastic alteration of structure, hindering also the re-binding of FAD. The presence of FMN in the dialysis buffer has some stabilizing effect, resulting in a less drastic conformational change and higher ability to recombine with FAD in the absence of added thiols, but the results obtained are very poor with respect to the procedure generally used in our laboratory and are not in agreement with the results reported by BRADY and BEYCHOK (1968, 1969) for the pig heart enzyme. Since in all cases no flocculation occurred during the

preparation of the apoenzymes, the differences obtained are not due to total unfolding, but to partially irreversible changes in protein conformation. The shape of the CD curves obtained for the guanidine-HCl treated preparations, however, clearly indicates that the amount of random structure has increased (GREENFIELD and FASMAN, 1969). No conclusions can be drawn about a possible contribution of the β-form to the secondary structure of the enzyme.

SUMMARY

A method for the isolation and purification of a reversible transhydrogenase from *Azotobacter vinelandii* is described (CHAPTER 3). The purification of the enzyme is hampered by association-dissociation phenomena, resulting in large losses of transhydrogenase activity. The relation between these losses and removal of lipoamide dehydrogenase, pyruvate dehydrogenase complex and a NADPH-ferricyanide diaphorase activity suggests the existence of a multi-enzyme complex, dissociation of this complex resulting in association of the transhydrogenase molecules.

The purified transhydrogenase is a flavoprotein with FAD as prosthetic group. The absorption spectrum of the $NADP^+$-free enzyme is characterized by a maximum at 442 nm. A minimum molecular weight of 60,000 daltons can be calculated from the experimentally determined extinction coefficient at 442 nm. The oxidized enzyme is stable at elevated temperatures and at high dilution; storage at $-20°$ results in aggregation of the enzyme. The reduced enzyme is thermolabile; inactivation at elevated temperatures can be prevented by addition of FAD. It is difficult to prepare the apoenzyme and incubation with FAD only results in partial restoration of transhydrogenase activity.

Ultracentrifugation and light-scattering studies demonstrate that the transhydrogenase preparations are inhomogeneous. In two types of enzyme preparations three sedimentation coefficients ($s_{20,w}$) are determined: 24, 48 and 88 S, respectively. By addition of NADPH and $NADP^+$ upon sedimentation of the enzyme a relation is demonstrated between the 48 and 88 S components. The sedimentation coefficient of the main component is concentration independent beyond 1 mg/ml. From light-scattering experiments a molecular weight (M_z) of 30–50 million daltons is determined; the calculated length for a rod-like structure is 10,000–15,000 Å.

Electron microscopic investigations (CHAPTER 4) confirm the inhomogeneity of the transhydrogenase preparations. Long helical-like structures up to 10,000 Å are present apart from large amounts of rod-like structures and separate fragments. The diameter of both the threads and rods is 116–120 Å. No clear-cut substructures are observable; possibly they represent projections of sphericle particles; the threads may represent spiral-like structures. Addition of $NADP^+$ to the enzyme solution can result in fragmentation of the thread-like structures, but the dissociation is never complete. Extensive removal of $NADP^+$ results in more homogeneous preparations with structures up to 15,000–18,000 Å in length. The ratio NADPH/$NADP^+$ seems to be regulatory for the length of the structure. Other nucleotides have no clear-cut effect on the structure of the enzyme.

In some preparations a totally unknown, ladder-like structure is observed. The constituents are very similar to the thread-like structures of the transhydrogenase and the tetramer-like structures, present in pyruvate dehydrogenase

complex preparations. Only transhydrogenase and transacetylase activities are detectable in these preparations. This structure supports the idea of a complex between the transhydrogenase and the pyruvate dehydrogenase. The ladder-like structures resist the influence of the different nucleotides.

Ammonium sulfate crystalline suspensions of the enzyme show regular structures, some kind of 'stacked disc' structures; solubilisation results in the appearance of thread-like structures, fragments and rosettes, but no close relation between the different species can be established.

From an examination of the different purification stages it can be concluded that the thread-like transhydrogenase structure is not a purification artefact due to the procedure followed; however, a relation seems to exist between the presence of the thread-like structures, the concentration of the transhydrogenase and the removal of the pyruvate dehydrogenase complex.

Spectral studies (CHAPTER 5) have shown that 1 mole $NADP^+$ (per mole of flavin) can be easily bound to the oxidized enzyme. This results in a spectral shift in the region 300–500 nm of the absorption spectrum, a quenching of flavin fluorescence and a shift of the emission maximum; moreover it affects the ORD and CD characteristics. The dissociation constant (K_D) of this $NADP^+$ complex is $\sim$ 3–4 μM. Changes in the 300–350 nm region of the absorption spectrum at higher $NADP^+$ concentrations point to the possible existence of a second binding site for $NADP^+$. These shifts are possibly due to either changes in polarity around the flavin, or to interaction between $NADP^+$ and the isoalloxazine ring of the flavin, or to weakening of ribityl side chain interactions; protein conformational changes, however, cannot be excluded.

Anaerobic titrations of the transhydrogenase with NAD(P)H in the presence of NADase show that two moles of reductant are required to reduce one mole of enzyme-bound flavin; this observation is confirmed by titrations with sodium dithionite. The existence of an unknown reducible group X next to the flavin is proposed. On the basis of the differences found in the titrations with dithionite, with NADPH in the absence and presence of $NADP^+$ and with NADH in the absence and presence of $NADP^+$ and NAD^+ a reduction scheme is proposed. The titration experiments show that NAD^+ and $NADP^+$ interact in a different manner with the different forms of the enzyme, e.g. $NADP^+$ has a higher affinity for the oxidized enzeym, while NAD^+ has a higher affinity for the reduced enzyme. Furthermore the level of reduction of the enzyme-bound flavin is determined by the ratio of reduced and oxidized pyridine nucleotides. Titration experiments of the reduced enzyme with $NADP^+$ and photoreduction experiments support the proposals. On the basis of these findings a model is proposed giving an explanation for a specific hydrogen transfer from the 4B site of NADH to the 4B site of $NADP^+$.

Kinetic studies (CHAPTER 6) performed with naturally occurring coenzymes and their thio-analogues point to the existence of a ping-pong bi-bi mechanism for the NADH-$TNAD^+$ and NADPH-$TNAD^+$ reactions. The inhibition of NAD^+ with respect to NADH in the reaction NADH-$TNAD^+$ and the dependence of the reaction velocity on $[NADPH]^2$ in the reaction NADPH-

$TNAD^+$ in the presence of $NADP^+$, however, exclude this mechanism. A ternary complex mechanism is proposed, in which the enzyme is first reduced to the 4-equivalent reduced state by 2 moles of donor before 2 moles of acceptor are bound to the reduced enzyme; the possibility of complex formation of the oxidised enzyme with $NADP^+$ is included in the scheme. The kinetic patterns of the NADPH-$TNAD^+$ reaction in the absence and presence of $NADP^+$ can be explained by this mechanism. The explanation of the kinetic patterns of the NADH-$TNAD^+$ reaction can be given by slightly modifying the mechanism in such a way that the sequence of addition of the acceptor molecule and the second donor molecule is changed and assuming irreversible binding of the first acceptor molecule to the reduced enzyme; this latter assumption is justified by the high affinity of NAD^+ for the reduced enzyme. The reactions of $NADP^+$ and $TNADP^+$ with NAD(P)H proceed due to the reversible binding of both substrates according to a rapid equilibrium random bi-bi mechanism. The data of the reaction NADH-$NADP^+$ and the $NADP^+$ inhibition patterns of the reaction NADPH-$TNADP^+$ are consistent with this mechanism. The proposed ternary complex or random bi-bi mechanisms are more reasonable for a 4B-4B hydrogen transfer than a ping-pong bi-bi mechanism.

In CHAPTER 7 results are presented from studies on *Azotobacter* lipoamide dehydrogenase. The results show that the *Azotobacter* enzyme has several properties in common with the pig heart lipoamide dehydrogenase. Gel filtration and ultracentrifugation studies show that the holoenzyme and the apoenzyme have a molecular weight of 102,000 and 52,000 daltons, respectively, supporting the idea of the existence of a monomer-dimer system. The apoenzyme-FAD complex, however, does not show a pronounced DCIP activity; the absorption spectrum points to a more polar environment of the flavin.

Kinetic studies with reduced lipoamide and NAD^+ support, as proposed for the pig heart enzyme, an ordered bi-bi mechanism. Assuming this mechanism, kinetic parameters are calculated which are in the same order of magnitude as for the pig heart enzyme. The affinity of the *Azotobacter* enzyme for both substrates, however, is much higher.

The apoenzyme prepared according to the acid ammonium sulfate procedure is very stable and can be easily reconstituted with FAD; the recombination process is temperature and FAD dependent. Preparation of the apoenzyme by dialysis against guanidine-HCl, however, results in a totally different structure, as concluded from recombination experiments and from the different characteristics with respect to the holoenzyme and the acid ammonium sulfate treated enzyme.

SAMENVATTING

In Hoofdstuk 3 wordt een methode voor de isolering en zuivering van het enzym transhydrogenase uit de bacterie *Azotobacter vinelandii* beschreven. Gebleken is, dat de zuivering bemoeilijkt wordt door associatie-dissociatie verschijnselen, wat kan resulteren in grote verliezen aan transhydrogenase-activiteit. Het verband tussen de verliezen aan transhydrogenase-activiteit en de verwijdering van lipoïnezuur dehydrogenase, pyrodruivenzuur-dehydrogenase-complex en een NADPH-ferricyanide diaforase doet het bestaan van een multi-enzymcomplex veronderstellen; dissociatie van de transhydrogenase van dit complex zou dan resulteren in associatie of aggregatie van de enzym moleculen.

De gezuiverde transhydrogenase is een flavoproteïne met FAD als prosthetische groep. Het absorptie-spectrum van het $NADP^+$-vrije enzym wordt gekenmerkt door een maximum bij 442 nm. Een minimum molecuulgewicht van ca. 60.000 daltons kan worden berekend uit een experimenteel bepaalde waarde van de extinctiecoëfficient bij 442 nm. Het geoxydeerde enzym is stabiel, zowel bij verhoogde temperatuur als in verdunde oplossing; bewaren bij $-20°$ echter resulteert in aggregatie t.g.v. concentratieverhoging. Het gereduceerde enzym is thermolabiel; inactivering bij verhoogde temperatuur kan worden voorkomen door toevoeging van FAD. Het apoenzym is moeilijk te bereiden en incubatie met FAD resulteert slechts in een zeer onvolledige terugkeer van de transhydrogenase-activiteit.

Ultracentrifuge- en lichtverstrooiingsproeven hebben aangetoond dat de transhydrogenasepreparaten niet homogeen zijn. In 2 typen transhydrogenasepreparaten zijn 3 sedimentatieconstanten ($s_{20,w}$) bepaald, resp. 24, 48 en 88 S. Door toevoeging van NADPH en $NADP^+$ tijdens sedimentatieproeven kon een relatie worden aangetoond tussen de 48 en 88 S componenten. De sedimentatieconstante van de hoofdcomponent blijkt onafhankelijk te zijn van de concentratie in het gebied boven 1 mg/ml. Uit de lichtverstrooiingsproeven is d.m.v. ZIMM-relaties een molecuulgewicht van 30–50 miljoen daltons bepaald voor de grootste structuren; de uit deze metingen berekende lengte voor een draadvormig molecuul is 10.000–15.000 *Å*.

Electronenmicroscopische onderzoekingen (Hoofdstuk 4) hebben bevestigd dat de transhydrogenasepreparaten niet homogeen zijn. Zeer lange draadvormige structuren met lengten tot 10.000 *Å*, zijn aanwezig naast vele kortere draden en losse structuren. De doorsnee van de draad is 116–120 *Å*. Geen duidelijke substructuren zijn waar te nemen, hoewel een spiraalvorm tot de mogelijkheden behoort. Toevoeging van $NADP^+$ aan de enzymoplossing kan resulteren in het uiteenvallen van de draden in kleine fragmenten; dit dissociatiegedrag echter is niet altijd volledig. Volledige verwijdering van $NADP^+$ maakt de preparaten homogener wat de lengte van de draden betreft; draden met een lengte > 15.000 *Å* waren nu aantoonbaar. De verhouding NADPH/

$NADP^+$ lijkt regelend te zijn voor de lengte van de draad. Andere nucleotiden hebben geen duidelijke invloed op de structuur. In bepaalde preparaten is een totaal onbekende laddervormige structuur aangetroffen. De samenstellende elementen vertonen wat hun afmetingen en voorkomen betreft, overeenkomsten met de transhydrogenasedraad en de tetrameerstructuren, welke aanwezig zijn in pyrodruivenzuurdehydrogenase-complexpreparaten. Alleen een transhydrogenase- en een transacetylase-activiteit is in deze preparaten aantoonbaar. Deze structuur ondersteunt de veronderstelling van een mogelijke complexvorming van de transhydrogenase met het pyrodruivenzuurdehydrogenase-complex. De ladderstructuren zijn bestand tegen de inwerking van de verschillende nucleotiden. Ammoniumsulfaat kristalsuspensies van de transhydrogenase vertonen zeer regelmatige structuren, welke in bundels voorkomen; bij oplossen zijn draden, brokstukken en rozetten waarneembaar, doch een nauwe relatie tussen de verschillende structuren kon niet worden vastgesteld.

Uit onderzoekingen aan de verschillende zuiveringsstadia kan worden geconcludeerd dat de draadvorm geen artefact t.g.v. de zuiveringsprocedure is; er lijkt een relatie te bestaan tussen de aanwezigheid van de draadvorm, de concentratie van de transhydrogenase en de verdwijning van het pyrodruivenzuurdehydrogenase-complex.

Spectrale studies (Hoofdstuk 5) hebben aangetoond dat 1 molecuul $NADP^+$ (per molecuul flavine) zich gemakkelijk kan binden aan het geoxydeerde enzym. Deze complexvorming resulteert in verschuivingen in het absorptiespectrum, doving van de flavine fluorescentie-emissie en verschuiving van het emissiemaximum, en beïnvloeding van de ORD- en CD-karakteristieken. Een dissociatieconstante (K_D) voor dit $NADP^+$-complex van ca. 3–4 μM kan worden berekend. Veranderingen in het 300–350 nm gebied van het absorptiespectrum bij hogere $NADP^+$-concentraties wijzen op het mogelijke bestaan van een 2e bindingsplaats voor $NADP^+$. Deze verschuivingen zijn geïnterpreteerd als een gevolg van veranderingen in polariteit in de omgeving van het flavine, òf van interactie van $NADP^+$ en de isoalloxazinering van het flavine, òf van een vermindering van de ribityl-isoalloxazine-interacties; eiwitconformatieveranderingen kunnen echter niet worden uitgesloten.

Anaerobe titraties van de transhydrogenase met NAD(P)H in aanwezigheid van NADase laten zien dat 2 moleculen reductant nodig zijn om één molecuul enzymgebonden flavine te reduceren; titraties met Na-dithioniet hebben deze waarneming bevestigd. Dit leidde tot de veronderstelling dat naast FAD nog een 2e reduceerbare groep aanwezig zou moeten zijn in de transhydrogenase. Op basis van de verschillen welke gevonden worden bij de titraties met dithioniet, met NADPH in aan- en afwezigheid van $NADP^+$ en met NADH in aan- en afwezigheid van NAD^+ en $NADP^+$ wordt een reductie-schema voorgesteld. De titratie-experimenten tonen aan dat NAD^+ en $NADP^+$ op een verschillende manier met de verschillende vormen van het enzym een interactie geven, d.w.z. $NADP^+$ heeft een hogere affiniteit voor het geoxydeerde enzym, terwijl NAD^+ een hogere affiniteit bezit voor het gereduceerde enzym. Bovendien blijkt het reductie-niveau van het enzymgebonden flavine bepaald te worden

door de verhouding van de gereduceerde en geoxydeerde vormen van de pyridine nucleotiden. Titratieproeven van de gereduceerde enzymen met $NADP^+$ en fotoreductie-experimenten ondersteunen deze hypothese. Op basis van deze gegevens wordt een model voorgesteld, waarin de interactie van N-1 van de isoalloxazinering met N-1 van het geoxydeerde pyridine nucleotide en binding van het gereduceerde pyridine nucleotide op N-5 een aannemelijke verklaring lijkt te geven voor een specifieke overdracht van waterstof van een 4B-plaats naar een 4B-plaats.

Kinetische studies (Hoofdstuk 6) welke werden uitgevoerd met de in de natuur voorkomende coenzymen en zijn thio-analogen, en waarbij de transhydrogenase-reactie in beide richtingen werd bestudeerd, wezen aanvankelijk op het bestaan van een '*ping-pong bi-bi*' mechanisme. De remmingspatronen van NAD^+ t.o.v. NADH in de reactie NADH → $TNAD^+$ en de afhankelijkheid van de snelheid van $[NADPH]^2$ in de reactie NADPH → $TNAD^+$ in aanwezigheid van $NADP^+$ sloten dit mechanisme echter uit. Een ternair complex mechanisme wordt nu voorgesteld, waarbij 2 donormoleculen het enzym reduceren tot een 4-equivalenten gereduceerde toestand alvorens 2 acceptormoleculen gebonden worden; de mogelijkheid van complexvorming van het geoxydeerde enzym met $NADP^+$ is in het schema opgenomen. Met dit mechanisme kunnen alle kinetische beelden in de NADPH-$TNAD^+$ reactie worden verklaard. De verklaringen voor de NADH-$TNAD^+$ reactie zijn op basis van de spectrale studies gevonden in een iets gewijzigde volgorde van donor- en acceptorbinding; de binding van het eerste acceptormolecuul moet echter irreversibel verondersteld worden, wat op basis van de hoge affiniteit van NAD^+ voor het gereduceerde enzym gerechtvaardigd lijkt. De reacties van $NADP^+$ en $TNADP^+$ met NAD(P)H, waarbij reversibele substraten zijn betrokken, zullen waarschijnlijk volgens een '*rapid equilibrium random bi-bi*' mechanisme verlopen. Dit voorgestelde ternair complex mechanisme is waarschijnlijker bij een 4B-4B waterstofoverdracht dan een '*ping-pong bi-bi*' mechanisme.

In Hoofdstuk 7 worden enkele resultaten besproken welke zijn verkregen met lipoïnezuur dehydrogenase uit *Azotobacter vinelandii*. De resultaten wijzen duidelijk op een aantal overeenkomsten met het varkenshartenzym. Gelfiltratie- en ultracentrifugeproeven hebben aangetoond dat het holoenzym een molecuulgewicht heeft van 102.000 daltons en het apoenzym van 52.000 daltons; deze ondersteunen het bestaan van een monomeer-dimeer systeem. Het apoenzym-FAD complex heeft echter geen uitgesproken hoge DCIP-activiteit; het absorptiespectrum wijst op een meer polaire omgeving van het flavine.

Kinetische studies met gereduceerd lipoamide en NAD^+ ondersteunen het voor het varkenshartenzym voorgestelde '*ordered bi-bi*' mechanisme. De op basis van dit mechanisme berekende kinetische parameters zijn in dezelfde orde van grootte als berekend voor het varkenshartenzym, hoewel de affiniteit van het *Azotobacter* enzym voor de beide substraten groter is.

Het apoenzym bereid volgens de zure ammoniumsulfaatprocedure is zeer stabiel en kan gemakkelijk met FAD gereconstitueerd worden; het recombinatie-proces verloopt langzamer bij lage temperatuur en wordt geremd door hoge

concentraties FAD. Bereiding van het apoenzym d.m.v. dialyse tegen guanidine-HCl echter resulteert in een totaal andere structuur; de recombinatie met FAD verloopt slechts gedeeltelijk en de CD-karakteristieken verschillen duidelijk met die van het eerstgenoemde apoenzym en het holoenzym.

REFERENCES

ACKERS, G. R., Biochemistry, 3 (1964) 723.

AKI, K., TAKAGI, T., ISEMURA, I., and YAMANO, T., Biochim. Biophys. Acta, **112** (1966) 193.

ASANO, A., IMAI, I., and SATO, R., Biochim. Biophys. Acta, **143** (1967) 477.

BASU, D. R., and BURMA, D. P., J. Biol. Chem., **235** (1960) 509.

BEINERT, H., and SANDS, R. H., in Free Radicals in Biological Systems, ed. M. S. BLOIS, W. H. BROWN, R. M. LEMMON, R. O. LINDBLOM and M. WEISSBLUTH, Acad. Press, New York, 1961, p. 17.

BENESI, H. A., and HILDEBRAND, J. A., J. Amer. Chem. Soc., **71** (1949) 2703.

BRADY, A. H., and BEYCHOK, S., Biochem. Biophys. Res. Comm., **32** (1968) 186.

BRADY, A. H., and BEYCHOK, S., J. Biol. Chem., **244** (1969) 1634.

CHANCE, B., in The Mechanism of Enzyme Action, ed. W. D. MCELROY and B. GLASS, John's Hopkins Press, Baltimore, 1955.

CHUNG, A. E., J. of Bacteriology, **102** (1970) 438.

CLELAND, W. W., Biochim. Biophys. Acta, **67** (1963) 104.

COHEN, P. T., Dissertation Brandeis University, 1967, University Microfilms Inc., Ann Arbor, No 67–16542.

COHEN, P. T., and KAPLAN, N. O., J. Biol. Chem., **245** (1970a) 2825.

COHEN, P. T., and KAPLAN, N. O., J. Biol. Chem., **245** (1970b) 4666.

COLMAN, R. F., and BLACK, S., J. Biol. Chem., **240** (1965) 1796.

COLOWICK, S. P., KAPLAN, N. O., NEUFELD, E. F., and CIOTTI, M. M., J. Biol. Chem., **195** (1952) 95.

CONWAY, A., and KOSHLAND, JR., D. E., Biochemistry, **7** (1968) 4011.

CRANE, F. L., and BEINERT, H., J. Am. Chem. Soc., **76** (1954) 4491.

DANIELSON, L., and ERNSTER, L., Biochem. Biophys. Res. Comm., **10** (1963a) 91.

DANIELSON, L., and ERNSTER, L., in Energy-Linked Functions of Mitochondria, ed. B. CHANCE, Acad. Press Inc., New York, 1963b, p. 157.

DERVARTANIAN, D. V., and VEEGER, C., Biochim. Biophys. Acta, **92** (1964) 233.

DERVARTANIAN, D. V., Ph. D. Dissertation, University of Amsterdam, 1965.

DERVARTANIAN, D. V., ZEYLEMAKER, W. P., and VEEGER, C., in Flavins and Flavoproteins, ed. E. C. SLATER, B. B. A. Library, **Vol. 8**, Elsevier Publ. Co., Amsterdam, 1966, p. 183.

DE KOK, A., and VEEGER, C., Biochim. Biophys. Acta, **131** (1967) 589.

DE KOK, A., BRÜSTLEIN, M., HEMMERICH, P., and VEEGER, C., 1970, to be published.

DE KOK, A., Thesis, University of Amsterdam, Mededelingen Landbouwhogeschool Wageningen, **70–1** (1970).

DE KOK, A., VEEGER, C., and HEMMERICH, P., in Flavins and Flavoproteins, ed. H. KAMIN, University Park Press, Baltimore, 1970.

DIXON, M., and KLEPPE, K., Biochim. Biophys. Acta, **167** (1968) 227.

DOLIN, M. I., J. Biol. Chem., **235** (1960) 544.

DOLIN, M. I., in Flavins and Flavoproteins, ed. E. C. SLATER, B.B.A. Library, **Vol. 8**, Elsevier Publ. Co., Amsterdam, 1966, p. 171.

DOLIN, M. I., unpublished results.

DOTY, P., and STEINER, R. F., J. Chem. Phys., **28** (1950) **1**, 211.

EDMONDSON, D. E., and TOLLIN, G., Private communication from G. TOLLIN to C. VEEGER and taken from a dissertation submitted by D. E. EDMONDSON in partial fulfilment of requirements for a Ph.D. degree, University of Arizona, 1970.

EHRENBERG, A., and LUDWIG, G. D., Science, **127** (1958) 1177.

EISENKRAFT, B., Thesis, University of Amsterdam, Mededelingen Landbouwhogeschool Wageningen, **69–15** (1969).

ELEY, M., LEE, J., LHOSTE, J. M., LEE, C. Y., CORMIER, M. J., and HEMMERICH, P., Biochemistry, **9** (1970) 2902.

ESTABROOK, R. W., and NISSLEY, S. P., in Symp. Funktionelle Morphologische Organisation der Zelle, ed. P. KARLSON, Springer-Verlag, Heidelberg, 1963, p. 119.
FASMAN, G. D., in Methods in Enzymology, ed. S. P. COLOWICK and N. O. KAPLAN, Acad. Press, New York, 1963, Vol. VI, p. 942.
FERDINAND, W., Biochem. J., **98** (1966) 278.
FIESER, L. F., J. Amer. Chem. Soc., **46** (1924) 2639.
FOUST, G. P., MAYHEW, S. G., and MASSEY, V., J. Biol. Chem., **244** (1969a) 964.
FOUST, G. P., BURLEIGH, B. D., JR., MAYHEW, S. G., WILLIAMS, C. H., JR., and MASSEY, V., Anal. Biochem., **27** (1969b) 530.
FRISELL, W. R., and MACKENZIE, C. G., J. Biol. Chem., **237** (1962) 94.
GOLDMAN, D. S., Biochim. Biophys. Acta, **45** (1960) 279.
GORNALL, A. G., BARDAWILL, C. J., and DAVID, M. M., J. Biol. Chem., **177** (1949) 751.
GREENFIELD, N., and FASMAN, G. D., Biochemistry, **8** (1969) 4108.
HAAS, E., Biochem. Zeitschr., **290** (1937) 291.
HAYAKAWA, T., HIRASHIMA, M., IDE, S., HAMADA, M., OKABE, K., and KOIKE, M., J. Biol. Chem., **241** (1966) 4694.
HEMMERICH, P., NAGELSCHNEIDER, G., and VEEGER, C., FEBS Letters, **8** (1970) 69.
HESP, B., CALVIN, M., and HOSAKAWA, K., J. Biol. Chem., **244** (1969) 5644.
ICÉN, A., Scan. J. Clin. Lab. Invest., **20** (1967) 96.
IDE, S., HAYAKAWA, T., OKABE, K., and KOIKE, M., J. Biol. Chem., **242** (1967) 54.
ITZHAKI, R. F., and GILL, D. M., Analyt. Biochem., **9** (1964) 401.
JACOBI, G., and ÖHLERS, U., Z. Pflanzenphysiol., **58** (1968) 193.
JONES, C. W., and REDFEARN, E. R., Biochim. Biophys. Acta, **113** (1966) 467.
JONES, C. W., and REDFEARN, E. R., Biochim. Biophys. Acta, **143** (1967) 354.
KALSE, J. F., and VEEGER, C., Biochim. Biophys. Acta, **159** (1968) 193.
KAPLAN, N. O., COLOWICK, S. P., and NEUFELD, E. F., J. Biol. Chem., **195** (1952) 107.
KAPLAN, N. O., COLOWICK, S. P., NEUFELD, E. F., and CIOTTI, M. M., J. Biol. Chem., **205** (1953) 17.
KAPLAN, N. O., COLOWICK, S. P., ZATMAN, L. J., and CIOTTI, M. M., J. Biol. Chem., **205** (1953) 31.
KAPLAN, N. O., SWARTZ, M. N., FRECH, M. E., and CIOTTI, M. M., Proc. Natl. Acad. Sci., **42** (1956) 481.
KAPLAN, N. O., in Methods in Enzymology, ed. S. P. COLOWICK and N. O. KAPLAN, Acad. Press, New York, 1955, Vol. II, p. 660, 664.
KAUFMAN, B., and KAPLAN, N. O., J. Biol. Chem., **236** (1961) 2133.
KAWAHARA, Y., MISAKA, E., and NAKANISHI, K., J. Biochem., **63** (1968) 77.
KAWASAKI, T., SATOH, K., and KAPLAN, N. O., Biochem. Biophys. Res. Comm., **17** (1964) 648.
KEISTER, D. L., SAN PIETRO, A., and STOLTZENBACH, F. E., J. Biol. Chem., **235** (1960) 2989.
KEISTER, D. L., SAN PIETRO, A., and STOLTZENBACH, F. E., Biochim. Biophys. Acta, **98** (1962) 235.
KEISTER, D. L., Brookhaven Symp. Biol., **19** (1966) 255.
KEISTER, D. L., and HEMMES, R. B., J. Biol. Chem., **241** (1966) 2820.
KEISTER, D. L., and YIKE, N. J., Biochem. Biophys. Res. Comm., **214** (1966) 519.
KEISTER, D. L., and YIKE, N. J., Biochemistry, **6** (1967) 3847.
KILGOUR, G. L., FELTON, S. P., and HUENNEKENS, F. M., J. Am. Chem. Soc., **79** (1957) 2254.
KIRSCHNER, K., EIGEN, M., BITTMAN, R., and VOIGT, B., Proc. Natl. Acad. Sci., **56** (1966) 1661.
KLINGENBERG, M., and SLENCZKA, W., Biochem. Zeitschr., **331** (1959) 486.
KOIKE, M., SHAH, P. C., and REED, L. J., J. Biol. Chem., **235** (1960) 1939.
KOIKE, M., and REED, L. J., J. Biol. Chem., **236** (1961) PC 33.
KOIKE, M., REED, L. J., and CARROLL, R., Biochem. Biophys. Res. Comm., **7** (1962) 16.
KOIKE, M., REED, L. J., and CARROLL, R., J. Biol. Chem., **238** (1963) 30.
KOIKE, M., personal communication.
KOSHLAND, JR., D. E., NEMETHY, G., and FILMER, D., Biochemistry, **5** (1966) 365.

KOSTER, J. F., and VEEGER, C., Biochim. Biophys. Acta, **151** (1968) 1.
KOSTER, J. F., Thesis, University of Amsterdam, Mededelingen Landbouwhogeschool Wageningen, 69–8 (1969).
KRAMAR, R., MÜLLER, M., and SALVENMOSER, F., Biochim. Biophys. Acta, **162** (1968) 289.
KREBS, H. A., and KORNBERG, H. L., Ergebn. Physiol., **49** (1957) 212.
KRUL, J., unpublished results.
LEE, C. P., and ERNSTER, L., Biochim. Biophys. Acta, **81** (1964) 187.
LEE, C. P., SIMARD-DUQUESNE, N., HOBERMAN, H. D., and ERNSTER, L., Biochim. Biophys. Acta, **105** (1965) 397.
LI, T. K., ULMER, D. D., and VALLEE, B. L., Biochem. Zeitschr., **1** (1962) 114.
LINEWEAVER, H., and BURK, D., J. Am. Chem. Soc., **56** (1934) 658.
LOUIE, D. D., and KAPLAN, N. O., Fed. Proc., **28** (1969) 342.
LOUIE, D. D., and KAPLAN, N. O., in Pyridine Nucleotide Dependent Dehydrogenases, ed. H. SUND, Springer-Verlag, Berlin, 1970a, p. 351.
LOUIE, D. D., and KAPLAN, N. O., J. Biol. Chem., **245** (1970b) 5691.
LUBIN, M., J. Mol. Biol., **39** (1969) 219.
LUSTY, C. J., J. Biol. Chem., **238** (1963) 3443.
MAHLER, H. R., and CORDES, E. H., 'Biological Chemistry', Harper and Row, New York, 1969, p. 255.
MARTIN, R. G., and AMES, B. N., J. Biol. Chem., **236** (1961) 1372.
MASSEY, V., Biochim. Biophys. Acta, **30** (1958) 205.
MASSEY, V., Biochim. Biophys. Acta, **37** (1960) 314.
MASSEY, V., GIBSON, Q. H., and VEEGER, C., Biochem. J., **77** (1960) 341.
MASSEY, V., and VEEGER, C., Biochim. Biophys. Acta, **40** (1960) 184.
MASSEY, V., and VEEGER, C., Biochim. Biophys. Acta, **48** (1961) 33.
MASSEY, V., and PALMER, G., J. Biol. Chem., **237** (1962) 2347.
MASSEY, V., The Enzymes, ed. P. D. BOYER, H. A. LARDY and K. MYRBÄCK, **Vol. 7**, Acad. Press, New York, 1963, p. 275.
MASSEY, V., and GIBSON, Q. H., Fed. Proc., **23** (1964) 18.
MASSEY, V., and GANTHER, H., Biochemistry, **4** (1965) 1161.
MASSEY, V., and WILLIAMS, C. H., JR., J. Biol. Chem., **248** (1965) 4478.
MASSEY, V., and PALMER, G., Biochemistry, **5** (1966) 3181.
MASSEY, V., PALMER, G., WILLIAMS JR., C. H., SWOBODA, B. E. P., and SANDS, R. H., in Flavins and Flavoproteins, ed. E. C. SLATER, B.B.A. Library, **Vol. 8**, Elsevier Publ. Co., Amsterdam, 1966, p. 133.
MASSEY, V., MATTHEWS, R. G., FOUST, G. P., HOWELL, L. G., WILLIAMS, C. H., JR., ZANETTI, G., and RONCHI, S., in Pyridine Necleotide Dependent Dehydrogenases, ed. H. SUND, Springer-Verlag, Berlin, 1970, p. 393.
MATTHEWS, J., and REED, L. J., J. Biol. Chem., **238** (1963) 1869.
MAYHEW, S. G., and MASSEY, V., J. Biol. Chem., **244** (1969) 794.
MCCORMICK, D. B., KOSTER, J. F., and VEEGER, C., Eur. J. Biochem., **2** (1967) 387.
MELLEMA, J. E., VAN BRUGGEN, E. F. J., GRUBER, M., Biochim, Biophys. Acta, **140** (1967) 180.
MILES, D. W., and URRY, D. W., Biochemistry, **7** (1968) 2791.
MISAKA, E., and NAKANISHI, R., J. Biochem., **58** (1965) 436.
MONOD, J., WYMAN, J., and CHANGEUX, J. P., J. Mol. Biol., **12** (1965) 103.
MORTENSON, L. E., VALENTINE, R. C., and CARNAHAN, J. E., J. Biol. Chem., **238** (1963) 794.
MURTHY, P. S., and BRODY, A. F., J. Biol. Chem., **239** (1964) 4292.
NAKAMURA, T., YOSHIMURA, J., and OGURA, Y., J. Biochem., **57** (1965) 554.
ORLANDO, J. A., SABO, D., and CURNYN, C., Plant Physiol., **41** (1966) 937.
ORLANDO, J. A., Archiv. Biochem. Biophys., **141** (1970) 111.
PANDIT-HOVENKAMP, N. G., in Oxidation and Phosphorylation, ed. R. W. ESTABROOK and M. E. PULLMAN, Acad. Press, New York, 1966.
PENZER, G. R., and RADDA, G. K., Quart. Revs., **21** (1967) 43.
PESCH, L. A., and PETERSON, J., Biochim. Biophys. Acta, **96** (1965) 390.

REED, L. J., KOIKE, M., LEVITCH, M. E., and LEACH, F. R., J. Biol. Chem., **232** (1959) 143.
REED, L. J., and COX, D. J., Ann. Rev. Biochemistry, **35** (1966) 60.
REED, L. J., and WILLMS, C. R., in Methods in Enzymology, **Vol. IX**, ed. W. A. WOOD, Acad. Press, New York, 1966, p. 247.
REED, L. J., LINN, T. C., PETTIT, F. H., Proc. Natl. Acad. Sci., **62** (1969) 234.
ROBERTON, A. M., and GRIFFITHS, Biochem. J., **94** (1965) 30P.
RYDSTRÖM, J., TEXEIRA DA CRUZ, A., and ERNSTER, L., Eur. J. Biochem., **17** (1970) 56.
SAN PIETRO, A., KAPLAN, N. O., and COLOWICK, S. P., J. Biol. Chem., **212** (1955) 941.
SAVAGE, N., Biochem. J., **67** (1957) 146.
SCHACHMAN, H. K., in 'Ultracentrifugation in Biochemistry', Acad. Press, New York, 1959, p. 102.
SCOTT, E., DUNCAN, I. W., and EKSTRAND, V., J. Biol. Chem., **238** (1963) 3928.
SHIN, M., TAGAWA, K., and ARNON, D. L., Biochem. Zeitschr., **338** (1963) 84.
SIEGEL, L. M., and MONTY, K. J., Biochem. Biophys. Res. Comm., **19** (1965) 494.
SIEGEL, L. M., and MONTY, K. J., Biochim. Biophys. Acta, **112** (1966) 346.
SLATER, E. C., Discussions Faraday Soc., **20** (1955) 231.
STAAL, G. E. J., and VEEGER, C., Biochim. Biophys. Acta, **185** (1969) 49.
STAAL, G. E. J., VISSER, J., and VEEGER, C., Biochim. Biophys. Acta, **185** (1969) 39.
STAAL, G. E. J., VOETBERG, H., and VEEGER, C., unpublished results.
STACEY, K. A., 'Light-scattering in Physical Chemistry', Butterworth Scientific Publications, 1956.
STRAUB, F. B., Biochem. J., **33** (1939) 787.
STRITTMATTER, P., Fed. Proc., **24** (1956) 1156.
STRITTMATTER, P., J. Biol. Chem., **234** (1959) 2665.
STRITTMATTER, P., J. Biol. Chem., **236** (1961) 2329.
SVEDBERG, T., and PEDERSON, K. O., 'The Ultracentrifuge', Oxford University Press, New York, 1940.
SWEENY, J. R., and FISHER, J. R., Biochemistry, **7** (1968) 561.
SWEETMAN, A. J., and GRIFFITHS, D. E., Biochem. J., **121** (1970) 131.
SWINGLE, S. M., and TISELIUS, A., Biochem. J., **48** (1951) 191.
THELANDER, L., Eur. J. Biochem., **4** (1968) 407.
THEORELL, H., Proc. 4th Int. Congr. Biochem., ed. O. HOFFMANN-OSTENHOF, Pergamon Press, London, 1960, **Vol. VIII**, p. 167.
TISSIÈRES, A., HOVENKAMP, H. G., and SLATER, E. C., Biochim. Biophys. Acta, **25** (1957) 336.
URRY, D. W., and LI, T. K., Archiv. Biochem. Biophys., **128** (1969) 802.
VAN DEN BROEK, H. W. J., and VEEGER, C., FEBS Letters, **1** (1968) 301.
VAN DEN BROEK, H. W. J., and VEEGER, C., in Pyridine Nucleotide Dependent Dehydrogenases, ed. H. SUND, Springer-Verlag, Berlin, 1970, p. 335.
VAN DEN BROEK, H. W. J., and VEEGER, C., unpublished results.
VEEGER, C., and MASSEY, V., Biochim. Biophys. Acta, **67** (1963) 679.
VEEGER, C., DERVARTANIAN, D. V., KALSE, J. F., DE KOK, A., and KOSTER, J. F., in Flavins and Flavoproteins, ed. E. C. SLATER, B.B.A. Library, **Vol. 8**, Elsevier, Publ. Co., Amsterdam, 1966, p. 242.
VEEGER, C., VOETBERG, H., VISSER, J., STAAL, G. E. J., and KOSTER, J. F., in Flavins and Flavoproteins, ed. H. KAMIN, University Park Press, Baltimore, 1970.
VEEGER, C., VOETBERG, H., PRONK, J., and VISSER, A. J. W. G., Proc. Werner Gren Symposium on Structure and Function of Oxidation-Reduction Enzymes (1970), ed. A. EHRENBERG, Pergamon Press, to be published.
VISSER, J., and VEEGER, C., Biochim. Biophys. Acta, **159** (1968) 265.
VISSER, J., VOETBERG, H., and VEEGER, C., in Pyridine Nucleotide Dependent Dehydrogenases, ed. H. SUND, Springer-Verlag, Berlin, 1970, p. 359.
VISSER, J., and VEEGER, C., Biochim. Biophys. Acta, **206** (1970) 224.
VISSER, J., Thesis, Agricultural University Wageningen, Mededelingen Landbouwhogeschool Wageningen, **70–7** (1970).
VOETBERG, H., and VEEGER, C., to be published.

WARBURG, O., and CHRISTIAN, W., Biochem. Zeitschr., **298** (1938) 150.
WEBER, M. M., and KAPLAN, N. O., J. Biol. Chem., **225** (1957) 909.
WILLMS, C. R., OLIVER, R. M., HENNEY JR., H. R., MUKHERJEE, B. B., and REED, L. J., J. Biol. Chem., **242** (1967) 889.
WREN, A., and MASSEY, V., Biochim. Biophys. Acta, **110** (1965) 329.
ZANETTI, G., and FORTI, G., J. Biol. Chem., **241** (1966) 279.
ZANETTI, G., and WILLIAMS, C. H., J. Biol. Chem., **242** (1967) 5232.
ZANETTI, G., WILLIAMS, C. H., and MASSEY, V., J. Biol. Chem., **243** (1968) 4013.
ZEYLEMAKER, W. P., DER VARTANIAN, D. V., VEEGER, C., and SLATER, E. C., Biochim. Biophys. Acta, **178** (1969) 213.
ZEYLEMAKER, W. P., Thesis, University of Amsterdam, Mondeel Offsetdrukkerij, Amsterdam, 1969.
ZIMM, B. H., J. Chem. Phys., **16** (1948) 1093.